PREPARATION AND PROPERTIES OF ELECTRICALLY CONDUCTING COPOLYMERS FORMED BY ELECTROPOLYMERIZATION OF HETEROCYCLIC COMPOUNDS

by

Eric Mackenzie Peters

B.Sc., Trinity Western University (B.C.), 1983

A THESIS SUBMITTED IN PARTIAL FULFILLMENT

OF THE REQUIREMENTS FOR THE DEGREE OF

MASTERS OF SCIENCE

in the Department

of

Chemistry

APPROVAL

Name: Eric Mackenzie Peters

Degree: Master of Science in Chemistry

Title of Thesis: Preparation and Properties of Electrically Conducting Copolymers Formed by Electropolymerization of Heterocyclic Compounds

Examination Committee:

Chairperson: Professor Paul Percival

Professor B. Lionel Funt
Senior Supervisor
Professor of Chemistry, SFU.

Professor Robert J. Cushley
Professor of Chemistry, SFU.

Professor Alden G. Sherwood
Associate Professor of Chemistry, SFU.

Professor Edward J. Wells
Associate Professor of Chemistry, SFU.

Date Approved: 7 April 1987

PARTIAL COPYRIGHT LICENSE

I hereby grant to Simon Fraser University the right to lend my thesis, project or extended essay (the title of which is shown below) to users of the Simon Fraser University Library, and to make partial or single copies only for such users or in response to a request from the library of any other university, or other educational institution, on its own behalf or for one of its users. I further agree that permission for multiple copying of this work for scholarly purposes may be granted by me or the Dean of Graduate Studies. It is understood that copying or publication of this work for financial gain shall not be allowed without my written permission.

Title of Thesis/Project/Extended Essay

Preparation and Properties of Electrically Conducting Copolymers Formed by Electropolymerization of Heterocyclic Compounds

Author: _____
(signature)

Eric Mackenzie Peters
(name)

April 24/87.
(date)

ABSTRACT

Various heterocyclic compounds can be electrochemically oxidized to form electrically conducting polymers. This work explores the effect of polymerizing two different heterocyclic compounds, to form a conducting copolymer.

For this study pyrrole (PY) and 2,2-bithiophene (BT) were electrochemically polymerized to form a copolymer. Various feed ratios of the two monomers were polymerized, in two different solvents, to low conversion and the polymers were analyzed for their mer ratios. The data were interpreted using the Copolymerization Equation and sets of reactivity ratios were determined for the polymers formed at two electrode potentials in each solvent system.

The oxidation potentials of the copolymers were determined through cyclic voltammetry and spectrophotometry and were found to be intermediate to those of the two parent homopolymers.

Absorption spectra in the UV-visible range were obtained. The absorption peaks of the reduced copolymers were intermediate to those of the homopolymers.

The electrical conductivity varied with the mer composition of the copolymer. The copolymers were found to have conductivities that were less than those of their parent homopolymers.

The surface structure and morphology of copolymers were examined using electron microscopy and compared to those of homopolymers.

DEDICATION

I would like to dedicate this thesis to my father, MacKenzie Peters and my grandfather, Don Skitch. Two men who have impressed me with their ingenuity and versatility over the years. From the time that I first toddled after them to the barn to stick my fingers into their work and ask questions, they have demonstrated their many skills and patience to me. Teaching me lessons, untaught and showing me love, unexpressed.

ACKNOWLEDGEMENTS

I would like to thank Dr. John Van Dyke for his assistance throughout the course of this work. The many discussions and patient direction were invaluable to the completion of this thesis.

I would also like to thank Dr. B.L. Funt for his supervision of the course of this work.

I would like to express my appreciation to Dr. Onkar S. Rajora of the S.F.U. Physics department, the late Dr. W. M. Leung the former director of Energy Mines and Resourses, Devon Coal Research Facility, Don Enns of Cantest in Vancouver, M. K. Yang of the S.F.U. Biology department and Greg Owen of the S.F.U. Chemistry department for their assistance in the analysis of the conducting copolymers.

I am also grateful to the members of the lab and my friends that assisted me during the my research, S.V. Lowen, S. Holdcroft, F. Orfino, G.H. Fritzke, R. McCloud, and A. Chan.

The assistance of the various members of the Department of Chemistry, and the technical assistance of the personnel of S.F.U.'s Glassblowing, Electronic, and Machine Shops was also appreciated.

Finally I would like to thank my wife June for her support. Without it the writing of this thesis would have been a difficult task.

TABLE OF CONTENTS

LIST OF TABLES

LIST OF FIGURES

CHAPTER I. INTRODUCTION

Section I.1 Conducting Polymers

Since 1977, increasing interest has been focused on a new class of material, doped organic polymers with high conductivities. The driving force in the development of these conductive polymers is the search for new materials which combine the light weight, toughness and resiliency, versatility in shaping, and corrosion resistance of plastics, with the conductivity of metals.

These conductive polymers can be chemically synthesized as polyacetylene [1,2], polyparaphenylene [3], or polythiophene [4] or can be electrochemically grafted on an electrode as polypyrrole [5], polythiophene [6], or polyfuran [7]. The electrochemical approach to polymerization has the advantage that the properties of the polymers can be changed by varying the electrolysis conditions (eg. electrode overpotential, current density, and electrolyte) in a controlled way, thus facilitating the study of conduction in a variety of polymers. Further encouraging features of the electrochemically prepared polymer systems are the degrees of freedom available to modify the electrical and physical properties through anion substitution [8], derivatization [9-12], copolymerization [13-17], and formation of composites with other polymers [18-21]. These attributes have encouraged researchers to believe that answers to the intractible nature of these polymers can be found.

The first conducting polymer to be electrochemically polymerized was polypyrrole (PPY)[22], but research interest in

the polymer did not build until Diaz et al. [5,23,24] successfully demonstrated electro-oxidation polymerization in acetonitrile. Other analogs of the heterocyclic pyrrole were electrochemically polymerized soon after; these include thiophene [6], azulene [25,26], furan [7], and selenophene [27]. Other electrochemically polymerized conducting polymers include six membered aromatic rings such as benzene [28] and aniline [29] and multi-ring aromatic systems such as pyrene [25,25], carbazole [25,26], indole [6], dithienothiophene [30], etc.

Of these electrochemically prepared polymers polypyrrole (PPY) and polythiophene (PT) have been examined most extensively because they were the first polymers to be investigated and they have significantly higher conductivity than most of the other electrochemically prepared polymers. Much of the physical, kinetic, and theoretical analysis of aromatic conducting polymer systems has been directed at these two polymers. Which are intractible as homopolymers. Extensive work has been aimed at preparing derivatives in order to improve their physical and mechanical properties. To date, there is only one commercial product using these polymers, an electrostatic brush in photocopiers made by the Xerox Corporation [31].

This thesis is also concerned with the modification of PPY and PT in an attempt to improve their properties, but unlike earlier attempts, copolymerization of the two polymer units is used.

Section I.2 2,2'-Bithiophene and Pyrrole

One of the most important decisions made at the beginning

of this research was the selection of monomers for copolymerization. Pyrrole (PY) and thiophene were the logical choices because they were already well researched and the N atom in the PY ring and the S atom in the thiophene ring made the analysis of the copolymer much easier than any other combination of available monomers. On the other hand, the oxidation potential of the thiophene monomer to form polymer is greater than the destructive irreversible oxidation of PPY thus thiophene could not be used. Thiophene is polymerized at potentials greater than +2.02 Volts (V)[6] vs a saturated calomel electrode (SCE), whereas PPY [32] is oxidized at potentials greater than +1.6 V and the structure of the polymer is changed. The dimer of the thiophene monomer, 2,2'-bithiophene (BT), polymerizes at potentials greater than 1.3 V [33] and poly(2,2'-bithiophene) (PBT) has similar properties to that of PT [34]. In fact, until the recent publication by J. Roncali et al. [34] the properties of PBT and PT were considered identical. As the copolymerization of BT with PY would closely model the PY-thiophene theoretical copolymer and the monomers could theoretically be polymerized together without the irreversable oxidation of the PY units in the chain, BT and PY were chosen as the monomer pair for copolymerization.

Both PY and thiophene are heterocyclic five-membered rings. When polymerized, the rings are joined at the α position and are coplanar [35]. The simple aromatic structure is in Figure I.1.a. A resonance form of the aromatic structure called the quinoid structure is given in Figure I.1.b. For PPY and PT the simple aromatic resonance structure is more stable than the quinoid structure. The difference in stability is 14.4 Kcal/mole for PPY

Figure.I.1 STRUCTURE DIAGRAMS FOR HETEROCYCLIC POLYMERS
a) Aromatic Resonance Form
b) Quinoid Resonance Form
c) Polaron Schematic
d) Bipolaron Schematic

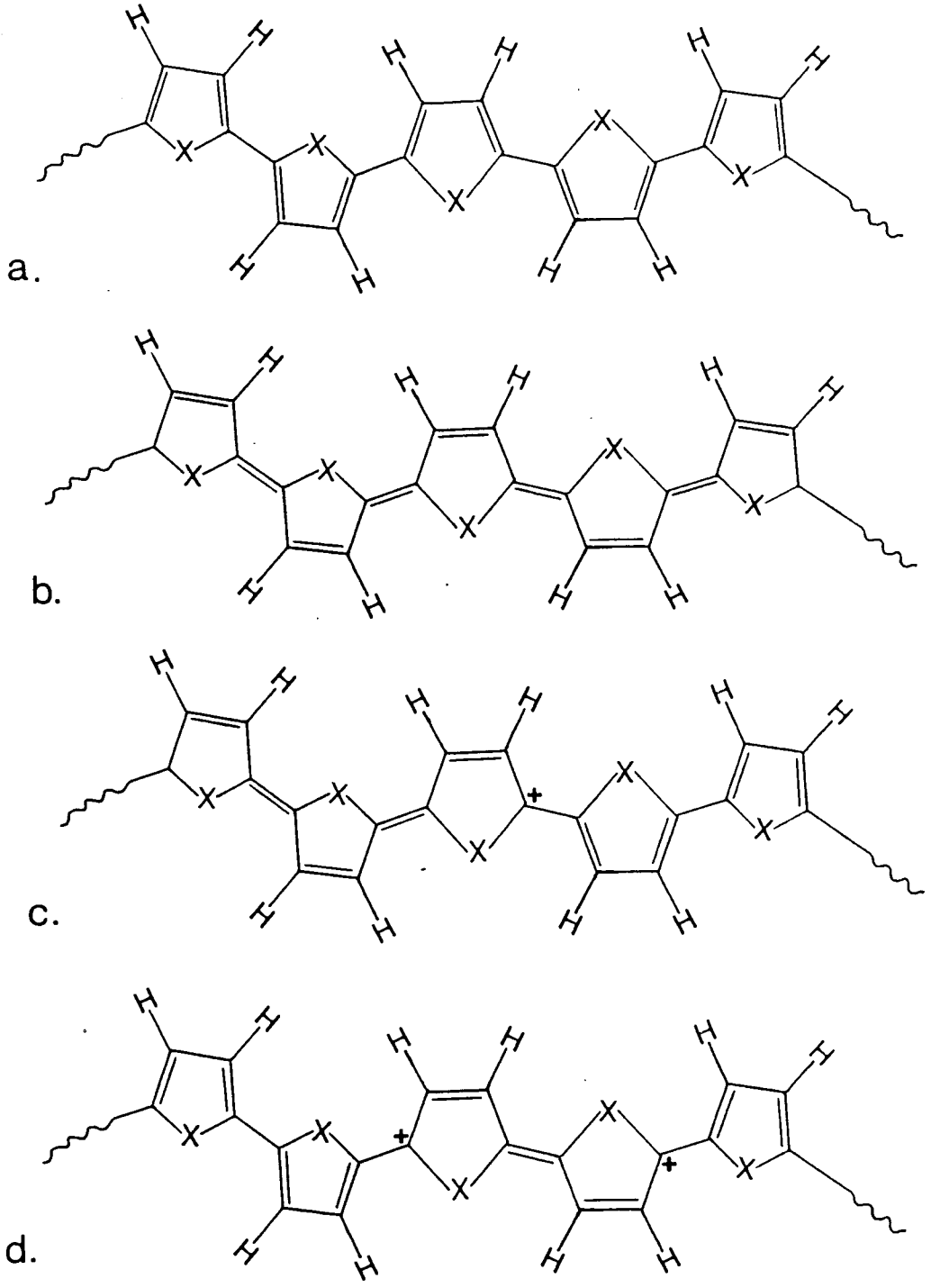

Figure.I.1

and 16.1 Kcal/mole for PT [36]. Thus the aromatic form of the polymer is favored, but there is a small amount of β-β carbon shortening indicating some exo conjugation.

When the neutral polymers are oxidized, positive charges are formed along the chain which are balanced by negative charges from doping anions. The positive charges on the polymer films create strong geometric modifications of the polymer lattice matrix. The average length of α-β carbon bonds are increased and the length of the β-β carbon bonds are shortened [36] indicating that the quinoid structure is more favored upon doping.

Section I.3 Electrical Conduction in Polypyrrole and Poly(2,2'-Bithiophene

The mechanism of electrical conduction in these organic polymers is still controversial. Conduction could result from the movement of a single positive charge (a polaron, Figure I.1.c) or a pair of positive charges (a bipolaron, Figure I.1.d) along the polymer chain. Optical and ESR [37-40] data give evidence for the formation of both polarons and bipolarons in doped conducting polymers such as PPY and PBT. The polaron state is characterized by its spin 1/2, which gives rise to an ESR signal, and by the three optical absorption peaks within the band gap [41]. The bipolaron state does not have an ESR signal as the spin state is zero; also it has only two optical absorption peaks. The absorption peak corresponding to the transitions between the bonding and antibonding polaron levels is missing.

Although both bipolarons and polarons are formed in doped

PPY and PBT, many authors [36,40,42-46,81] consider the fundamental charge carrying species to be the bipolaron. Theoretical calculations show that energy is gained if one bipolaron is formed rather than two polarons [41]. Experimental support for the bipolaron theory is that the spin concentrations in the conducting polymer can not be correlated with the conductivity of the polymer [41,47,81].

Theoretically, the polymer chain is first ionized to produce a polaron (cation-radical). The polaron is associated with the doping anion and can not contribute significantly to conduction. As the chain is oxidized further, higher concentrations of polarons are formed. Each polaron is theoretically more easily oxidized than the polymer chain itself, (to form a second polaron) and thus bipolarons (dications) are formed. Also as the concentration of polarons increase adjacent polarons interact to produce more bipolarons [45].

Recently this theoretical mechanism of conduction has been questioned. Using the theoretical energy difference between a bipolaron and two polarons, Conwell [48] calculated that the concentration of polarons in PPY at room temperature would be negligible, suggesting that the energy difference calculated was far too great. By in situ ESR-electrochemical experiments and coulometry with optics M. Nechtschein et al. [41] confirmed Conwell's calculations determining that the energy for the creation of the bipolaron is almost equivalent to that for the creation of two polarons. These results suggest that the polarons may play a role in the conduction of electricity in the polymers along with the bipolarons.

The significance of differences between interchain and intrachain electron transfer have yet to be addressed by researchers. Kaneto et al.[49] found that the electrical conductivities of PT films were highly anisotropic, having conductivities that were 0.6 S/cm parallel and 1.0×10^{-4} S/cm perpendicular to the surface of the film. Using wideangle X ray diffraction and scanning electron microscopy M. Ito et al.[50] have determined that the alignment of the polymer chains is responsible for the anisotropic conductivity. This would suggest that intrachain conduction is far easier than interchain conduction. The interchain movement of polarons (Figure I.2.a) at low doping levels would have a very large activation barrier as it would require the reorganization of the bond lengths to the end of the polymer chain [45]. The movement of bipolarons (Figure I.2.b) between the chains has a much lower activation barrier as only a small segment of the chain must be rearranged. Recently S. Tasaka et al. [51] have developed techniques using Langmuir-Blodgett films to model these conducting polymer films and examine inter vs intra chain conduction. As the mechanism of conduction is still unclear there is much work to be done using these types of modelling to reveal the microscale conductivity of the polymers.

Section I.4 Electrochemical Polymerization of Polypyrrole and Poly(2,2'-bithiophene)

Conventional electrochemical polymerization begins with the oxidation or reduction of a monomer or an initiator at an electrode to form an anion, cation or radical, followed by

Figure.I.2 INTER CHAIN MOVEMENT OF CHARGE CONDUCTION SPECIES
a) Transfer of a Polaron between Polymer Chains
b) Transfer of a Bipolaron between Polymer Chains

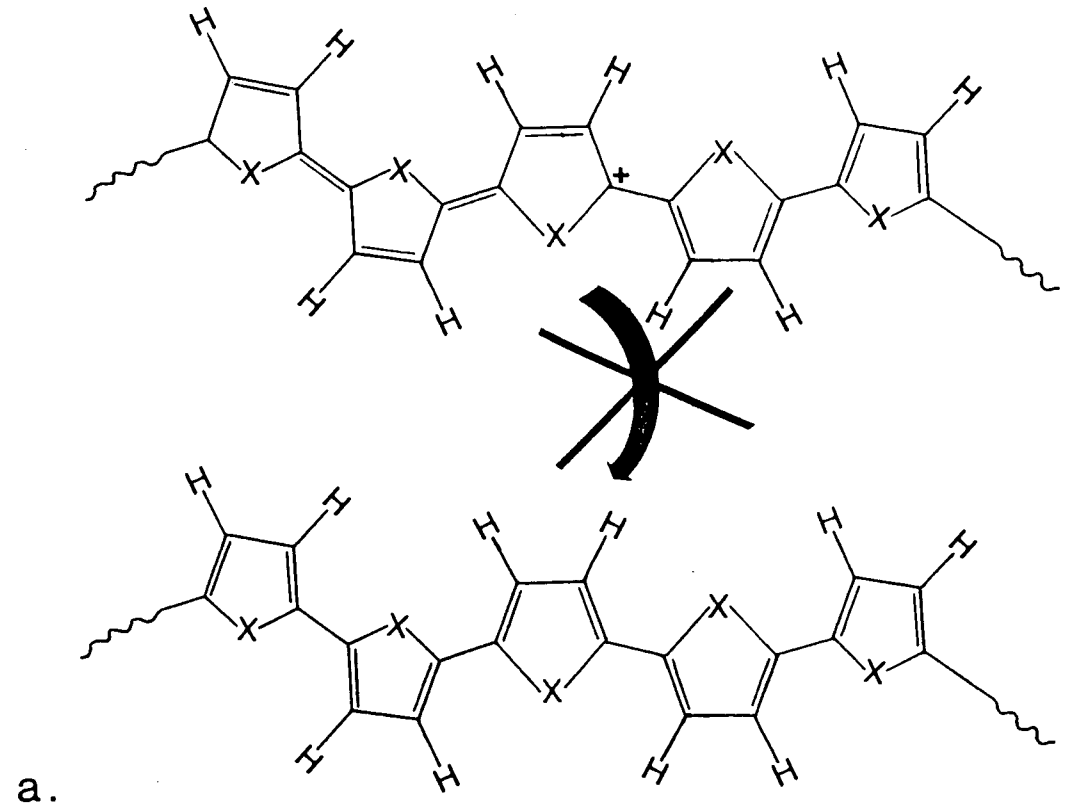

a.

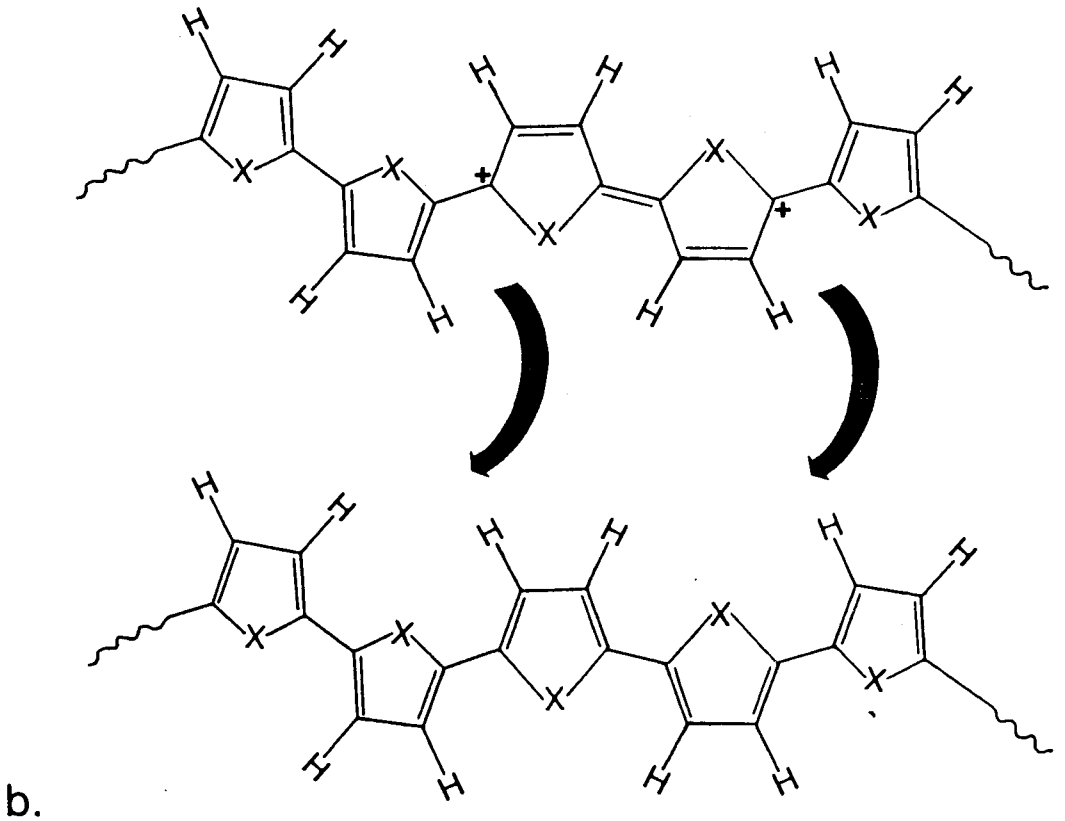

b.

Figure.I.2

anionic, cationic or free radical chain polymerization in solution. Electrochemical polymerization of BT and PY does not follow this normal mechanism. The reaction mechanism proposed by E.M. Genies et al. [52] (Figure I.3) indicates that the monomer and the polymer are oxidized at the electrode in step I. In this step the heterocyclic ring of the monomer or polymer loses an electron to the electrode to form a highly reactive radical-cation. In step II two radical-cations combine to form a dication dimer or polymer and in step III two hydrogen ions are expelled from the polymer. The polymer chain must be oxidized by the electrode again for addition of more monomer units to the chain. The solubility of the polymer chains decrease rapidly with increasing chain length in all solvents so that essentially all the polymer is formed on the electrode.

The polymer films are formed in their oxidized state and are doped with the anion of the electrolyte. The anion can be removed from the film by applying a negative potential on the electrode and reducing the film. Electrodes in their reduced (or neutral) form can be reoxidized using the same or another anion, chemically or electrochemically. Chemical reduction of an oxidized films is also possible.

PPY and PBT have been doped with a variety of electron acceptors [53] including ClO_4^-, BF_4^-, AsF_5^-, and I^-, but not successfully with electron donors [36]. Other conducting polymers such as polyparaphenylene and polyacetylene can be doped with electron donors (Li and Na) or electron acceptors to yield highly conductive complexes.

Figure.I.3 REACTION MECHANISM FOR ELECTROPOLYMERIZATION OF HETEROCYCLIC POLYMERS

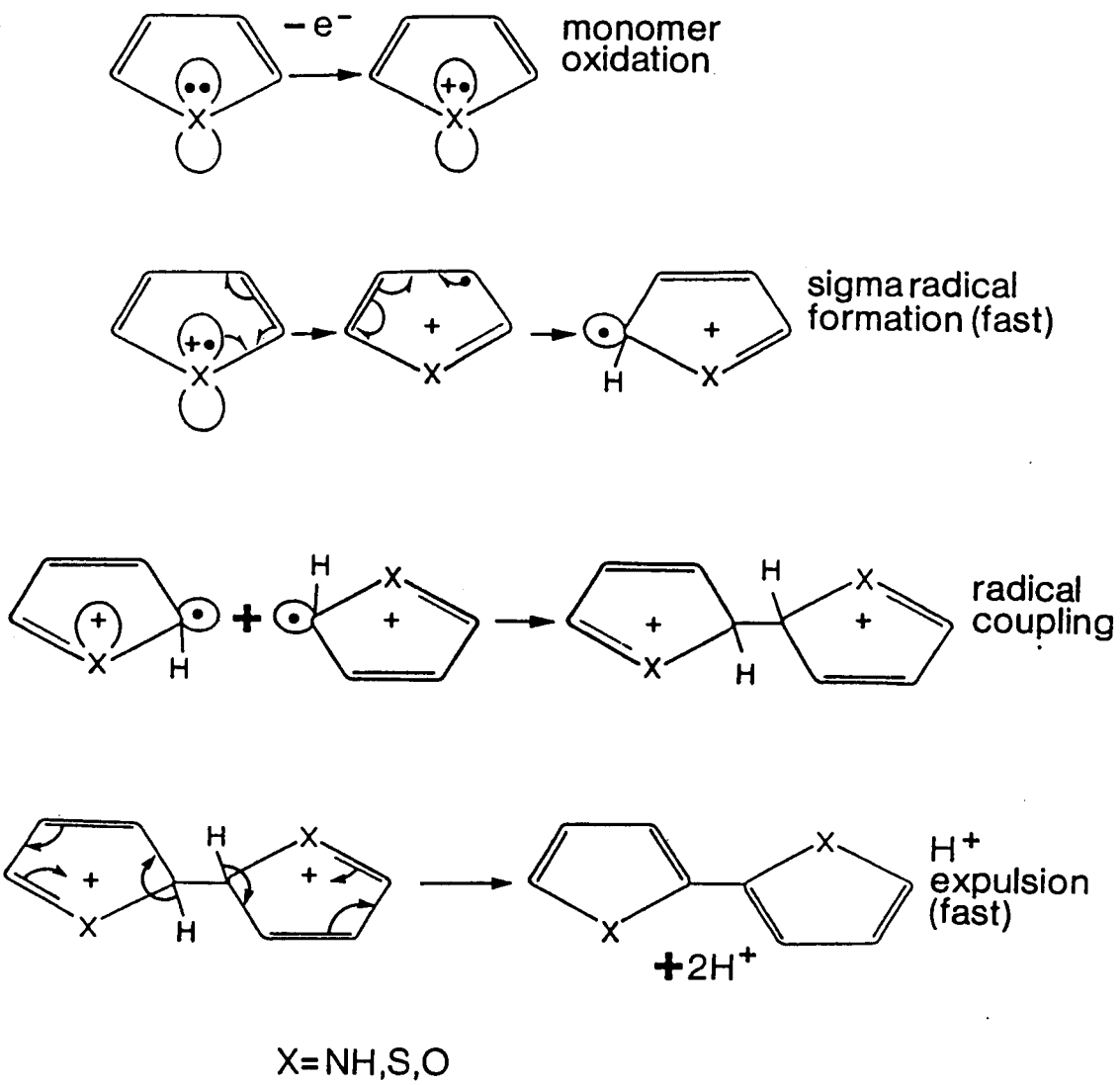
−e⁻
monomer oxidation
sigma radical formation (fast)
radical coupling
H⁺ expulsion (fast)
+2H⁺
X=NH,S,O

Figure.I.3

Section I.5 Conducting Copolymers, Composites and Derivatives.

Many of the plastics, synthetic fibers and rubbers used forty years ago were made of a single homopolymer. Improvements in the resiliency, strength, and resistance to degradation by radiation, heat, and chemicals of these materials over the last forty years are primarily due to the modification of these homopolymers by blending with different polymers, stablizers, inhibitors and other additives and by copolymerizing the homopolymers with other polymers. Conducting polymers are still primarily in the simple homopolymer stage of their development. To improve their intractable nature conducting homopolymers will probably need to be modified as was the case with the synthetic materials created forty years ago.

Some conducting homopolymers have been processed from liquid AsF_3 [54,55] and liquid I_2 [56], but these procedures suffer from industrial impracticability due to the corrosive and toxic natures of the solvents used. The procedures reportedly did not improve the poor physical and mechanical properties of the conductive polymers. The extended π bonding of these polymers should limit the flexibility of the polymer chain; thus the polymers will be copolymerized, derivatized or made into composites with other non conducting polymers, to provide the resiliency and flexibility needed for the envisioned applications.

Recently efforts to modify the physical properties of PPY and PT through forming composites with other polymers [57], copolymerization [58] and derivatization [51,16] have shown that remarkable improvements are possible using these techniques.

PPY has been used to form conducting composites with, latexes [57], polyvinylalcohol (PVA) [60,61], polyvinylchloride [21,20,62], and polyacetylene [18]. PBT was polymerized within a tetrahydrofuran polymer [76]. Methylthiophene (MeT) and polymethylmethacrylate (PMMA) [63], were electropolymerized together to form a conducting composite. In most cases mechanical properties of the films were improved slightly but the conductivities were less than that of PPY or poly(3-methylthiophene) alone. All of these syntheses except reference 11 and 3 require two steps involving a preliminary step of coating the electrode or substratum with the nonconductive polymer, followed by electropolymerization or chemical polymerization [60] of the conducting polymer within the coated polymer's matrix. Obviously a limited amount of polymer can be produced by these methods as the thickness of the film is limited by the monomer's ability to diffuse through the nonconducting film.

S.J. Jasne et al.[57] and J. Roncali et al. [63] have recently formed conducting composite films by electropolymerization of solutions containing monomer and nonconducting polymer chains. S.J. Jasne et al. polymerized pyrrole in latex and water solutions. The films produced are fully processable because the major component of each film's composition is a thermoplastic and/or soluble latex polymer. The conductivity of these films range from 10^{-3} to 5 S/cm and appears to be uniform throughout the films. Roncali et al. polymerized 3-methylthiophene in the presence of poly(methyl-

methacrylate) in a 50/50 methylene chloride/ nitrobenzene solvent mixture. The preliminary report indicated that the mechanical properties of the composite were superior to the homopolymers but did not mention anything about attempts to dissolve or melt the composite films. The composite films gave conductivities ranging from 0.1 to 30 S/cm. The thickness of these composite films is not limited by the porosity of the nonconducting component; therefore this technique shows the potential for use in many applications.

Derivatives of PPY and PT can take two different forms: polymers from substituted rings of pyrrole or thiophene, or polymers doped with large anion groups which change the polymer's structure. Most of the substituted monomers are copolymerized together with other monomers; therefore this type of derivatization will be reviewed with the other forms of copolymers. This section will concentrate on anion substitution in the homopolymers.

Researchers initially investigated doping of PPY and PT films with the goal of improving the conductivity and anion switching time. Thus, relatively small organically soluble anions such as ClO_4^-, BF_4^-, PF_6^-, and $CF_3SO_3^-$ [10] were used as dopants. Later researchers found that larger anions such as the glutamatic acid anion [64,68] or ferrocyanide [65] could be incorporated as dopants.

Recently electroactive polymers such as potassium poly(vinylsulfate) and sodium poly(styrenesulfonate) have been used as dopants for the polymerization of PPY [59]. These polymeric dopants improve the mechanical properties of the PPY

film increasing the tensile strength 2-5 times. The conductivity of these polymer-doped films is high, but very little of the polymeric dopant can be removed from the film (i.e. less than 2% is released from the films), thus, normal electrochromic switching of the film is not observed [59]. Incomplete undoping of the polymeric dopants implies there is a tight network of PPY intertwined with the polymeric dopant in these films.

Large polymeric dopants such as those mentioned above may overcome the physical and mechanical properties of these polymers, but the film's inability to oxidize and reduce may limit their applications.

Copolymers in general exhibit physical and mechanical properties different from those of either parent homopolymer or the composite of the parent homopolymers. Copolymerization modifies the symmetry of the polymer chain and modulates intramolecular and intermolecular forces [67], so properties such as melting point, glass temperature, crystallinity, solubility, elasticity, permeability, and chemical reactivity can be varied within wide limits. Many of these properties can not even be significantly altered by composite blending; thus copolymerization can be a much more powerful technique for the modification of conducting polymers than the two methods mentioned before.

Copolymerization can be defined as polymerization in which two or more structurally distinct monomers are incorporated into the same polymer chain. The sequence in which these monomer units are polymerized into the chain is not defined. Thus there

are four distinct copolymer types: statistical or random copolymers, alternating copolymers, block copolymers and graft copolymers. Three of the four types of conducting copolymers have been polymerized using common techniques ie. block, random and graft. Alternating polymers have been electropolymerized using dimers and trimers containing two different monomer rings [71,72].

In statistical (random) copolymers the comonomers appear in irregular, unspecified sequences along the polymer chain. For example monomers A and B give:

A + B ---------> BAAABBABBABABABBBBA

For graft copolymers, chains of one comononmer are pendant from a backbone of the other. For example:

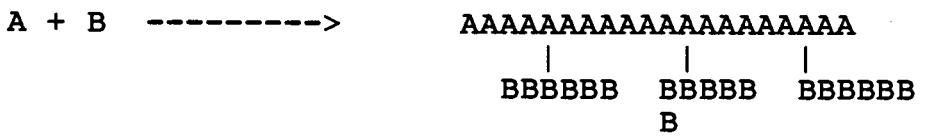

For block copolymers, chains of one comonomer are joined to chains of the other. For example:

A + B ---------> AAAAABBBBBAAAAABBBBB

For alternating copolymers, the comonomers add in an alternating sequence along the polymer chain. For example:

A + B ----------> ABABABABABABABABABA

For conducting polymers the synthesis of graft copolymers is significantly different than statistical or block copolymers. Graft copolymers are polymerized chemically while most statistical or block copolymers are polymerized electrochemically. Graft and statistical copolymerization represent two distinctly different methods for the modification

of the physical properties of conducting polymers.

The first random copolymerization of conducting polymers was the copolymerization of pyrrole with its derivative, 3-methylpyrrole [14,66]. The copolymerization did not significantly change the mechanical properties of the conducting polymers, as mechanical properties of the homopolymers are similar, but modification of the conductivity, chemical reactivity and electromagnetic spectra were observed. Since these first attempts at random copolymerization of conducting polymers, two important areas of copolymerization research have emerged. These are the uses of copolymerization a) to enhance the mechanical properties and improve processability and b) to modify the chemical reactivity and physical properties.

Soluble processable conducting polymers have been formed from substituted thiophenes. R.L. Blankespoor and L.L. Miller [68] have formed a soluble polymer by electropolymerizing 3-methoxythiophene, and M. Sato et al. [69] have electropolymerized 3-alkylthiophenes with large alkyl substituent groups (> pentyl) to form highly conducting soluble polymers (95-11 S cm^{-1}).

R. L. Elsenbaumer et al. [58] chemically polymerized a series of poly(3-alkylthiophenes) to compare the solubility and conductivity of the polymer vs. the chain length of the alkyl groups. Elsenbaumer found that the solubility increases with increasing chain length of the alkyl substituent (ie. n-butyl > ethyl >> methyl) while the conductivity changes only slightly (3-4 S cm^{-1}).

Recently Elsenbaumer found that copolymerized 3-alkylthiophenes had greater conductivity than their corresponding homopolymers (10-50 S cm^{-1}) [70]. Copolymerization also increased the molecular weight of the polymer chains and improved the mechanical properties of the films formed. It is thought that copolymerization helps to relieve the steric interactions between the substituent alkyl groups, during polymerization, and in the copolymer chain, resulting in the increased chain length and improved film-forming properties [70].

These improvements in the physical properties of soluble conducting polymers by copolymerization may mean that copolymerization will be an important process in further improvements in the polymers.

Copolymerization of conducting polymers for the modification of chemical reactivity has taken many different forms. M.S. Wrighton et al.[17] copolymerized pyrrole and N-(3-trimethyl - oxysily)-propyl)pyrrole, to improve the adhesion of the PPY to the surface of an n-type Si, for protection of the semiconductor against photocorrosion. O.Inganas et al.[71], S. Naitoh et al.[72], and we [73] have polymerized pyrrole, thiophene and their dimers and trimers to modify the oxidation potential, colour and other physical and chemical properties from that of the two homopolymers. Pyrrole and thiophene have been copolymerized with other conducting [13-15,74,75] and nonconducting [77] polymers to produce similar modifications. Results from S. Naitoh and this thesis have shown the most significant modification of the oxidation potential and other

physical parameters by copolymerization.

Pyrrole and thiophene were chosen as monomers by this and other research groups [71,72,78,80] for copolymerization, for a variety of factors including : ease of analysis, separation of homopolymer oxidation potentials, and characterization done on the homopolymers. Thus pyrrole and thiophene are ideal model monomers for the study of conducting polymer copolymerization reactivity ratios and compositional effects, the main research thrust of this thesis. Control of copolymer composition shown by this research will be an important factor in the application of these processable conducting polymers to commercial needs.

Block copolymers can easily be electropolymerized (see Section V.3.3). Thin layers of different polymers can be polymerized on an electrode by simply moving the electrode between two monomer solutions and applying a potential on the electrode for a short time. Unfortunately these copolymers are of little interest as the physical properties of the copolymer change little from those of the constituent homopolymers.

A.I. Nazzal and G.B. Street [79] grafted PPY onto polystyrene by copolymerizing styrene and 4-chloromethylstyrene, attaching pyrrole groups to the pendant methyl group and electrochemically grafting PPY onto the attached pyrrole. The films produced by this method exhibited electrical conductivities comparable to that of polypyrrole. Unfortunately the copolymerization did not seem to improve the solubility, processability or mechanical properties greatly from those of PPY.

Commercial applications for conducting polymers will soon be a reality with the improvement and implementation of some of the polymerization techniques reviewed here. Copolymerization and control of the copolymer's composition will be an important factor in this success. Techniques outlined in this thesis should provide this control.

CHAPTER II DETERMINATION OF COPOLYMER COMPOSITION

Section II.1 Copolymerization Theory

As mentioned in the preceding section, copolymerization can be defined as polymerization in which two or more structurally distinct monomers are incorporated into the same polymer chain. If two monomers are polymerized in the same reaction mixture, one expects to obtain a copolymer. This copolymer will not normally contain monomer units in the same ratio as the reaction mixture, because the reactivities of the two monomers are generally different. As the reaction mixture is a two component system the relative reactivity of each monomer must be defined in terms of its reactivity to the other monomer and to itself, a reactivity ratio.

Normally the copolymerization of two monomers, M_1 and M_2, can be thought of as four separate reactions:

$$R\text{----}M_1^* + M_1 \xrightarrow{k_{11}} R\text{----}M_1M_1^* \quad \text{rate} = k_{11}[M_1^*][M_1] \quad [2.1]$$

$$R\text{----}M_1^* + M_2 \xrightarrow{k_{12}} R\text{----}M_1M_2^* \quad \text{rate} = k_{12}[M_1^*][M_2] \quad [2.2]$$

$$R\text{----}M_2^* + M_1 \xrightarrow{k_{21}} R\text{----}M_2M_1^* \quad \text{rate} = k_{21}[M_2^*][M_1] \quad [2.3]$$

$$R\text{----}M_2^* + M_2 \xrightarrow{k_{22}} R\text{----}M_2M_2^* \quad \text{rate} = k_{22}[M_2^*][M_2] \quad [2.4]$$

M_1^* and M_2^* represent the active centers at the end of a propagating polymer chain [83]. These propagating species are normally radicals, anions, cations or carbocations. k_{11} is the rate constant for a propagating chain ending in M_1 adding to the monomer M_1 as given in the rate equation 2.1, k_{12} is the rate constant for equation 2.2 and so on.

Monomer M_1 disappears from the monomer mixture by reaction schemes 2.1 and 2.3, while monomer M_2 disappears by reaction schemes 2.2 and 2.4. The rates of consumption of the two monomers, which are equal to their rates of incorporation into the copolymer, are given by the equations;

$$\frac{-d[M_1]}{dt} = k_{11}[M_1^*][M_1] + k_{21}[M_2^*][M_1] \qquad [2.5]$$

$$\frac{-d[M_2]}{dt} = k_{12}[M_1^*][M_2] + k_{22}[M_2^*][M_2] \qquad [2.6]$$

Although these rates $-d[M_1]/dt$ and $-d[M_2]/dt$ can be determined by analysis of the reaction mixture, it is more informative to consider the ratio $d[M_1]/d[M_2]$, because the rate constants k_1 and k_2 of the parent homopolymers are not identical to constants k_{11} and k_{22} due to the possible interactions of the two monomers in solution. The behavior of the monomers in homopolymerization does not give direct information about their behavior in copolymerization. Dividing equation 2.5 by equation 2.6 gives;

$$\frac{d[M_1]}{d[M_2]} = \frac{k_{11}[M_1^*][M_1] + k_{21}[M_2^*][M_1]}{k_{12}[M_1^*][M_1] + k_{22}[M_2^*][M_1]} \qquad [2.7]$$

For a steady-state condition for M_1^* and M_2^*;

$$k_{21}[M_2^*][M_1] = k_{12}[M_1^*][M_2] \qquad [2.8]$$

on elimination of the active center concentrations ($[M_1^*]$ and $[M_2^*]$) from equation 2.7, the copolymer composition is obtained as;

$$\frac{d[M_1]}{d[M_2]} = \frac{[M_1]}{[M_2]} * \frac{r_1[M_1] + [M_2]}{[M_1] + r_2[M_2]} \qquad [2.9]$$

where r_1 and r_2 are "reactivity ratios" defined as;

$$r_1 = k_{11}/k_{12} \text{ and } r_2 = k_{22}/k_{21}$$

Equation 2.9 is the standard equation used to interpret of chain-growth copolymerization and has been used to correlate most of the copolymerization data. Although the equation was published independently and in the same year by three separate research groups namely, Alfrey and Goldfinger [84], Mayo and Lewis [85] and Wall [86], it is commonly called the Mayo-Lewis Equation [87].

In oxidative electropolymerization PY and BT do not polymerize by chain-growth polymerization but radical-cation coupling. The various steps in the copolymerization of these polymers are considered as follows:

Stage 1 - Oxidation of the monomers

$$M_1 \xrightarrow{k_a} M_1^{+\cdot} \qquad [2.10]$$

$$M_2 \xrightarrow{k_b} M_2^{+\cdot} \qquad [2.11]$$

Stage 2 - Coupling of radical cations

$$R\text{----}M_1^{+\cdot} + M_1^{+\cdot} \xrightarrow{k_{11}} R\text{----}M_1^{+}M_1^{+} \qquad [2.12]$$

$$R\text{----}M_1^{+\cdot} + M_2^{+\cdot} \xrightarrow{k_{12}} R\text{----}M_1^{+}M_2^{+} \qquad [2.13]$$

$$R\text{----}M_2^{+\cdot} + M_1^{+\cdot} \xrightarrow{k_{21}} R\text{----}M_2^{+}M_1^{+} \qquad [2.14]$$

$$R\text{----}M_2^{+\cdot} + M_2^{+\cdot} \xrightarrow{k_{22}} R\text{----}M_2^{+}M_2^{+} \qquad [2.15]$$

Stage 3 - Proton expulsion

$$R\text{----}M_1^{+}M_1^{+} \xrightarrow{k_{aa}} R\text{----}M_1M_1 + 2H^{+} \qquad [2.16]$$

$$R\text{----}M_1^{+}M_2^{+} \xrightarrow{k_{ab}} R\text{----}M_1M_2 + 2H^{+} \qquad [2.17]$$

$$R\text{----}M_2^{+}M_1^{+} \xrightarrow{k_{ba}} R\text{----}M_2M_1 + 2H^{+} \qquad [2.18]$$

$$R\text{----}M_2^{+}M_2^{+} \xrightarrow{k_{bb}} R\text{----}M_2M_2 + 2H^{+} \qquad [2.19]$$

Reactions 2.10 and 2.11 correspond to the oxidation of the monomers to form radical cations. These then couple with oxidized polymer in reactions 2.12-2.15. The protons are expelled in the reactions 2.16-2.19 and the process repeated. This reaction scheme is modelled on the mechanism proposed by Diaz [52] and previously adopted by our research group for homopolymerization [33].

If stage 1 is rate controlling then reactions 2.10 and 2.11 will determine the ratio of the monomers oxidized initially. The ratio of oxidized monomers $[M_1^{+\cdot}]/[M_2^{+\cdot}]$ will depend not only on how much the over potential exceeds the oxidation potential, but also on the concentration of the monomer. The results will fit the Mayo-Lewis Equation, but the incorporation of the monomers would not be due to any selectivity in the reactivity of the monomers, as in equation 2.12-2.15 (see Appendex I).

If stage 2 is the rate controlling stage, then these reactions (equations 2.12 - 2.15) will determine the composition of the over all product. Direct application of the Mayo-Lewis Equation to the equations in stage 2 will provide meaningful information about the selectivity and reactivity of the monomers, even though the Mayo-Lewis Equation has only previously been applied to chain growth polymerization.

If stage 3 is the rate controlling stage then the ratios must be understood in terms of the relative rates of proton expulsion. The rates of proton expulsion could be fit to the Mayo-Lewis Equation if the positive charges were confined

exclusively to the coupled cations at the end of the chain. However the charges are more likely to be spread along the chain as in the case of the homopolymers (Fig I.1). Since the stability of the cation will be affected not only by the mer units (M_1 & M_2), as shown in equations 2.16-2.19, but also by the several units that were added previously, any selectivity in the addition of monomers would be difficult to explain using stage 3 as the rate limiting step. Recent evidence in our Labs using deuterium isotopes suggests that proton expulsion is not rate determining.

The Mayo-Lewis Equation was derived from the simple copolymerization equations 2.1-2.4 [84-86]. These equations were formulated with the assumption that the rate of addition of monomer to a free growing active center depends only on the nature of the active center [90]. This assumption is violated for polymerization mechanisms other than chain addition, as they have more than one active center, and for polymerization of monomers which are highly polar or sterically hindered, as the monomers affect the nature of the addition reaction. The original derivations of the Mayo-Lewis Equation also required the assumption that a steady state of active centers (M^*) was established. It is difficult to make this assumption when, as in this case, formation of polymer does not require an active center, but like step-growth polymerization can grow by joining oligmeric groups. The size of such groups is limited only by their solubility in the polymerizing solvent. To accommodate for the violation of the assumption of the steady state

approximation and to extend the Mayo-Lewis Equation to more than two monomers, new derivations were formulated.

One alternative derivation of the Mayo-Lewis Equation which does not follow Dostal's [90] assumptions and does not require the steady state assumption, uses probability equations instead [88,89]. For example the probability of the addition of a monomer M_1 to a polymer chain with an active center M_1^* is given by;

$$p_{11} = \frac{k_{11}[M_1^*][M_1]}{k_{11}[M_1^*][M_1] + k_{12}[M_1^*][M_2]} = \frac{r_1[M_1]}{r_1[M_1] + [M_2]}$$

$$= 1 - p_{12} \qquad [2.20]$$

Similarly the probabilities for the other three possible combinations are;

$$p_{12} = \frac{[M_2]}{r_1[M_1] + [M_2]} = 1 - p_{11} \qquad [2.21]$$

$$p_{22} = \frac{r_1[M_2]}{r_2[M_2] + [M_1]} = 1 - p_{21} \qquad [2.22]$$

$$p_{21} = \frac{[M_1]}{r_2[M_2] + [M_1]} = 1 - p_{22} \qquad [2.23]$$

For M_1 the probability of finding a sequence of n mer units in length is;

$$p_1 = p_{11}^{n-1}\, p_{12} \qquad [2.24]$$

From this the "weight" fraction of all M_1 in the copolymer is shown to be;

$$W_1 = \frac{p_{12}}{p_{11}} \qquad n\, p_{11}^{n} = \frac{1}{p_{12}} \qquad [2.25]$$

Similarly the "weight" fraction of M_2 sequences is;

$$W_2 = \frac{1}{p_{21}} \qquad [2.26]$$

The molecular composition of the copolymer $d[M_1]/d[M_2]$ is equal to the ratios of the "weight" fractions of the respective sequences of M_1 and M_2;

$$\frac{d[M_1]}{d[M_2]} = \frac{1/p_{12}}{1/p_{21}} = \frac{r_1[M_1]+[M_2]}{[M_2]} * \frac{[M_1]}{r_2[M_2]+[M_1]}$$

$$= \frac{[M_1]}{[M_1]} * \frac{r_1[M_1]+[M_2]}{[M_1]+r_2[M_2]} = [2.9] \qquad [2.27]$$

which is the Mayo-Lewis Equation. Thus the steady state assumption and Dostal equations are not required in the derivation of the Mayo-Lewis Equation.

Graphical presentation of the dependence of copolymer composition on monomer-feed composition was first reported by Wall [86]. The molar ratio for the mer units in the copolymer, $d[M_1]/d[M_2]$, is plotted against the molar ratio for the monomers in the reaction mixture, as in Figure II.1. The characteristic curve is completely analogous to the curve obtained for the distillation of binary systems. The reactivity ratios, calculated using the Mayo-Lewis Equation, define the shape of this curve. For example:

If $r_1=r_2=1$ then neither active center shows any selectivity in adding monomer, and the monomer enters the copolymer in amounts determined only by their relative concentrations in the monomer feed. The graphical representation is shown as the diagonal line A in Figure II.2.

If $r_1 r_2 = 1$ then both active centers show the same preference for

addition to one of the two monomers, so that the copolymer is always richer in the one monomer than the monomer feed mixture. This is a special case of the more general class for which $r_1 > 1$ and $r_2 < 1$ (Figure II.2, line C) and is often called ideal copolymerization. This is shown as line B in Figure II.2.

Figure.II.1 TYPICAL COPOLYMER COMPOSITION CURVE

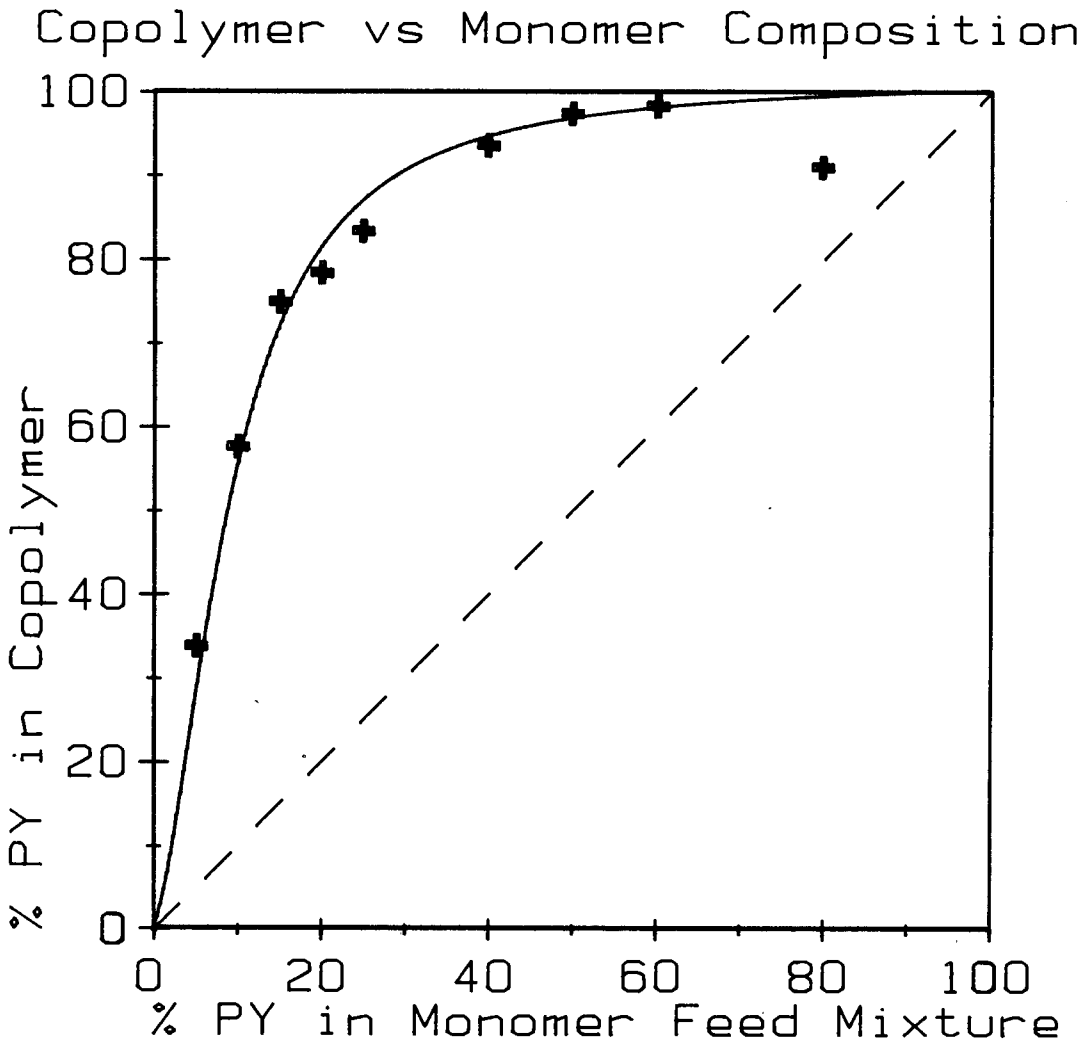
Copolymer vs Monomer Composition
100
80
60
40
20
0
% PY in Copolymer
0
20
40
60
80
100
% PY in Monomer Feed Mixture

Figure.II.1

If $r_1 = r_2 = 0$ then each active center adds exclusively to the other monomer forming an alternating polymer of 1:1 composition regardless of the monomer feed composition. This is graphically represented as line D of Figure II.2.

As different values for the reactivity ratios give significantly different shapes for the curves, their values can be roughly estimated from these plots. To approximate the parameters more precisely, one of the several procedures developed from the Mayo-Lewis Equation must be used. The three simplest procedures used are, "Fineman and Ross", "Jaacks" and "Mayo and Lewis" [91]. These are arithmetically correct, but if the uncertainties are large, defining the reactivity ratio values can be difficult. More complex methods of estimation, which require extensive computer calculations [92-95], fit better reactivity ratios to the data than can be obtained using the three methods mentioned above. These computer estimations account for uncertainties and numerically fit the best reactivity ratios to the data.

These computer defined reactivity ratios are not required for this work as we are only demonstrating proof of concept; thus the copolymer reactivity ratios will not be used to predict copolymer composition. Therefore, for this analysis a modified "Fineman and Ross" (F&R) procedure will be used because of its simplicity.

Figure.II.2 COMPOSITION CURVES FOR VARIOUS REACTIVITY RATIOS
A) $r_1 = r_2 = 1$
B) $r_1 r_2 = 1$
C) $r_1 > 1$, $r_2 < 1$
D) $r_1 = r_2 = 0$

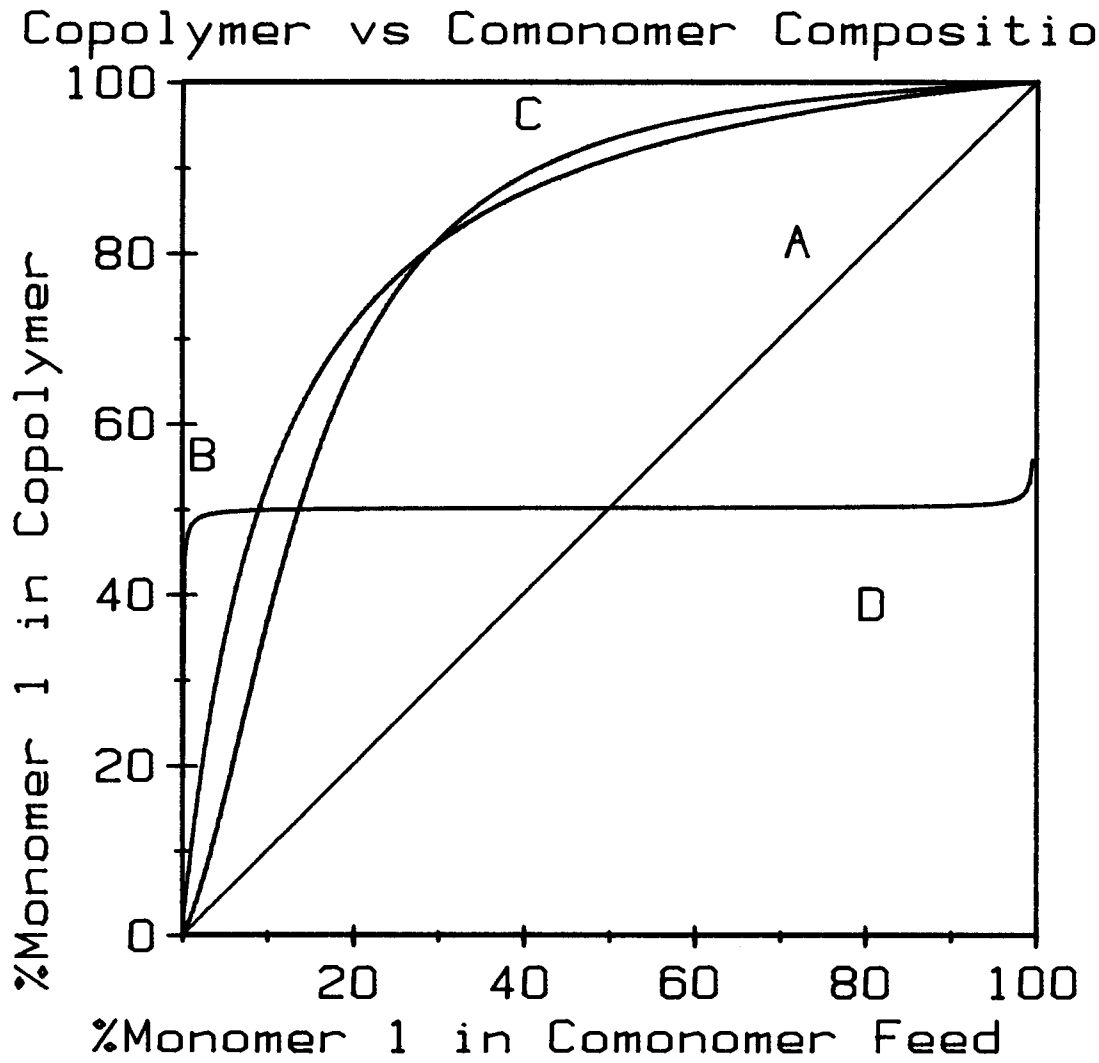
Copolymer vs Comonomer Composition
100
80
60
40
20
0
%Monomer 1 in Copolymer
A
B
C
D
20
40
60
80
100
%Monomer 1 in Comonomer Feed

Figure.II.2

Section II.2 Experimental

II.2.1 Purifications

For these experiments two solvents were used, acetonitrile (ACN) and propylene carbonate (PC). ACN (reagent grade) was dried by refluxing with CaH_2, then distilled and stored over a molecular sieve in a N_2 atmosphere. PC (reagent grade) was also dried by refluxing with CaH_2 but was distilled in a spinning band column of ca. 100 theoretical plates. PC was also stored over a molecular sieve in a N_2 atmosphere. Solvent purities were checked using gas chromatography (5890A Hewlett Packard).

2,2'-Bithiophene (BT) was obtained from two different sources, Aldrich Chemicals and Kodak Chemicals. BT (Aldrich) was decolourized with activated charcoal, recrystallized three times and then sublimed to form white crystals with a melting point 32.5 C. BT (Kodak) needed only to be sublimed once to form white crystals of equivalent purity.

Pyrrole was distilled in a spinning band column of ca. 100 theoretical plates. The distillate was dried by refluxing with CaH_2 and stored over molecular sieves in a N_2 atmosphere.

Tetrabutylammonium perchlorate (TBAP) (Polarographic grade, G.F. Smith) and lithium perchlorate ($LiClO_4$) (Alfa Inorganics) were dried under reduced pressure.

II.2.2 Apparatus

Two identical H type cells were constructed from "Pyrex" glass (Figure.II.3). The two compartments of the cells were separated by fritted glass disks of medium porosity. Each compartment had a volume of approximately 30 ml. The caps on the cells were constructed from Teflon and all the large outlets to

Figure.II.3 DIAGRAM OF POLYMERIZATION CELL

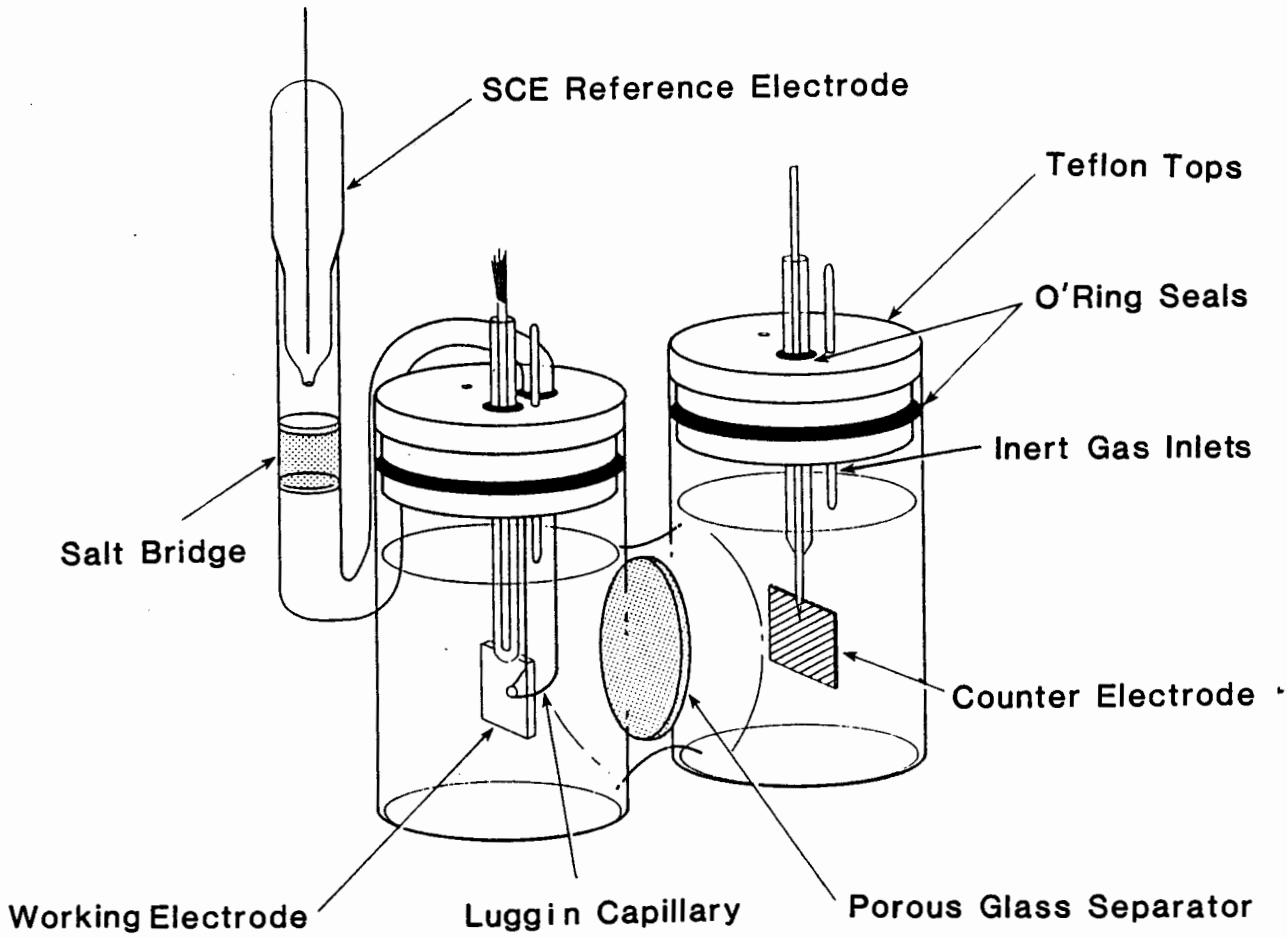
SCE Reference Electrode
Teflon Tops
O'Ring Seals
Inert Gas Inlets
Salt Bridge
Counter Electrode
Working Electrode
Luggin Capillary
Porous Glass Separator

Figure.II.3

the cells were sealed with silicone rubber O rings. The small outlets for the Teflon tubing of the gas purge lines did not require seals.

The cell was fitted with a saturated calomel reference electrode (SCE) (Fisher Scientific). The SCE was separated from the working compartment by a Luggin capillary and a KCl salt bridge.

The counter electrodes were constructed from Pt. An approximately 4 cm^2 piece of thin Pt sheet were spot welded to a Pt wire. The Pt wires were soldered to nickel wires with silver solder. The wires were sealed within 4 mm diameter "Pyrex" glass tubes by melting the glass with a torch so that it joined onto the Pt wires.

The working electrodes were constructed from sheets of Sb-doped SnO_2-coated conducting glass. The glass was cut into 1.5 cm by 2.0 cm pieces using a diamond knife. Wires were connected to the pieces of glass by spotting the edges of the glass with an amalgam of In-Ga (for improved conduction through the SnO_2 interface) and then gluing the wires over the spots with conducting silver dag (Achenson). Adhesion of the wires to the electrodes was improved through the coating of the silver dag with 48 hour epoxy (Conap Easypoxi). The wires were covered with 4 mm diameter "Pyrex" glass tubing and the tubing was sealed to the electrodes with the Conap epoxy.

A small, Teflon, magnetic, stir bar was used to agitate the polymerization solution in the working compartment. The stir bar was spun at a constant rate by a magnet attached to an electric motor. The rate of rotation of the stir bar was checked during

each polymerization with a Cole-Palmer strobe light.

II.2.3 Polymerization

Before polymerization each part of the cell was carefully washed and dried in an oven at 90°C for 4 hrs to remove water from the surface of the cell. The cells were flushed with Ar before being charged with 50 ml of monomer solution. The monomer solutions contained varying concentrations of the two monomers BT and PY in 0.1 M TBAP/ACN or 0.1M $LiClO_4$/PC electrolyte solvent mixtures. The monomer solutions were bubbled with Ar before polymerization to remove any O_2 that might remain in solution. An Ar atmosphere was maintained throughout the reaction and the solutions were stirred at a constant rate, to minimize the effects of localized depletion of the monomers.

The working electrode potential was maintained at a selected value by a potentiostat (SFU electronic shop construction) and monitored using a Fluke 8840A multimeter. The charge transferred was recorded using an Electrosynthesis # 640 coulometer and monitored by recording the current vs time on a Cole-Palmer chart recorder. The polymerizations were conducted in the range where BT can be oxidized ($\geq$ 1.3 V) and below the potentials where irrevesible oxidation of pyrrole may occur ($\geq$ 1.6 V) (1).

The polymerizations were confined to < 10 % conversion of the monomer to polymer. After the reaction, all samples were washed with clean solvent, to remove electrolyte from surface and dried under reduced pressure (0.15 mm Hg) for 24 hours. Samples from the PC solvent polymerizations were dried an additional 24 hours in a vacuum oven at 0.20 mm Hg and 90°C.

Counter electrodes from the polymerizations in PC were removed from the cell after polymerization and washed with water. Li metal which had plated onto the electrode reacted with the water. As Li will react with minute amounts of water in solution, the reaction mixtures must have been extremely dry to allow the Li to form on the counter electrode.

After drying, the samples were removed from the electrodes and mechanically broken into small pieces for gravimetric microanalysis. The C, N, and H contents were determined using a Carlo Erba elemental analyzer, model # 1106, and S contents were determined using a LECO induction furnace.

Section II.3 Results and Discussion

II.3.1 Microanalysis

Four sets of samples were polymerized, two sets in each of the two solvent systems, TBAP/ACN and $LiClO_4$/PC. The samples were first polymerized at 1.3 V and 1.5 V vs SCE in the TBAP/ACN solvent system and then at 1.3 V and 1.4 V vs SCE in the $LiClO_4$/PC system. The $LiClO_4$/PC system was designed to remove any possible N contamination of the sample that might have occurred from inclusion of solvent or electrolyte in the polymers. Although chronologically the TBAP/ACN samples were polymerized first for ease of analysis description the $LiClO_4$/PC microanalysis results will be described first.

II.3.1.a Copolymerization at 1.3 V in the $LiClO_4$/PC Solvent System

The results of microanalysis of 10 samples polymerized at 1.3 V are listed in Table II.1. The samples were polymerized to

low conversion so that the monomer mixture did not change substantially during the course of polymerization and the composition of the samples approximates the composition of the initial polymers. The requirements of low conversion, and low monomer concentration for optimum coating of the electrode, had to be balanced against obtaining a minimal sample weight for microanalysis. Approximately 20 mg of each sample was obtained.

Because the polymers contain an undetermined amount of perchlorate anion to balance the charge in the oxidized polymers, the ratio of PY to BT mer units cannot be established by the absolute quantities of N or S. Rather the ratios of N/S, N/C or S/C must be used to determine the polymer composition. The mole percent PY mer units in the copolymer were calculated from these three ratios using the following equations. The results are listed in Table II.1.

$$\text{Mole \% PY} = \frac{(96.0888)(N/C)}{14.0067 + (48.0444)(N/C)} \qquad [2.28]$$

$$\text{Mole \% PY} = \frac{64.128 - (96.0888)(S/C)}{64.128 - (48.0444)(S/C)} \qquad [2.29]$$

$$\text{Mole \% PY} = \frac{64.128\ (N/S)}{14.0067 + (64.128)(N/S)} \qquad [2.30]$$

In table II.1 the mole % PY calculations using the three different equations (2.28-2.30) give significantly different mole percent PY values. In theory these values should be equivalent, thus there must be some errors in the microanalysis results.

The value for the S content of PPY, sample # CO01 and the value for N content of PBT, sample # CO02, should both be zero.

Table II.1 MICROANALYSIS RESULTS FOR SAMPLES POLYMERIZED AT 1.3 V IN PROPYLENE CARBONATE

Code	Monomer Ratio [PY]/[BT]		Weight % in Copolymer C	N	S	Percent PY Units in the Copolymer Cal. using N/S	Percent PY Units in the Copolymer Cal. using N/C	Percent PY Units in the Copolymer Cal. using S/C
CO01-18-B	100.00	0.00	46.18	10.71	0.32	99.35	88.61	99.48
CO03-20-B	79.73	20.27	45.30	10.23	0.63	98.67	87.30	98.95
CO04-20-R	59.48	40.52	46.17	10.06	1.30	97.25	85.54	97.85
CO05-04-B	44.89	55.11	45.28	9.48	2.60	94.35	83.60	95.50
CO06-05-R	29.98	70.02	45.81	9.00	4.00	91.15	80.52	93.00
CO07-05-B	19.94	80.06	44.64	8.42	7.60	83.53	78.57	85.38
CO08-06-R	15.18	84.82	43.83	8.40	6.30	85.92	79.33	87.93
CO09-07-B	10.03	89.97	46.30	8.03	13.80	72.71	74.60	71.25
CO10-07-R	4.97	95.03	46.50	6.98	21.80	59.45	67.98	45.86
CO02-18-R	0.00	100.00	48.11	0.35	32.10	4.75	4.87	0.05

There is no possible source for N or S contamination in the polymerization solutions. Therefore the errors must be in the techniques used for microanalysis. S content analysis requires, the burning of the sample in the LECO furnace, the trapping of the gases and residue in a solution and the titration of the solution to determine the S content. Error occurs only if the previous sample had a high S content and a little S remains in the furnace chamber. Errors from this contamination would be random and therefore can not be predicted or corrected for. C,N and H analysis requires the burning of the samples in an O_2 rich atmosphere and the analysis of the resulting gases in a gas chromatograph. Values of C,N and H are automatically corrected for the inclusion of air in the sample by the subtraction of the peak areas of a standard. Values of N in CO02 will be considered as standard values subtraction and will be little affected by trapped air.

The trapping of solvent within the polymers will also affect the C concentration in these polymers. Table II.2 shows the effect of evacuation of sample 01-CO-86 at 90 C and 0.20 mm Hg, for an extended period of time. The N/C ratio increased over time as the solvent was removed from the polymer, but appears to reach a limit after the first 96 hours of drying. The last column in Table II.2 demonstrates how the N/C calculation of percent PY monomer units in the polymer is affected by the inclusion of solvent in the polymer. Similar effects would be observed for the S/C calculations.

Table II.2 Extraction of Solvent from Polymer

Drying Time	Drying Temp.	Weight % in sample # 01-CO-86		Weight Ratio N/C	Mole % PY Units in Poly.
		C	N		
24 hr.	20 C	43.50	8.99	0.21	83
+24 hr.	90 C	46.74	10.45	0.22	86
+48 hr.	90 C	45.49	10.48	0.23	88
+96 hr.	90 C	44.59	10.20	0.23	88

As solvent free samples are not assured even after evacuation of the samples for extended periods of time, only the N/S calculations can be used without correction for inclusion of solvent to determine the reactivity ratios. The other calculations (N/C and S/C) require a correction for the solvent included in the sample.

Several methods of normalization were tried to correct the values for inclusion of solvent. The most effective method was based on the assumption that S and N analysis values were correct and that the C values were high due to solvent trapped in the sample.

The theoretical N/C ratio for PPY derived from equation 2.28 is 0.2915. From microanalysis of sample # CO01, an experimental ratio of 0.2320 was obtained. The theoretical ratio of C atoms to N atoms is 4 to 1. Using the equation:

$$\text{Number of C atoms per N atom} = \frac{(14.0067)}{(0.2319)(12.0111)} = 5.029 \qquad [2.31]$$

the ratio of C to N was calculated to be 5.029 to 1.

The theoretical S/C ratio for PBT derived from equation 2.29 is 0.6674. The experimental S/C ratio of PBT, sample # CO2, is 0.6672 which is very close to the theoretical, but the

samples were dried extensively to remove trapped solvent between the C,H,N microanalysis and the S microanalysis. Thus comparison with PBT polymerized at 1.4 V is more informative. From microanalysis of PBT, sample # 11-CO-86, an experimental ratio of 0.5311 was found. Employing equation 2.32 the C to S ratio is calculated to be 5.026 to 1 which is similar to the ratio of C to N found for sample # C01.

$$\text{Number of C atoms per S atom} = \frac{(32.064)}{(0.5311)(12.0111)} = 5.026 \qquad [2.32]$$

As the ratio of C to S is almost equivalent to the ratio of C to N it can be assumed that the C contamination is approximately 1.03 C atoms per monomer ring unit for polymers dried in a vacuum for 24 hours at 90 C. Using this approximation the corrected formulas for the calculation of mole percent PY monomer units in the polymer were derived, using the N/C and S/C ratios. These corrected formulas are given equation 2.33 and 2.34.

$$\text{Mole \% PY} = \frac{(120.7672)(N/C)}{14.0067 + (60.3836)(N/C)} \qquad [2.33]$$

$$\text{Mole \% PY} = \frac{64.128 - (120.7672)(S/C)}{64.128 - (60.3836)(S/C)} \qquad [2.34]$$

Using equation 2.33 the new values for mole percent PY were calculated and are listed in Table II.3. Note that the corrected results for the N/C calculation more closely approximate the values calculated using the N/S and S/C ratios than those in table II.1.

In Figure II.4 the mole percent PY mer units in the polymer,

Table II.3 NORMALIZED RESULTS FOR 1.3 V PROPYLENE CARBONATE DATA

Code	Monomer Ratio [PY]/[BT]		Weight % in Copolymer C	N	S	Percent PY Units in the Copolymer Cal. using N/S	Percent PY Units in the Copolymer Cal. using N/C	Percent PY Units in the Copolymer Cal. using S/C
CO01-18-B	100.00	0.00	46.18	10.71	0.32	99.35	99.99	99.48
CO03-20-B	79.73	20.27	45.30	10.23	0.63	98.67	98.66	98.95
CO04-20-R	59.48	40.52	46.17	10.06	1.30	97.25	96.87	97.85
CO05-04-B	44.89	55.11	45.28	9.48	2.60	94.35	94.88	95.50
CO06-05-R	29.98	70.02	45.81	9.00	4.00	91.15	91.71	93.00
CO07-05-B	19.94	80.06	44.64	8.42	7.60	83.53	89.69	85.38
CO08-06-R	15.18	84.82	43.83	8.40	6.30	85.92	90.48	87.93
CO09-07-B	10.03	89.97	46.30	8.03	13.80	72.71	85.56	71.25
CO10-07-R	4.97	95.03	46.50	6.98	21.80	59.45	78.58	45.86
CO02-18-R	0.00	100.00	48.11	0.35	32.10	4.75	6.08	0.05

Figure.II.4 COMPOSITIONAL CURVE FOR COPOLYMERS POLYMERIZED AT 1.3 V IN PROPYLENE CARBONATE CALCULATED USING THE N/S RATIO

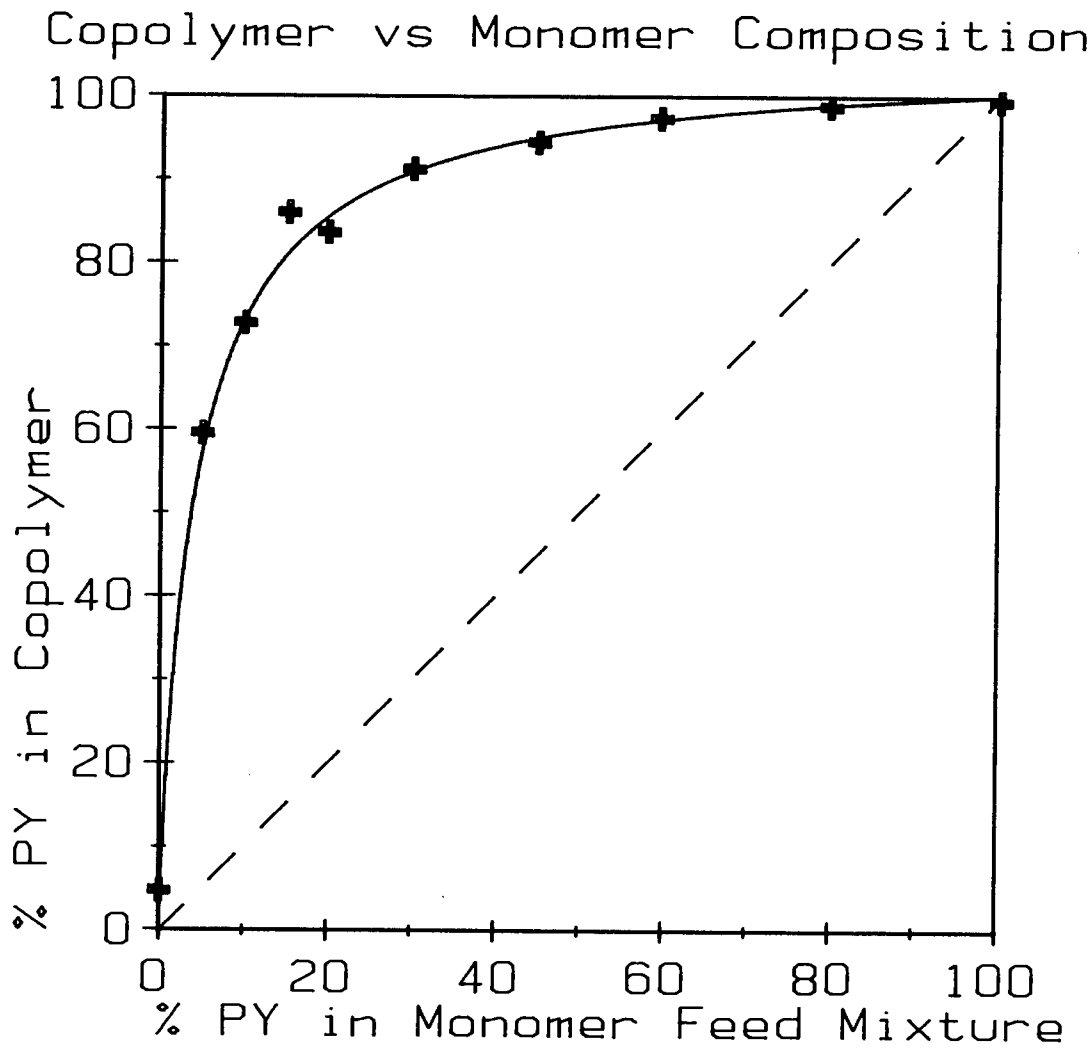
Copolymer vs Monomer Composition
100
80
60
40
20
0
% PY in Copolymer
0
20
40
60
80
100
% PY in Monomer Feed Mixture

FigureII.4

calculated using the N/S ratio, is plotted against the percent in the monomer polymerization mixture. This is the compositional PY curve for the copolymerization of PY and BT in PC at 1.3 V, and is similar to those in Figure II.1 & II.2.

Figures II.5.A and II.5.B are the compositional curves for the calculations using the N/C ratio. Line A is the curve for the percent PY values from Table II.1 and line B is the curve for the normalized values listed on Table II.3. The normalization moves the points away from the x axis to give a similar curve to that in Fig. II.4.

Figure II.6 is the compositional curve for the calculation using the S/C ratio. The curve is similar to the curve in Fig. II.4 from the N/S calculations.

II.3.1.b Copolymerization at 1.4 V in the $LiClO_4$/PC Solvent System

Results of microanalysis for 10 samples polymerized at 1.4 V are listed in Table II.4. The percent PY mer units for the polymer samples are calculated for all three ratios (N/S, N/C, and S/C) using Equations 2.28-2.30 and are listed in Table II.4. The values calculated using the N/C and S/C ratios are considerably different than those calculated using the N/S ratio, which indicates that some of the solvent is still trapped in the samples and the N/C and S/C calculations require normalization.

The N/C and S/C values are normalized using Equations 2.33 and 2.34 formulated in section II.3.1.a. Values from these calculations are listed in Table II.5.

The mole percent PY mer units in the polymer, calculated

Figure.II.5 COMPOSITIONAL CURVE FOR COPOLYMERS POLYMERIZED AT 1.3 V IN PROPYLENE CARBONATE CALCULATED USING THE N/C RATIO
A) Calculations using N/C Ratio
B) Normalized results

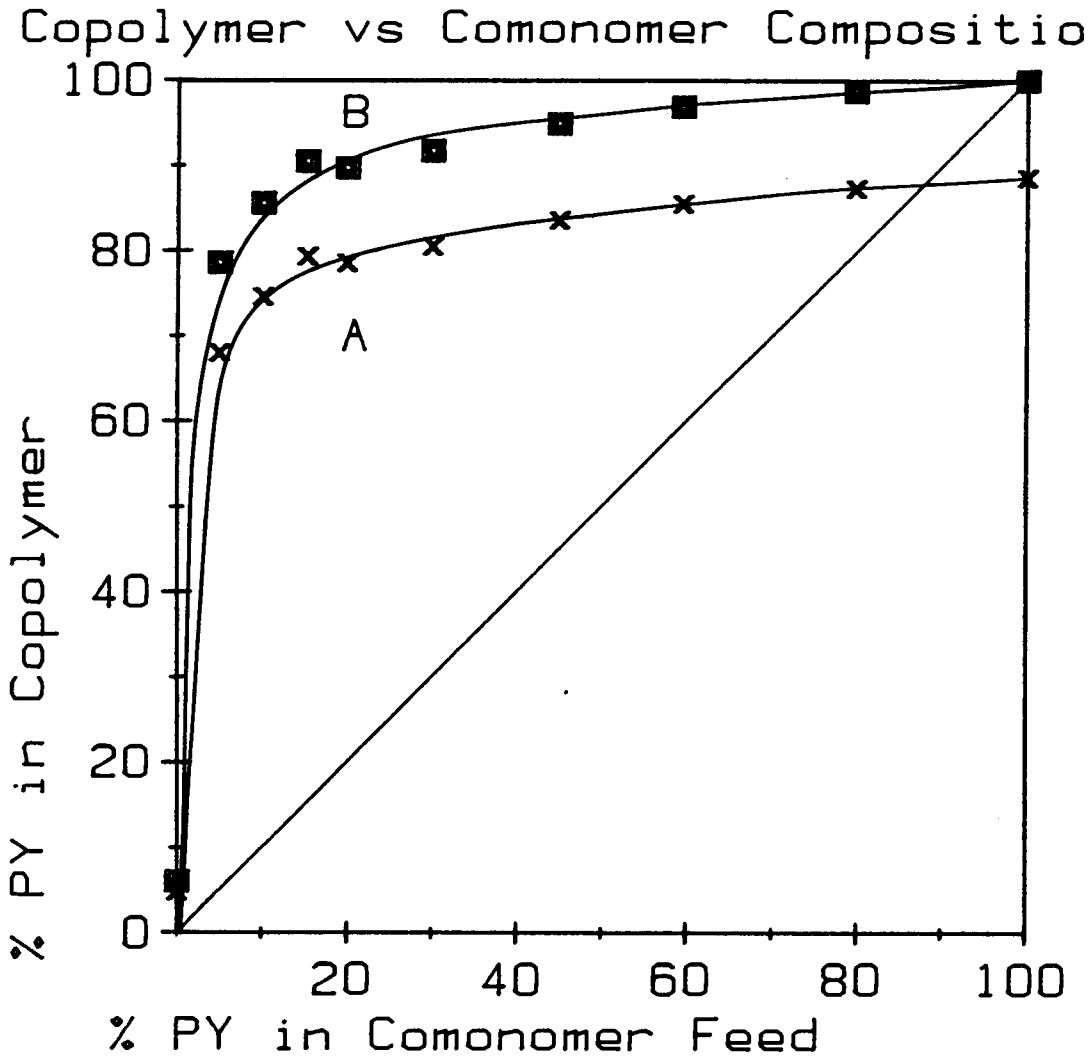
Copolymer vs Comonomer Composition
100
80
60
40
20
0
B
A
% PY in Copolymer
20
40
60
80
100
% PY in Comonomer Feed

FigureII.5

Figure.II.6 COMPOSITIONAL CURVE FOR COPOLYMERS POLYMERIZED AT 1.3 V IN PROPYLENE CARBONATE CALCULATED USING THE S/C RATIO

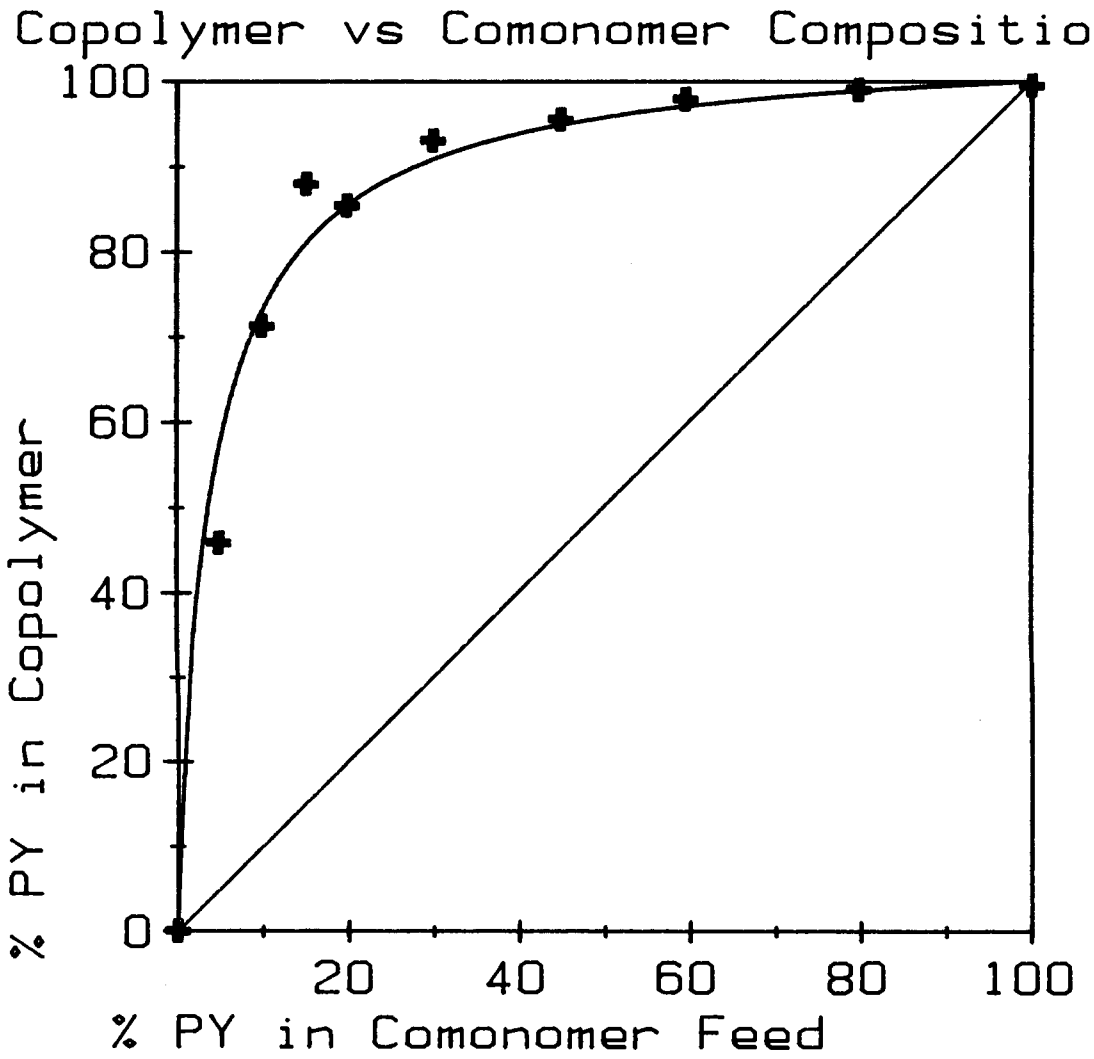
Copolymer vs Comonomer Composition
100
80
60
40
20
0
% PY in Copolymer
20
40
60
80
100
% PY in Comonomer Feed

Figure.II.6

Table II.4 MICROANALYSIS RESULTS FOR SAMPLES POLYMERIZED AT 1.4 V IN PROPYLENE CARBONATE

Code	Monomer Ratio [PY]/[BT]		Weight % in the Copolymer C	N	S	Cl	Percent PY Units in the Copolymer Cal. using N/S	Percent PY Units in the Copolymer Cal. using N/C	Percent PY Units in the Copolymer Cal. using S/C
12-CO-86	79.79	20.21	47.11	10.03	4.66		90.79	84.41	92.00
13-CO-86	60.05	39.95	46.72	10.39	0.93		98.08	86.55	98.49
14-CO-86	49.87	50.13	46.00	10.15	1.34		97.20	86.16	97.77
15-CO-86	39.82	60.18	45.88	9.30	3.02		93.38	82.03	94.81
05-CO-86	29.94	70.06	46.95	7.89				73.13	
06-CO-86	24.95	75.05	46.15	8.59	7.96		83.17	77.93	85.16
07-CO-86	19.98	80.02	47.16	7.35	9.36		78.24	69.67	82.53
08-CO-86	14.96	85.04	47.32	6.85	10.60	7.74	74.74	66.36	79.83
09-CO-86	9.92	90.08	47.36	4.54	15.40		57.44	49.49	67.79
10-CO-86	5.00	95.00	48.40	2.58	23.30	6.13	33.64	30.92	43.59
11-CO-86	0.00	100.00	47.26	0.00	25.10		0.00	0.00	33.91

Table II.5 NORMALIZED RESULTS FOR 1.4 V PROPYLENE CARBONATE DATA

Code	Monomer Ratio [PY]/[BT]		Weight % in the Copolymer C	N	S	Cl	Percent PY Units in the Copolymer Cal. using N/S	Percent PY Units in the Copolymer Cal. using N/C	Percent PY Units in the Copolymer Cal. using S/C
12-CO-86	79.79	20.21	47.11	10.03	4.66		90.79	95.72	89.73
13-CO-86	60.05	39.95	46.72	10.39	0.93		98.08	97.89	98.09
14-CO-86	49.87	50.13	46.00	10.15	1.34		97.20	97.50	97.18
15-CO-86	39.82	60.18	45.88	9.30	3.02		93.38	93.27	93.39
05-CO-86	29.94	70.06	46.95	7.89				84.02	
06-CO-86	24.95	75.05	46.15	8.59	7.96		83.17	89.04	80.61
07-CO-86	19.98	80.02	47.16	7.35	9.36		78.24	80.37	77.02
08-CO-86	14.96	85.04	47.32	6.85	10.60	7.74	74.74	76.85	73.27
09-CO-86	9.92	90.08	47.36	4.54	15.40		57.44	58.48	55.87
10-CO-86	5.00	95.00	48.40	2.58	23.30	6.13	33.64	37.37	17.09
11-CO-86	0.00	100.00	47.26	0.00	25.10		0.00	0.00	0.00

Figure.II.7 COMPOSITIONAL CURVE FOR COPOLYMERS POLYMERIZED AT 1.4 V IN PROPYLENE CARBONATE CALCULATED USING THE N/S RATIO

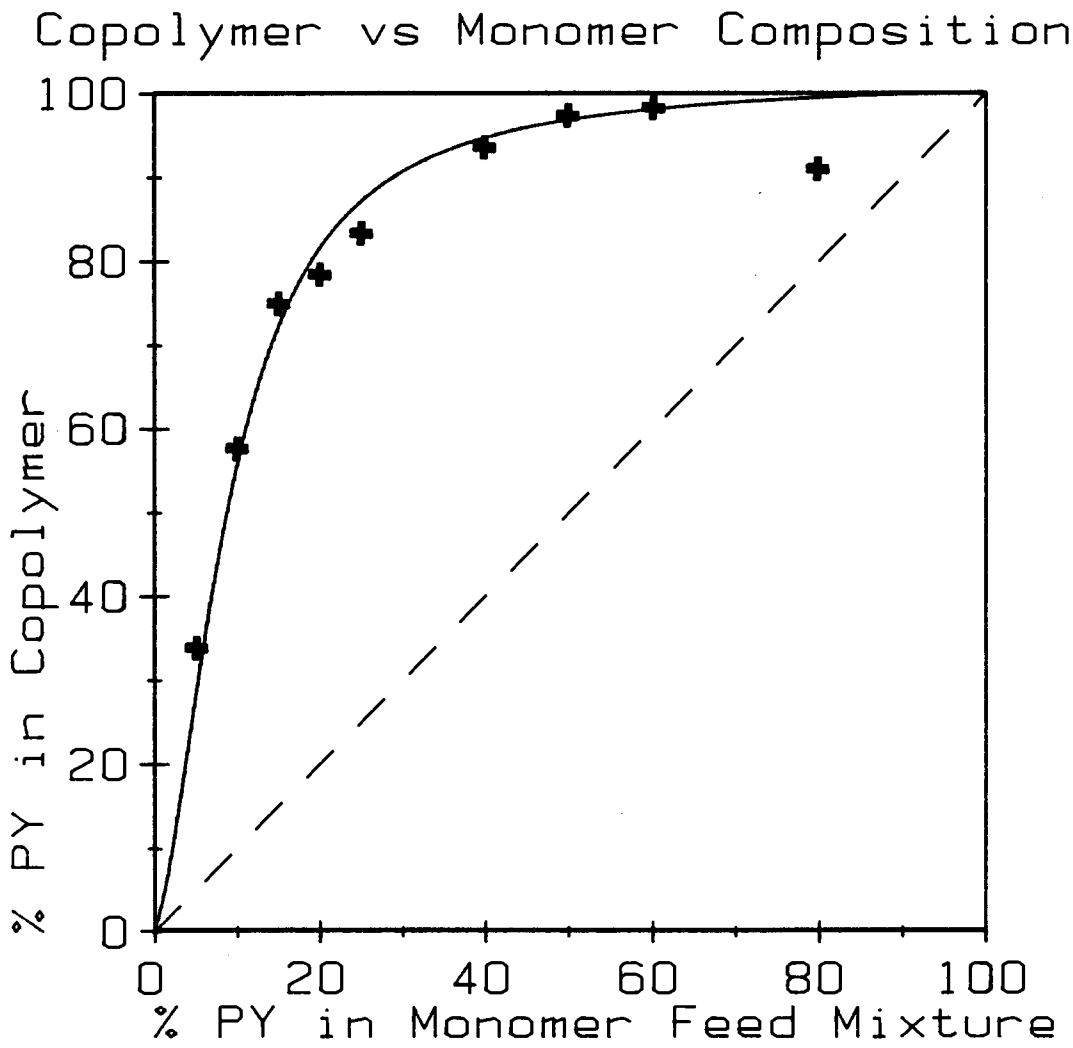
Copolymer vs Monomer Composition
100
80
60
40
20
0
% PY in Copolymer
0
20
40
60
80
100
% PY in Monomer Feed Mixture

Figure.II.7

Figure.II.8 COMPOSITIONAL CURVE FOR COPOLYMERS POLYMERIZED AT 1.4 V IN PROPYLENE CARBONATE CALCULATED USING THE N/C RATIO
A) Calculated using N/C Results
B) Normalized Results

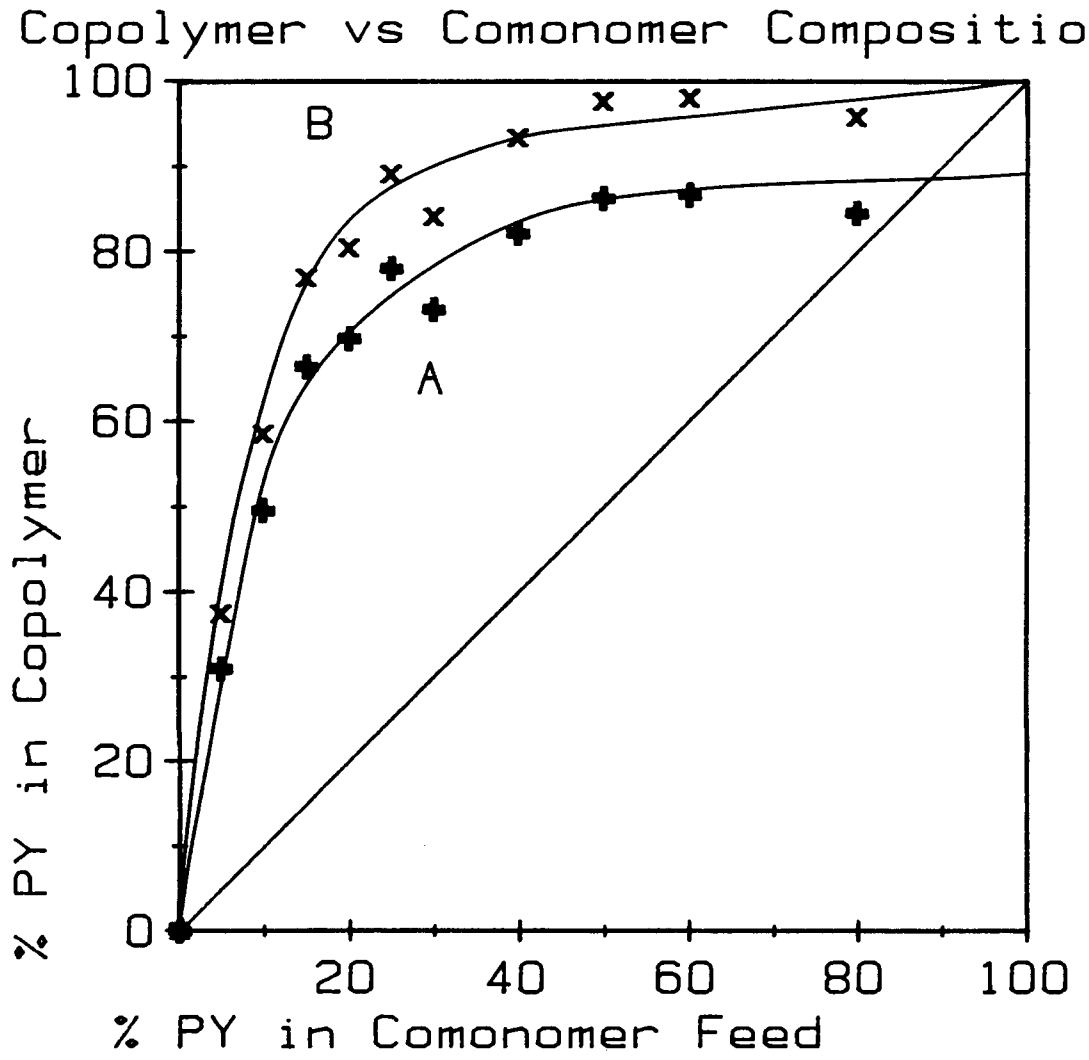
Copolymer vs Comonomer Composition
100
80
60
40
20
0
% PY in Copolymer
B
A
20
40
60
80
100
% PY in Comonomer Feed

Fig.II.8

using the N/S ratio, is plotted against the percent PY in the monomer polymerization mixture in Figure II.7. Figures II.8.A and II.8.B are the compositional curves for the calculations using the N/C ratios. Line A is the curve for the N/C values listed on Table II.4 and line B is the line for the normalized N/C values from Table II.5. The normalized N/C curve more closely approximates the N/S curve in Figure II.7 than that of line A. Figures II.9.A and II.9.B are the compositional curves for the calculations of percent PY calculated using the S/C ratios. Line A is the curve for the values listed on Table II.4 and line B is the curve for the values listed on Table II.5. Line B more closely approximates the curve in Figure II.7 than that of line A.

II.3.1.c Copolymerization at 1.3 V in the ACN/TBAP Solvent System

The results of microanalysis of 11 samples polymerized at 1.3 V vs SCE are listed in Table II.6. The mole percent PY mer units in the polymers are calculated using the equations 2.28-2.30 and the N/S, N/C and S/C ratios and are also listed in Table II.6. The values calculated from the N/C and S/C ratios vary significantly from those calculated from the N/S ratio due to incorporation of solvent and electrolyte in the polymer and errors in the microanalysis.

Unlike the results in section II.3.1.a and II.3.1.b the incorporation of solvent or supporting electrolyte in the polymers will affect the microanalysis values of N, as N is contained in the solvent (acetonitrile ACN) and the cation of the electrolyte (tetrabutylammomium). Solvent trapping is not as

Figure.II.9 COMPOSITIONAL CURVE FOR COPOLYMERS POLYMERIZED AT 1.4 V IN PROPYLENE CARBONATE CALCULATED USING THE S/C RATIO

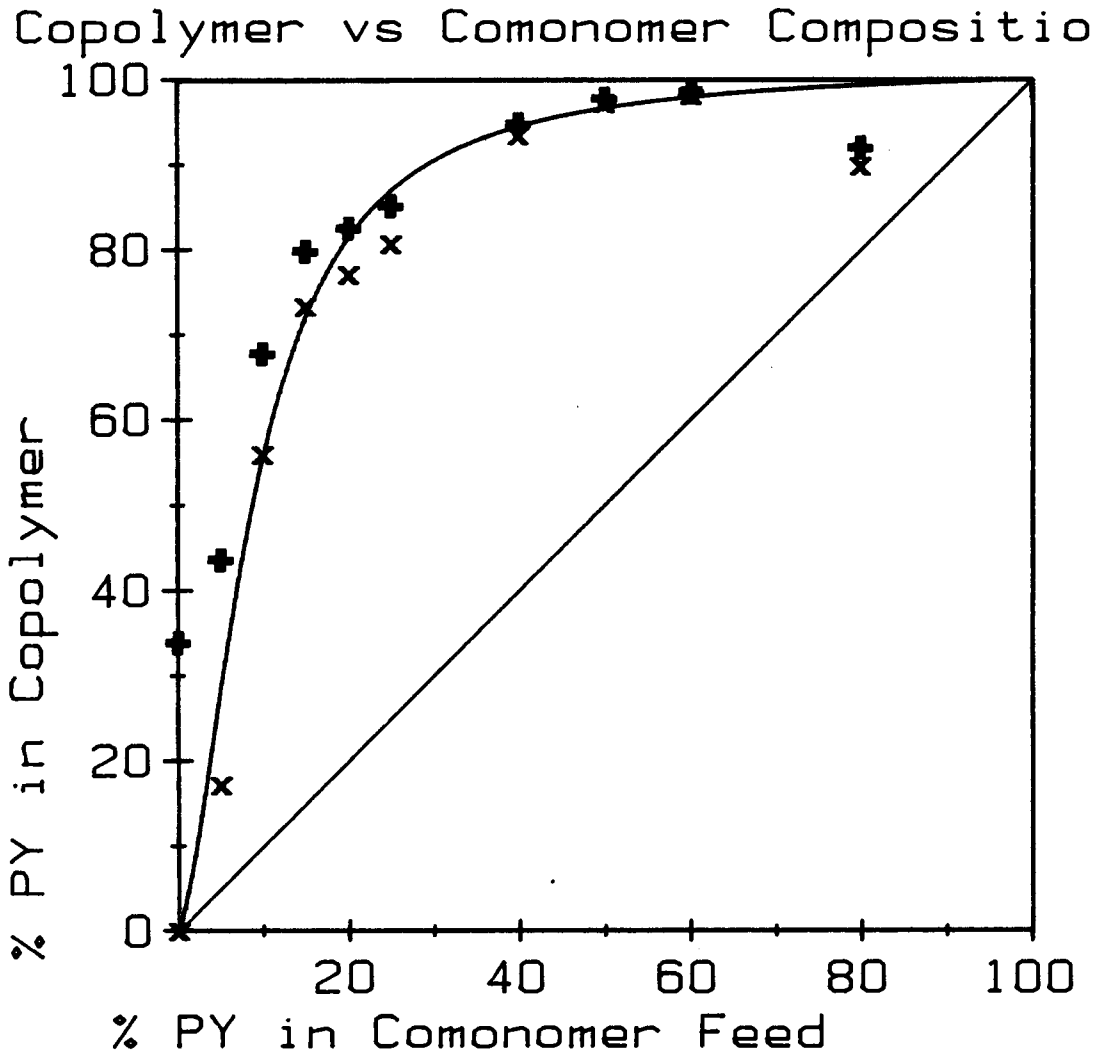
Copolymer vs Comonomer Composition
100
80
60
40
20
0
% PY in Copolymer
20
40
60
80
100
% PY in Comonomer Feed

Fig.II.9

Table II.6 MICROANALYSIS RESULTS FOR SAMPLES POLYMERIZED AT 1.3 V IN ACETONITRILE

Code	Monomer Ratio [PY]/[BT]		Weight % in Copolymer C	N	S	Percent PY Units in the Copolymer Cal. using N/S	Percent PY Units in the Copolymer Cal. using N/C	Percent PY Units in the Copolymer Cal. using S/C
1.0	100.00	0.00	44.40	10.50	0.50	98.97	89.57	99.15
2.0	95.10	4.90	45.60	11.90	1.10	98.02	94.47	98.16
3.0	90.40	9.60	46.20	10.10	0.70	98.51	85.71	98.85
4.0	73.60	26.40	44.70	10.30	2.60	94.77	88.29	95.44
5.0	65.70	34.30	40.90	10.10	2.10	95.66	91.72	96.00
6.0	54.30	45.70	41.70	9.70	4.60	90.61	88.76	90.99
7.0	51.50	48.50	42.20	8.60	2.50	94.03	82.29	95.36
8.0	34.60	65.40	44.90	7.80	9.30	79.34	74.68	81.63
9.0	25.10	74.90	46.10	7.80	8.20	81.33	73.45	84.62
10.0	10.10	89.90	44.90	4.60	16.90	55.48	52.01	60.73
11.0	0.00	100.00	48.30	1.60	48.90	13.03	20.41	0.00

great a problem for these samples as it was for the samples polymerized in PC, because ACN is much more volatile than PC. Evacuation of the samples for 24 hours at room temperature should have removed the solvent from the sample. Data from scanning electron microscopy (SEM), given in section III, shows that there are some crystals of electrolyte on the surface and within the matrix of the polymer films. The inclusion of the cations of the electrolyte may affect the microanalysis results to a small extent, but any significant N contamination from the electrolyte would mean that the polymers would be composed almost entirely of electrolyte, due to the relatively large molecular weight of the TBAP. This large a contamination was not evident in microscopic examination of the films surfaces or in SEM examination of the films.

As with the homopolymers in section II.3.1.a, the homopolymers PPY (sample #1) and PBT (sample #11) results show some error in the microanalysis. The N value in sample #11 can be partially explained by the inclusion of solvent and electrolyte into the sample, but errors due to microanalysis technique, like those evidenced by sample # CO1 in section II.3.1.a, may also contribute. The high error in S microanalysis of the samples, evidenced by the S value of sample #1, is partially due to the small amount of the sample left for S microanalysis, after C,N,H micrcoanalysis was completed. The low sample masses did not allow the results to be checked by multiple analysis and were even too small for a single accurate analysis. These errors were reduced for the $LiClO_4$/PC system by increasing the initial sample sizes.

Table II.7 NORMALIZED RESULTS FOR 1.3 V ACETONITRILE DATA

Code	Monomer Ratio [PY]/[BT]		Weight % in Copolymer C	N	S	Percent PY Units in the Copolymer Cal. using N/S	Percent PY Units in the Copolymer Cal. using N/C	Percent PY Units in the Copolymer Cal. using S/C
1.0	100.00	0.00	44.40	8.90	0.00	100.00	94.03	99.58
2.0	95.10	4.90	45.60	10.30	0.60	98.74	99.99	95.24
3.0	90.40	9.60	46.20	8.50	0.20	99.49	89.77	96.07
4.0	73.60	26.40	44.70	8.70	2.10	94.99	92.56	89.49
5.0	65.70	34.30	40.90	8.50	1.60	96.05	95.83	95.20
6.0	54.30	45.70	41.70	8.10	4.10	90.04	92.47	76.62
7.0	51.50	48.50	42.20	7.00	2.00	94.13	84.68	80.74
8.0	34.60	65.40	44.90	6.20	8.80	76.34	75.87	45.40
9.0	25.10	74.90	46.10	6.20	7.70	78.66	74.64	
10.0	10.10	89.90	44.90	3.00	16.40	45.58	45.65	
11.0	0.00	100.00	48.30	0.00	48.40	0.00	0.00	

To correct for the large errors in the N and S microanalysis values the N and S values for the homopolymers were subtracted from the rest of the data before the normalization. The corrected microanalysis data is listed in Table II.7. The new N/C ratio for PPY sample #1 is 0.201 which is less than 0.226 for sample #2 which is polymerized from a 95.1/4.9 (PY/BT) monomer ratio. Thus the ratio from sample #2 was used for the derivation of the normalization equation. Equation 2.31 was used to determine the ratio of C atoms to N atoms in the sample and a new equation (2.35) similar to Equation 2.32 was derived.

$$\text{Mole \% PY} = \frac{(124.0080)(N/C)}{14.0067 + (62.0040)(N/C)} \qquad [2.35]$$

Using Equation 2.35, values for the mole percent PY in the polymers were calculated and are listed on Table II.7.

The normalization of the S/C data used corrected S values in Table II.7. The S/C ratio of the PBT (sample #11) after the correction is 1.00 which is greater than the theoretical value of 0.6674. This ratio is greater than the S/C ratio for BT therefore there is significant error in this S microanalysis value. For this reason the normalization equation 2.26 is based on the number of C atoms per monomer ring found using the N/C ratio.

$$\text{Mole \% PY} = \frac{64.128 - (124.0080)(S/C)}{64.128 - (62.0040)(S/C)} \qquad [2.36]$$

Equation 2.36 and the corrected S/C ratios from Table II.7 are used to calculate the new mole percent PY which is listed in Table II.7.

The N/S mole percent PY values were also corrected using

Figure.II.10 COMPOSITIONAL CURVE FOR COPOLYMERS POLYMERIZED AT 1.3 V IN ACETONITRILE CALCULATED USING THE N/S RATIO
A) Calculated using N/S Results
B) Corrected N/S Results

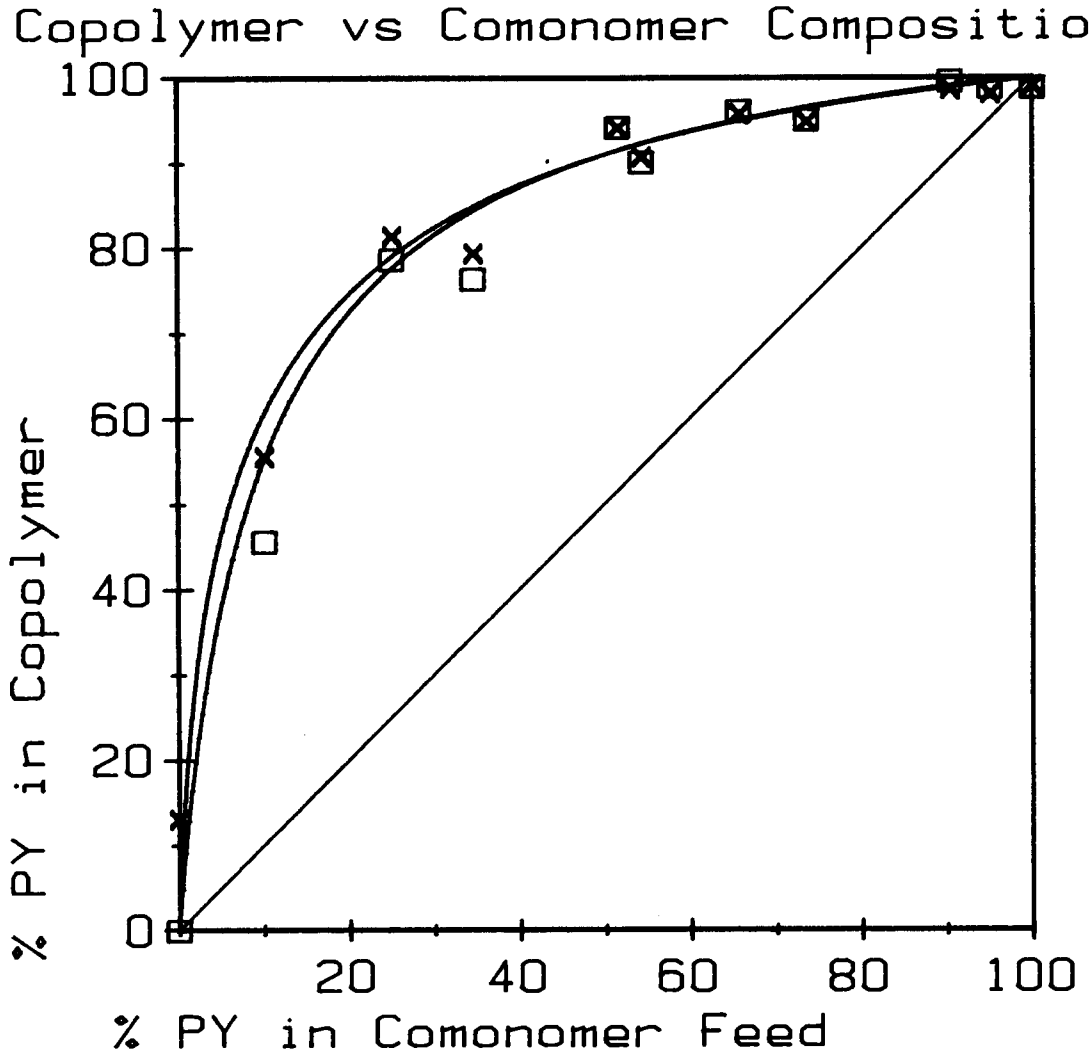
Copolymer vs Comonomer Composition
100
80
60
40
20
0
% PY in Copolymer
20
40
60
80
100
% PY in Comonomer Feed

Fig.II.10

the microanalysis data on Table II.7. Equation 2.30 was used to calculate the new mole percent PY values which are listed in Table II.7.

The mole percent PY in the polymers from Table II.6 and II.7, calculated using the N/S ratios, are plotted against the percent PY in the monomer mixture to give the compositional curves A and B respectively in Figure II.10. There are only slight differences between the normalized data (line B) and the data from Table II.6.

Figures II.11.A and II.11.B are the compositional curves for the calculations using the N/C ratios. Line A is the curve for the N/C values listed on Table II.6 and line B is the line for the normalized N/C values from Table II.7. The normalized N/C curve more closely approximates the N/S curves in Figure II.10 than that of line A. Figures II.12.A and II.12.B are the compositional curves for the calculations of percent PY calculated using the S/C ratios. Line A is the curve for the values listed on Table II.6 and line B is the curve for the values listed on Table II.7. The normalized values of line B do not appear to be as good a fit to the lines in Figure II.10 as are the values in line A. In this case the normalization of the data may not be necessary.

II.3.1.d Copolymerization at 1.5 V in the ACN/TBAP Solvent System

The results of microanalysis of 3 samples polymerized at 1.5 V vs SCE are listed in Table II.8. The mole percent PY mer units in the polymers are calculated using the equations 2.28-2.30 and the N/S, N/C and S/C ratios and are listed in Table

Figure.II.11 COMPOSITIONAL CURVE FOR COPOLYMERS POLYMERIZED AT 1.3 V IN ACETONITRILE CALCULATED USING THE N/C RATIO
A) Calculated using N/C results
B) Normalized Results

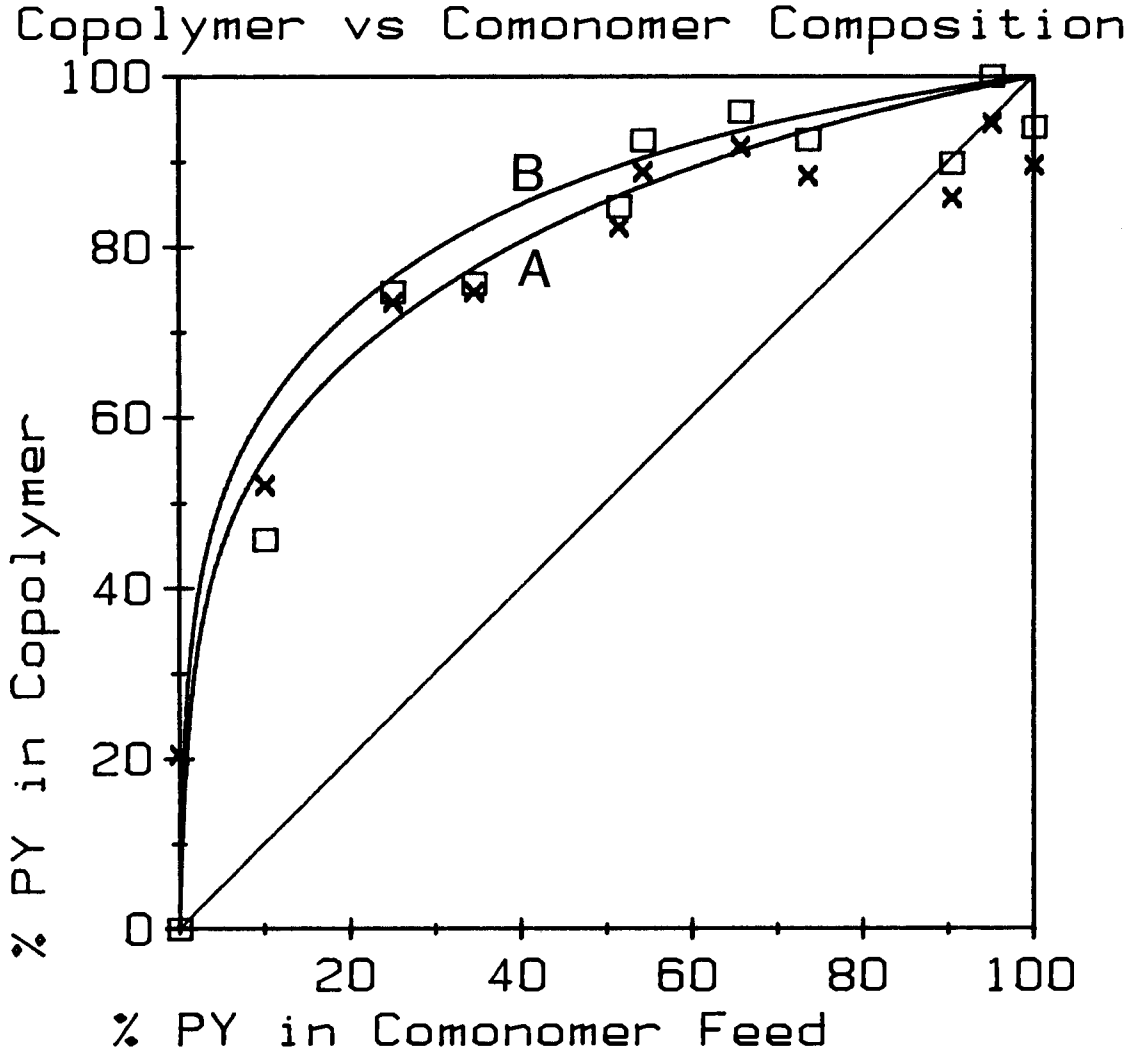
Copolymer vs Comonomer Composition
100
80
60
40
20
0
% PY in Copolymer
B
A
20
40
60
80
100
% PY in Comonomer Feed

Fig.II.11

Figure.II.12 COMPOSITIONAL CURVE FOR COPOLYMERS POLYMERIZED AT 1.3 V IN ACETONITRILE CALCULATED USING THE S/C RATIO
A) Calculated using the S/C REsults
B) Normalized Results

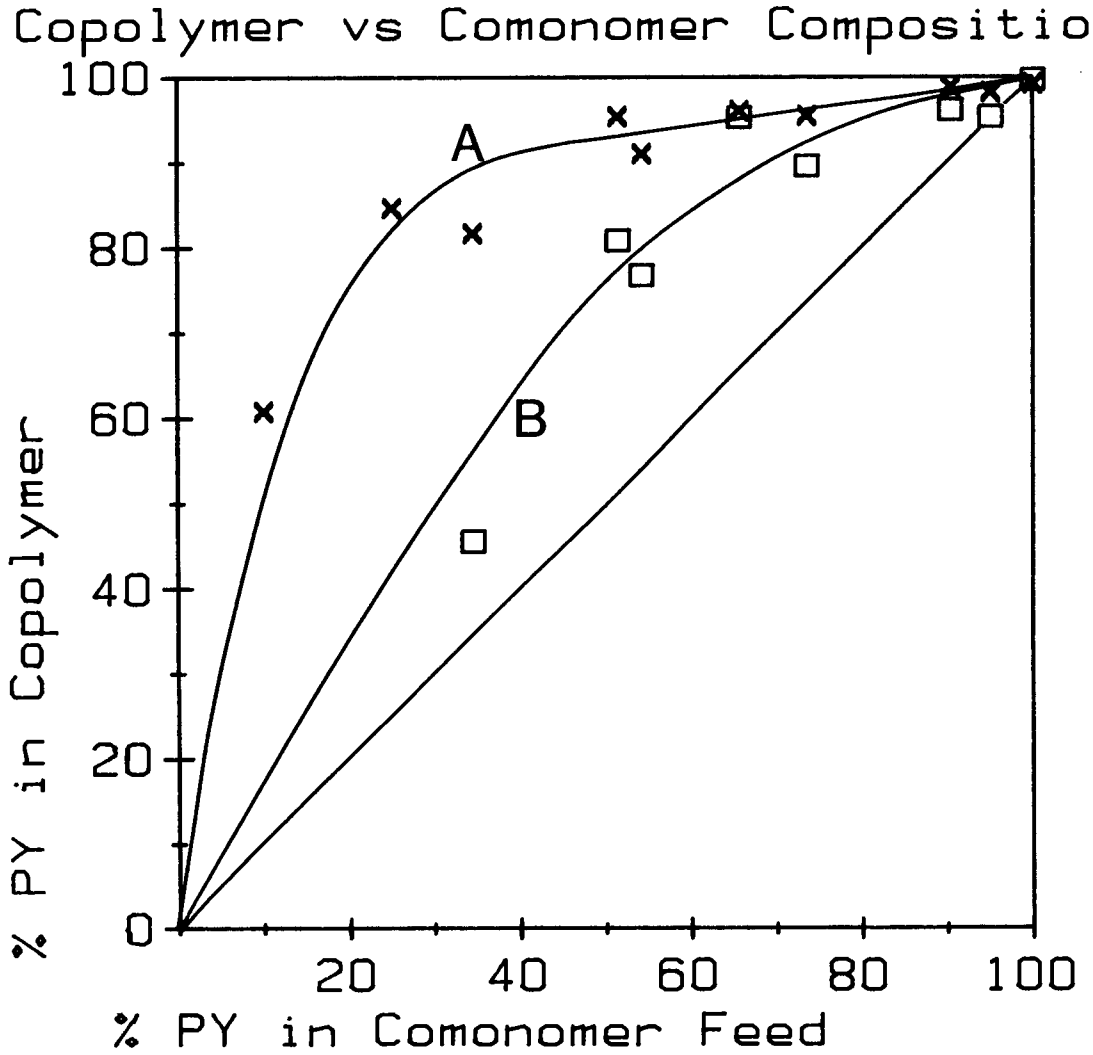
Copolymer vs Comonomer Composition
100
80
60
40
20
0
% PY in Copolymer
A
B
20
40
60
80
100
% PY in Comonomer Feed

Fig.II.12

Table II.8 MICROANALYSIS RESULTS FOR SAMPLES POLYMERIZED AT 1.5 V IN ACETONITRILE

Code	Monomer Ratio [PY]:[BT]		Weight % in Copolymer C	N	S	Percent PY Units in the Copolymer Cal. using N/S	Percent PY Units in the Copolymer Cal. using N/C	Percent PY Units in the Copolymer Cal. using S/C
1	58.8	41.2	42.9	9.4	5.7	88.30	85.82	88.95
2	50.3	49.7	41.2	8.1	9.0	80.47	80.55	80.43
3	9.9	90.1	46.8	2.6	27.9	29.91	32.01	19.29

II.8. Percent PY values calculated using the N/C and S/C ratios are significantly different to those calculated using the N/S ratio. If more than 3 samples had been analyzed then normalization might have been attempted, but with only 3 samples it would be very inaccurate.

The mole percent PY of the polymers are plotted against the percent PY in the monomer mixture for the data listed on Table II.8, in Figure II.13. The points on curves A, B, and C are the data from the N/S, N/C and S/C calculations respectively. The lines through the points are calculated from the reactivity ratios found in section II.3.2.b.

II.3.2 Calculation of Reactivity Ratios

The values of the reactivity ratios r_1 and r_2 from the Mayo-Lewis Equation (Equation 2.9):

$$\frac{d[M_1]}{d[M_2]} = \frac{[M_1]}{[M_2]} * \frac{r_1[M_1] + [M_2]}{[M_1] + r_2[M_2]} \qquad [2.9]$$

were obtained by a modification of the method of Fineman and Ross (2). We define F as the ratio of monomers in the polymerization mixture, $[M_1]/[M_2]$ and f as the ratio in the copolymer, $d[M_2]/d[M_1]$ and obtain the form:

$$F(1-f) = -r_2 + r_1F^2f \qquad [2.37]$$

The intercept and slope of the plot of F(1-f) vs. F^2f give $-r_2$ and r_1 respectively.

II.3.2.a Copolymerization at 1.3 V in the $LiClO_4$/PC Solvent System

For the mole percent PY in the polymer calculated using the N/S ratio (data listed in Table II.1) the values for the Fineman and Ross (F&R) linearization, F(1-f) and F^2f, were calculated and

Figure.II.13 COMPOSITIONAL CURVE FOR COPOLYMERS POLYMERIZED AT 1.5 V IN ACETONITRILE CALCULATED USING THE N/S RATIO, N/C RATIO AND S/C RATIO

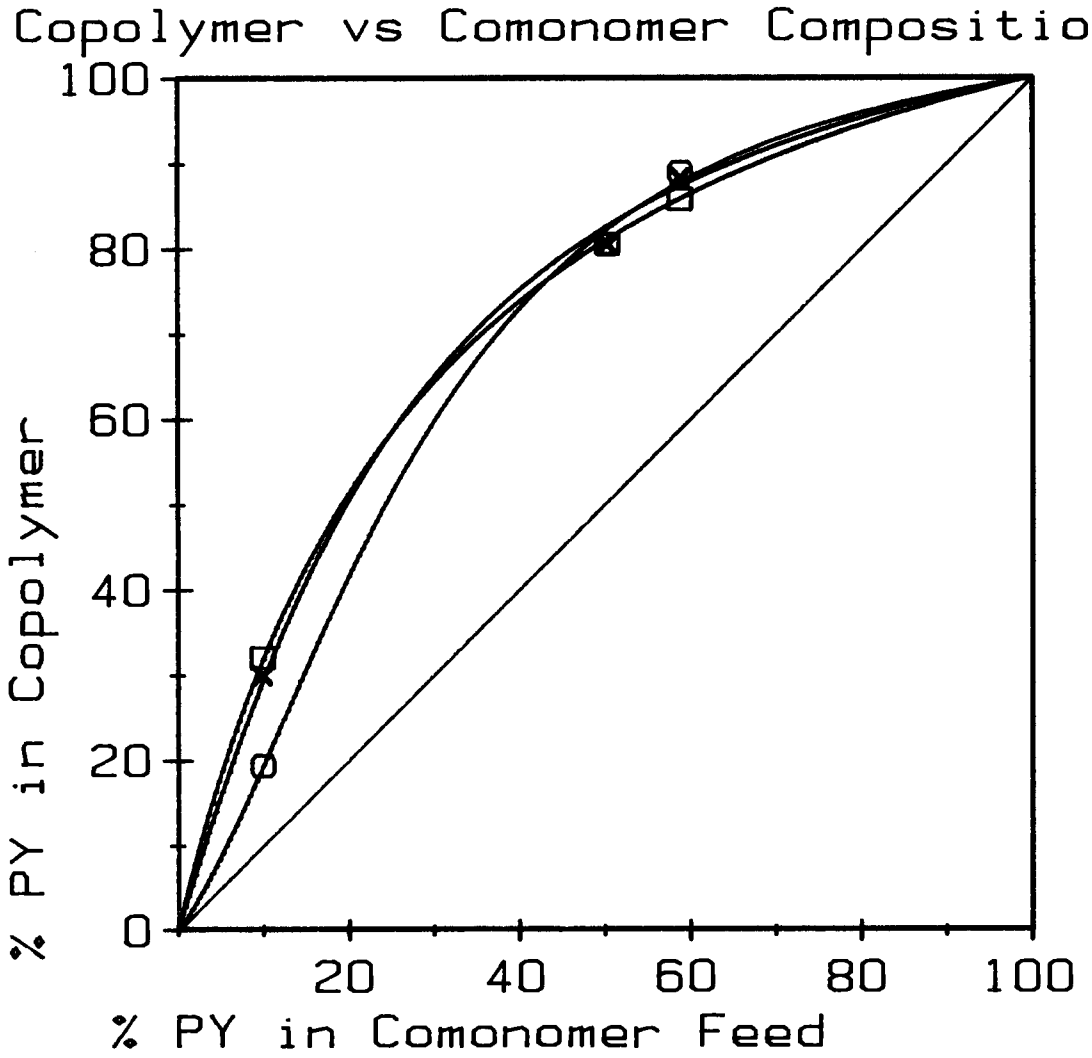
Copolymer vs Comonomer Composition
100
80
60
40
20
0
% PY in Copolymer
20
40
60
80
100
% PY in Comonomer Feed

Fig.II.13

Table II.9 VALUES FOR FINEMAN AND ROSS PLOT FOR SAMPLES POLYMERIZED AT 1.3 V IN PROPYLENE CARBONATE

Code	Monomer Ratio [PY]/[BT]		F	Percent PY Units in the Copolymer Cal. using N/S	f	F(1-f)	F*F*f
CO01-18-B	100.00	0.00		99.35			
CO03-20-B	79.73	20.27	3.932	98.67	0.0135	3.8796	0.2080
CO04-20-R	59.48	40.52	1.468	97.25	0.0282	1.4263	0.0608
CO05-04-B	44.89	55.11	0.815	94.35	0.0599	0.7658	0.0398
CO06-05-R	29.98	70.02	0.428	91.15	0.0971	0.3866	0.0178
CO07-05-B	19.94	80.06	0.249	83.53	0.1971	0.2000	0.0122
CO08-06-R	15.18	84.82	0.179	85.92	0.1638	0.1497	0.0052
CO09-07-B	10.03	89.97	0.112	72.71	0.3754	0.0697	0.0047
CO10-07-R	4.97	95.03	0.052	59.45	0.6822	0.0166	0.0019
CO02-18-R	0.00	100.00		0.00			

Figure.II.14 FINEMAN AND ROSS PLOT FOR COPOLYMERS POLYMERIZED AT 1.3 V IN PROPYLENE CARBONATE

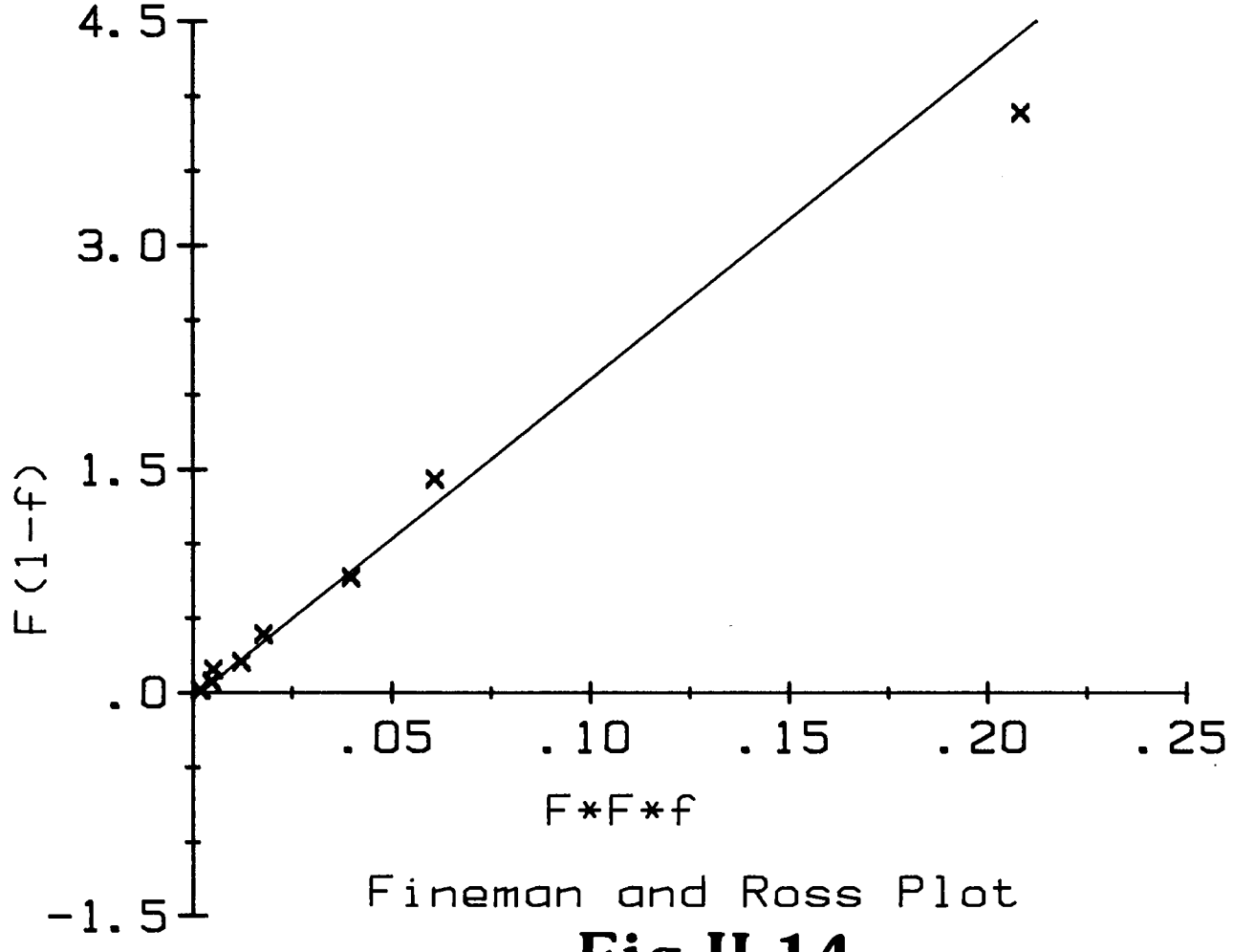

Fig.II.14

are listed in Table II.9. F(1-f) is plotted against F^2f in Figure II.14 to give a straight line with a slope of 23 and an intercept of -0.03. The slope and intercept were calculated using a linear regression of 7 of the 8 points. The point for sample # CO03 was dropped from the calculation because it disproportionately affects the slope and intercept values. Errors in the values for the points are unequally weighted using linear regression; thus points which are the farthest from the F(1-f), F^2f axis effect the slope and intercept of the line the greatest. The problem of unequal weighting of points is the greatest when as in Figure II.14, one reactivity ratio is close to zero and the other is relatively large (3,4).

The mole percent PY in the polymer, calculated using the N/C and S/C ratios, were used to calculate F(1-f) and F^2f and the values. These values were plotted to determine the reactivity ratios. The reactivity ratios and the correlation coefficients from the linear regression of 7 points are listed in Table II.10.

The normalized values listed on Table II.3, for the N/C ratios were used to calculate F(1-f) and F^2f. The reactivity ratios obtained for the 7 points are listed in Table II.10.

Table II.10 Reactivity Ratios for 1.3 V PC Polymerizations

Method Used for % PY in Poly. Calculations	Reactivity Ratio r_1 for PY (slope)	Reactivity Ratio r_2 for BT (-intercept)	Correlation Coefficient
N/S Ratio	23	0.03	0.98
N/C Ratio	3.2	-0.11	0.98
N/C (norm.)	20	-0.06	0.99
S/C Ratio	23	-0.03	0.99

Values for the reactivity ratios, calculated using the N/S, S/C and the normalized N/C methods are in good agreement with one another (Table II.10), but there are negative values for the reactivity ratio r_2 which by definition ($r_1 = k_{11}/k_{12}$ and $r_2 = k_{22}/k_{21}$) is impossible. r_2 is close to zero therefore small errors in the slope give rise to negative values for r_2. Accurate definition of values close to zero is difficult with the F&R technique. Other techniques could be used to minimize the effects of the errors on the determination of the reactivity ratios, but are impractical for this study as values derived will not be used for prediction of copolymer compositions.

II.3.2.b Copolymerization at 1.4 V in the $LiClO_4$/PC Solvent System

The F(1-f) and F^2f were calculated using the mole percent PY for the N/S ratio and are listed in Table II.11. These values are plotted in Figure II.15 to give a straight line with a slope of 38 and an intercept of -0.36. The point from sample # 12-CO-86 was dropped from the linear regression as it deviated greatly from the others and severely affected the analysis.

The values of PY calculated from the N/C and S/C values in

Table II.4 and II.5 were used to calculate F(1-f) and F^2f values for F&R plots. The reactivity ratios and the correlation coefficients for the linear regression of 8 points are listed on Table II.12.

Table II.12 Reactivity Ratios for 1.4 V PC Polymerizations

Method Used for % PY in Poly. Calculations	Reactivity Ratio r_1 for PY (slope)	Reactivity Ratio r_2 for BT (-intercept)	Correlation Coefficient
N/S Ratio	38	0.36	0.95
N/C Ratio	5.6	0.03	0.99
N/C (norm.)	34	0.21	0.95
S/C Ratio	46	0.28	0.87
S/C (norm.)	43	0.56	0.84

Table II.11 VALUES FOR FINEMAN AND ROSS PLOT FOR SAMPLES POLYMERIZED AT 1.4 V IN PROPYLENE CARBONATE

Code	Monomer [PY]/[BT]	Ratio	F	Percent PY Units in the Copolymer Cal. using N/S	f	F(1-f)	F*F*f
12-CO-86	79.79	20.21	3.9486	90.79	0.1015	3.5479	1.5822
13-CO-86	60.05	39.95	1.5030	98.08	0.0196	1.4736	0.0442
14-CO-86	49.87	50.13	0.9948	97.20	0.0288	0.9661	0.0285
15-CO-86	39.82	60.18	0.6618	93.38	0.0709	0.6148	0.0311
05-CO-86	29.94	70.06	0.4273				
06-CO-86	24.95	75.05	0.3324	83.17	0.2024	0.2651	0.0224
07-CO-86	19.98	80.02	0.2497	78.24	0.2781	0.1802	0.0173
08-CO-86	14.96	85.04	0.1759	74.74	0.3380	0.1164	0.0105
09-CO-86	9.92	90.08	0.1101	57.44	0.7409	0.0285	0.0090
10-CO-86	5.00	95.00	0.0526	33.64	1.9725	-0.0512	0.0055
11-CO-86	0.00	100.00	0.0000	0.00			

Figure.II.15 FINEMAN AND ROSS PLOT FOR COPOLYMERS POLYMERIZED AT 1.4 V IN PROPYLENE CARBONATE

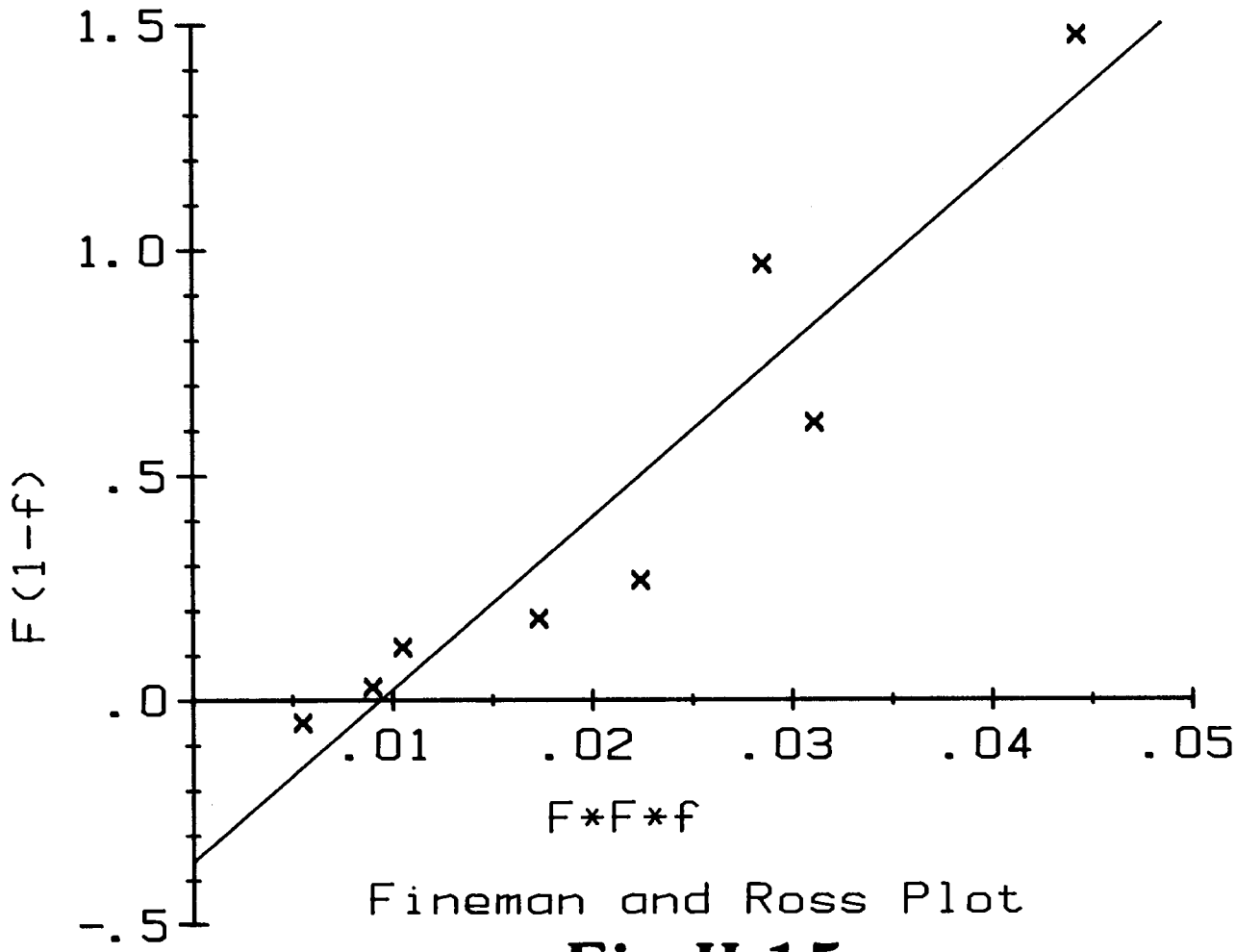

Fig.II.15

The reactivity ratios calculated by different ratios and methods vary significantly. The normalization of the N/C data significantly improves the reactivity ratio values with respect to the N/S values, but the normalization of the S/C data does not improve the values as greatly. The reactivity ratios values from the N/S calculations are close to the mean between the values for the normalized N/C and S/C calculations.

II.3.2.c Copolymerization at 1.3 V in the ACN/TBAP Solvent System

Values of $F(1-f)$ and F^2f were calculated from the N/S data in Table II.6 and II.7 and are listed in Table II.13. These values are plotted on Figure II.16 to give two straight lines with slopes of 10 and intercepts of -0.04 and -0.08. The 3 points from samples #2-4 were dropped from the linear regression as they deviated greatly from the others and severely affected the analysis.

Values from N/C and S/C data in Tables II.6 and II.7 were also used to calculate $F(1-f)$ and F^2f values for F&R plots. The reactivity ratios and the correlation coefficients for the linear regression of 6 points are listed on Table II.14.

Normalization of the N/S calculated values of % PY changes the reactivity ratios only slightly although the correlation coefficient for the points decreases significantly. The correlation coefficient for the points calculated using the S/C and N/C ratios also decrease significantly with normalization. Normalization of the N/C calculated values significantly improves the r_1 and r_2 values with respect to the N/S values. The reactivity ratios calculated using S/C ratios are improved

Table II.13 VALUES FOR FINEMAN AND ROSS PLOT FOR SAMPLES POLYMERIZED AT 1.3 V IN ACETONITRILE

Code	Monomer Ratio [PY]/[BT]		F	Percent PY Units in the Copolymer Cal. using N/S	f	F*F*f	(1-f)F
1.0	100.00	0.00		98.97	0.0104		
2.0	95.10	4.90	19.4082	98.02	0.0202	7.6051	19.0163
3.0	90.40	9.60	9.4167	98.51	0.0151	1.3423	9.2741
4.0	73.60	26.40	2.7879	94.77	0.0551	0.4285	2.6342
5.0	65.70	34.30	1.9155	95.66	0.0454	0.1666	1.8285
6.0	54.30	45.70	1.1882	90.61	0.1036	0.1462	1.0651
7.0	51.50	48.50	1.0619	94.03	0.0635	0.0716	0.9944
8.0	34.60	65.40	0.5291	79.34	0.2604	0.0729	0.3913
9.0	25.10	74.90	0.3351	81.33	0.2296	0.0258	0.2582
10.0	10.10	89.90	0.1123	55.48	0.8024	0.0101	0.0222
11.0	0.00	100.00	0.0000	0.00			

Figure.II.16 FINEMAN AND ROSS PLOT FOR COPOLYMER POLYMERIZED AT 1.3 V IN ACETONITRILE

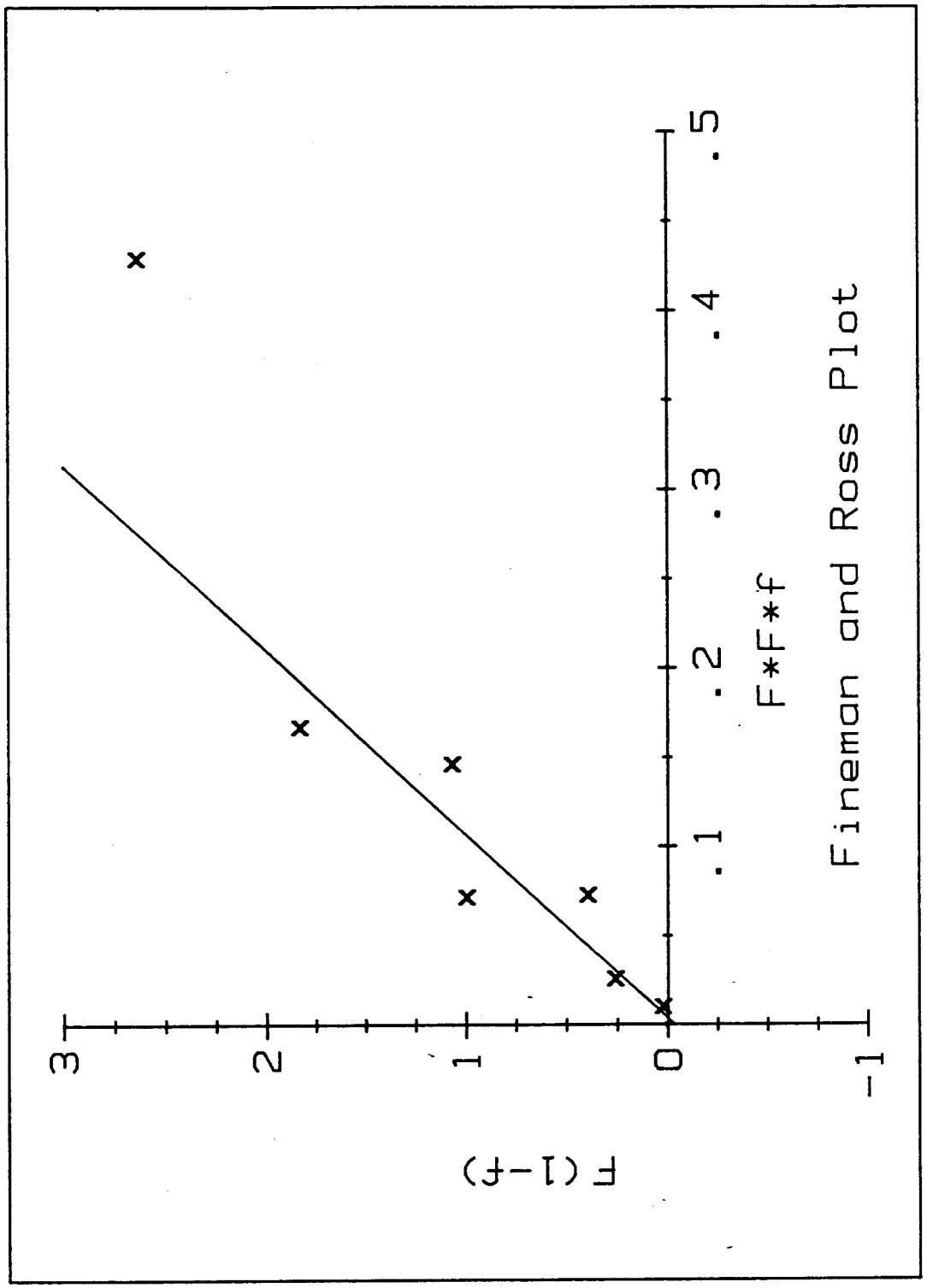

Fig.II.16

only slightly with normalization in parallel to the S/C ratios in Section II.3.2.b.

Table II.14 Reactivity Ratios for 1.3 V ACN Polymerizations

Method Used for % PY in Poly. Calculations	Reactivity Ratio r_1 for PY (slope)	Reactivity Ratio r_2 for BT (-intercept)	Correlation Coefficient
N/S Ratio	9.7	0.04	0.84
N/S (norm.)	9.8	0.08	0.71
N/C Ratio	5.0	0.03	0.96
N/C (norm.)	7.2	0.02	0.57
S/C Ratio	9.7	-0.06	0.79
S/C (norm.)	8.6	-0.03	0.63

From the data in Table II.14 the reactivity ratios can be determined to be 10 and 0.04. As mentioned in Section II.3.2.a, when one reactivity ratio is relatively large and the other is close to zero they are very difficult to accurately define using the F&R method (3,4). For this reason the r_2 reactivity ratio for the S/C calculation is a small negative value rather than positive.

II.3.2.d Copolymerization at 1.5 V in the ACN/TBAP Solvent System

Values of F(1-f) and F^2f were calculated using mole percent PY values calculated using the N/S ratio from Table II.8 and are listed in Table II.15. These values are plotted in Figure II.17 to give a line with a slope of 5.1 and an intercept of -0.31.

Values from the N/C and S/C mole percent PY calculations in Table II.8 were used to calculate F(1-f) and F^2f values for F&R plots. The reactivity ratios and the correlation coefficients

Table II.15 VALUES FOR FINEMAN AND ROSS PLOT FOR SAMPLES POLYMERIZED AT 1.5 V IN ACETONITRILE

Code	Monomer Ratio [PY]:[BT]		F	Percent PY Units in the Copolymer Cal. using N/S	f	F*F*f	(1-f)F
1	58.8	41.2	1.4272	88.30	0.1324	0.2698	1.2382
2	50.3	49.7	1.0121	80.47	0.2427	0.2486	0.7665
3	9.9	90.1	0.1099	29.91	2.3438	0.0283	-0.1477

Figure.II.17 FINEMAN AND ROSS PLOT FOR COPOLYMER POLYMERIZED AT 1.5 V IN ACETONITRILE

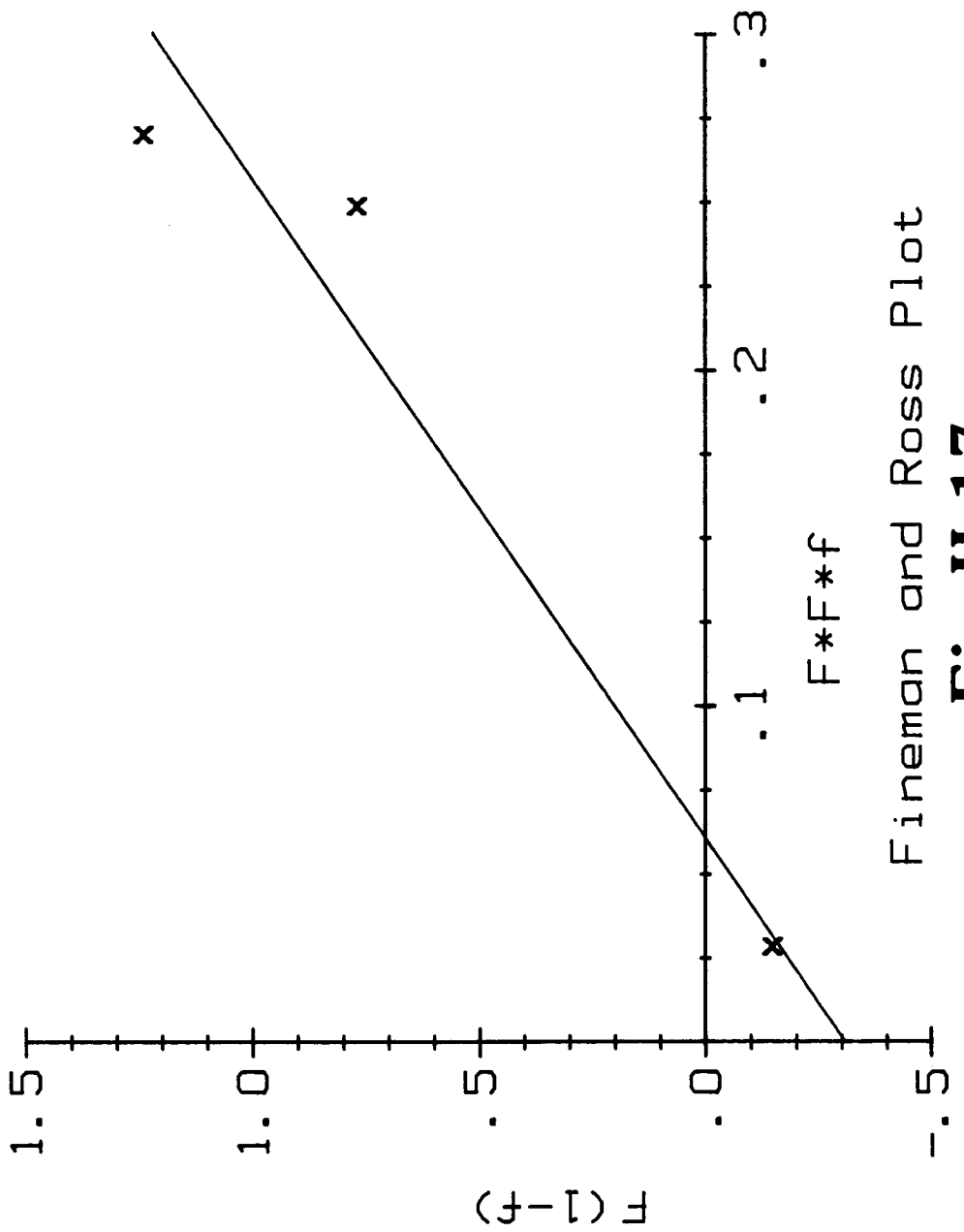

Fig.II.17

for the linear regression of 6 points are listed in Table II.16.

Table II.16 Reactivity Ratios for 1.5 V ACN Polymerizations

Method Used for % PY in Poly. Calculations	Reactivity Ratio r_1 for PY (slope)	Reactivity Ratio r_2 for BT (-intercept)	Correlation Coefficient
N/S Ratio	5.1	0.31	0.93
N/C Ratio	4.2	0.24	1.00
S/C Ratio	6.8	0.70	0.92

The reactivity ratio values from the three different ratio calculations vary significantly. Values from the N/C calculations give the best straight line fit, but the reactivity ratios from N/S calculations are intermediate between those for N/C and S/C, and are affected the least by errors in microanalysis. Thus the reactivity ratios would have to be considered close to those found using the N/S ratios.

II.3.3 Comparisons of Results

For all the copolymerization studies N/S data for appear to be the most accurate. Normalizations of the N/S, N/C and S/C data were attempted to correct for errors in microanalysis and to demonstrate the effects of trapped solvent on the data. Normalization of data may be required for monomer copolymerization systems that do not contain different atoms such as N and S in each monomer.

The reactivity ratios for the two solvent systems are listed in Table II.17. The PC/$LiClO_4$ system shows a greater

preference for PY over BT than the ACN/TBAP system at 1.3 Volts. In both systems increasing the electrode potential increases the relative rate of incorporation of BT into the polymer. The effect of electrode potential is shown graphically in Figure II.18 for the PC/$LiClO_4$ solvent system and in Figure II.19 for the ACN/TBAP solvent system.

Table II.17 Comparison of Reactivity Ratios

Method Used for % PY in Poly. Calculations	Reactivity Ratio r_1 for PY (slope)	Reactivity Ratio r_2 for BT (-intercept)
PC/$LiClO_4$		
1.3 Volts	23	0.03
1.4 Volts	38	0.36
ACN/TBAP		
1.3 Volts	9.7	0.04
1.5 Volts	5.1	0.31

Section II.3 Conclusions

This chapter has shown that the composition of these copolymers can be described by the reactivity ratios of the Mayo-Lewis Equation. These polymers were electropolymerized by radical cation coupling. We have been unable to find a description of such an approach to oxidative copolymerization or electrochemically induced reactions. Thus this is a completely new application of the equation to such systems. The electrode potential has also been shown to control the composition of the copolymers. Thus the composition of the copolymer is controlled by the feed ratios and the electrode potential. In principle

Figure.II.18 COMPARISON OF COMPOSITIONAL CURVES FOR COPOLYMERS POLYMERIZED AT 1.3 AND 1.5 V IN PROPYLENE CARBONATE
A) 1.3 V
B) 1.5 V

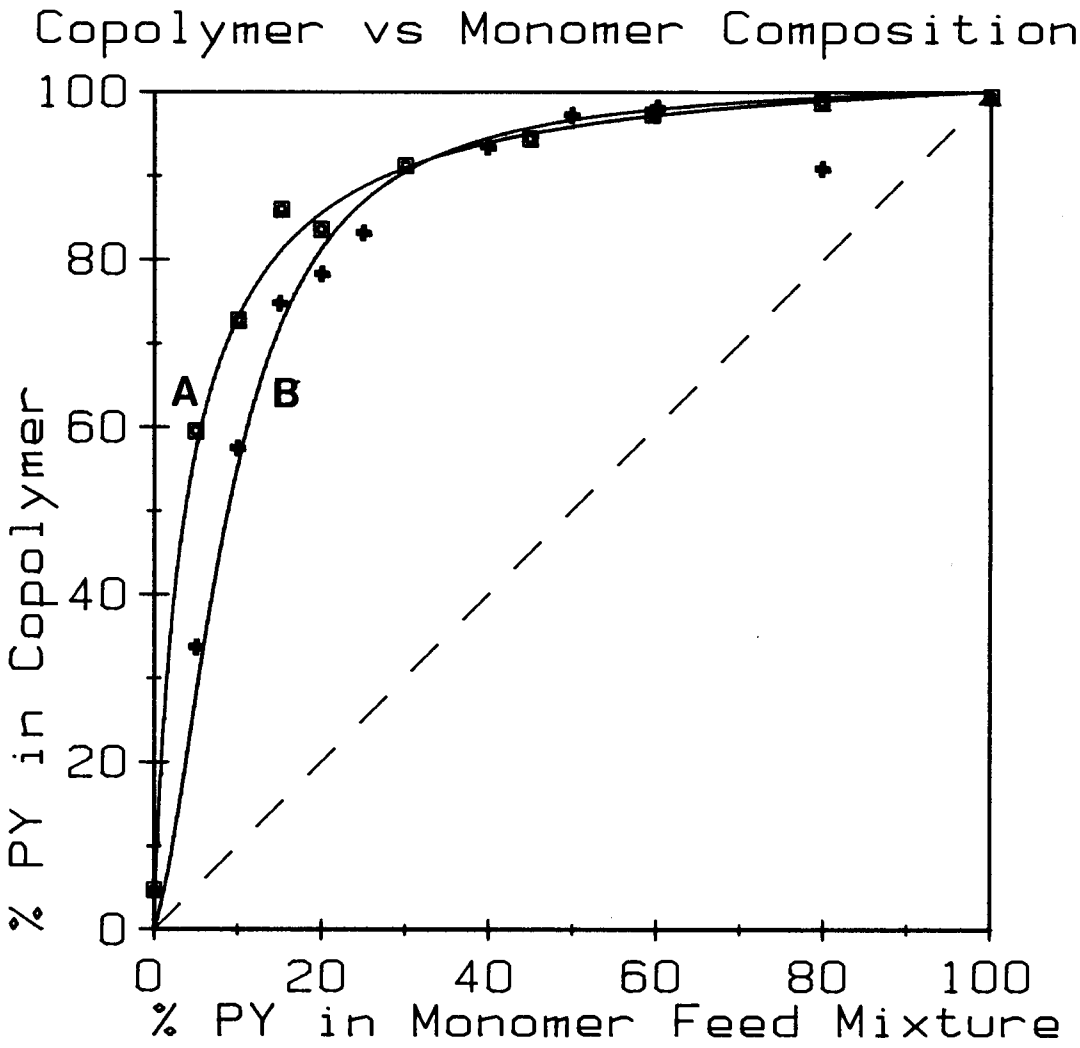
Copolymer vs Monomer Composition
100
80
60
40
20
0
% PY in Copolymer
A
B
0
20
40
60
80
100
% PY in Monomer Feed Mixture

Fig.II.18

Figure.II.19 COMPARISON OF COMPOSITIONAL CURVES FOR COPOLYMERS POLYMERIZED AT 1.3 AND 1.5 V IN ACETONITRILE
A) 1.3 V
B) 1.5 V

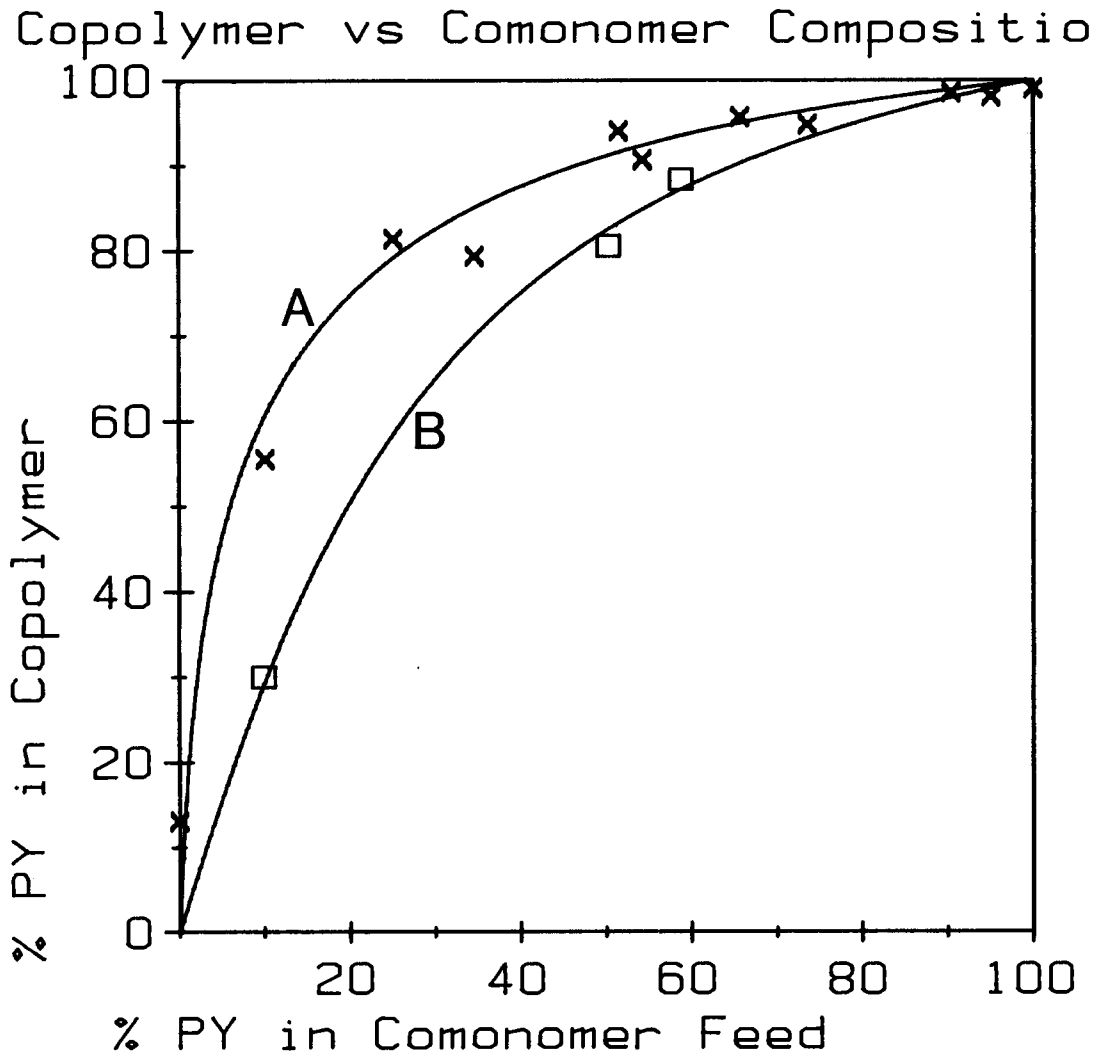
Copolymer vs Comonomer Composition
100
80
60
40
20
0
% PY in Copolymer
A
B
20
40
60
80
100
% PY in Comonomer Feed

Fig.II.19

copolymer compositions can be calculated for any feed ratio and potential for which the reactivity ratios have been determined.

CHAPTER III SCANNING ELECTRON MICROGRAPHS

Section III.1 Introduction

The surface morphologies of PPY [97-99,6,10] and PBT [100,6] have been examined using scanning electron microscopy (SEM). The surface morphologies of electrochemically polymerized conducting polymers change with increasing film thicknesses [100,6], different electrolytes [10], and different solvents [97]. No changes in surface morphologies were observed when the doping electrolytes were removed from the films [99] (ie. when the film is reduced from the doped to the neutral state), when neutral films were exposed to air [99], or when the doping anions were replaced with different anions [10]. The morphology of the surface facing the electrode is distinctly different to that facing the electrolyte. Cross sections of polymer films clearly show this distinction, the electrolyte surface being more irregular, than the surface next to the electrode [98].

SEM of polymer film cross sections have also been used to support electrical conductivity work. Kaneto et al.[49] found that the electrical conductivities of PT films were highly anisotropic; ie. the electrical conductivities parallel and perpendicular differed greatly. Tanaka et al.[8] reported that the conductivity of PT was affected by the temperature and the current density used during polymerization. M. Ito et al. [50] did wide-angle x-ray diffraction and SEM of PT and showed that the films had a fiber texture. The direction of the fibers' alignments changed, from parallel to the electrode at low current densities, to perpendicular at high current densities [50]. Ito et al. suggested that the fibers orient themselves with the

electric field at high current densities but, at lower current densities the field is not strong enough to align the polymer chains with the field.

Current densities on the electrodes during the polymerizations of PY and BT copolymers at +1.3 V, +1.4 V and +1.5 V in this work, do not vary significantly (< 20%). Thus it is difficult to explain the change in reactivity ratios with potential in terms of an effect of current density on fiber orientation. This chapter deals with the examinations of the copolymers for fiber texture to determine the polymer chain orientation on the edges. It was not expected to perceive any differences between the copolymers polymerized at the various potentials.

Section III.2 Experimential

Scanning electron micrographs were taken of two sets of samples. One set was polymerized in a TBAP/ACN solvent system on Pt electrodes and the other set was polymerized in a $LiClO_4$/PC solvent system on Sb-SnO_2 coated glass electrodes. Microanalysis was also done on the $LiClO_4$ polymerized samples so that the compositions of the samples were known.

III.2.1 Purifications

The solvents, monomers and electrolytes for these experiments were purified in the same manner as in section II.2.1.

III.2.2 Apparatus

The polymer samples polymerized in the $LiClO_4$/PC solvent

were also used for the copolymerization study in Chapter II. The apparatus used for their polymerization is described in Section II.2.2.

The other set of samples were polymerized specifically for SEM analysis. The samples were polymerized in a single compartment cell similar to the cell used for cyclic voltammetry in Section V.2.2. (Figure V.3).

The working electrode was made of thin Pt sheet. A thin strip (0.20 cm * 2.0 cm) of Pt sheet was spot welded onto a Pt wire and a 4 mm diameter pyrex tube was sealed to the Pt wire to form an electrode shaft.

The counter electrode was also made of thin Pt sheet. Four cm^2 of Pt sheet was welded onto a Pt wire and a 4 mm diameter pyrex glass tube was sealed to the Pt wire, using a torch to melt the glass.

A Fisher Scientific SCE was used as the reference electrode. The reference electrode was separated from the working compartment by a Luggin capillary and KCl salt bridge.

A highly modified ISI-DS130 dual stage scanning electron microscope was used to take pictures of the surfaces of these polymer films.

III.2.3 Polymerizations

The polymerization techniques for the samples in the PC solvent system are given in section II.2.3.

Before polymerization in ACN solutions the cell, cell tops and glassware were carefully washed and dried in an oven at 90 C to remove any H_2O from the surface of the cell and equipment.

Monomer solutions containing 0.1 M concentrations of BT, PY or both monomers, 0.1 M TBAP and acetonitrile were mixed in 25 ml volumetric flasks. The solvent and the electrolyte were added to the flask first, the solutions were bubbled with Ar to remove O_2 from the system and prevent the oxidation of the monomers and then the monomers were added to the solutions. The cells were flushed with Ar before they were charged with 15 ml of monomer solution. An Ar atmosphere was maintained in the cell throughout the reaction to prevent oxidization of the monomer.

The potential on the working electrode was maintained at a selected value relative to a SCE reference electrode by a potentiostat (SFU electronic shop construction) and monitored using a Fluke 8840A multimeter. The polymerization potential was set at 1.35 V for all polymerizations.

Only a small fraction of the 2.0 cm long electrode was dipped into the monomer solution for each polymerization. After each polymerization the small piece of the electrode on which polymer had formed was snipped off, washed with clean solvent and dried in a vacuum for 24 hours.

III.2.4 Scanning Electron Microscope Analysis

The pieces of polymer were mounted on graphite or aluminum studs with electrically conducting silver Electrodag 415 (Achenson) for examination in the scanning electron microscope. Samples polymerized in ACN solutions were not removed from the Pt electrode, A small piece of the electrode was mounted on the stud with the polymer coated on it. The pieces of polymer from the PC solutions, which had been removed from the electrodes were

mounted on edge and horizontally to get two different surface views of the same film. No coating of the films with metal was required as the films were analyzed in their conducting forms.

SEM photographs of the samples were obtained with magnifications of 100-20,000 X. The measurements were made using various tilt angles to compensate for irregularities in the surface of the films and to align the edges of the films with the detector. Photographs of ACN samples were initially taken at 25 kV, the electron acceleration voltage, but the films showed evidence of charging at these high potentials and clarity of the photos were enhanced by reduction to 5-10 kV.

Section III.3 Results and Discussion

III.3.1 Samples Polymerized in ACN Solutions

Three samples were prepared for SEM photographs: homopolymers of PY and BT and a 50:50 copolymer of BT and PY. SEM photographs were taken of the film's surfaces at magnifications of 245 and 1000 times. The surfaces of PPY and the copolymer (Figures III.1. and III.3) appeared very smooth, but PBT (Figure III.2) appeared very porous and almost sponge like. Small scratches from the mounting of the films on the studs can be seen in the surfaces. The texture lines across PPY and the copolymer are most likely from the duplication of the rolling lines of the Pt sheet on which they are polymerized.

Although the copolymer's surface morphology is distinctly different to PBT's morphology, it is quite similar to that of PPY. The only difference in the photographs of PPY and the

copolymer are the small areas of lighter intensity on the copolymer. Whether these areas are different polymer composition or not can only be speculation but they do not appear to be just electrolyte crystallized on the surface (Figure III.4)

III.3.2 Samples Polymerized in PC solutions

The surfaces of samples, polymerized at 1.4 V and 1.3 V in PC, were examined using SEM. The samples examined are listed in Table III.1 along with their compositions.

Figures III.5,6,8 are three different views of sample # C01 (PPY polymerized at 1.3 V). Figure III.5 is a photograph of the surface of the polymer which contacts the monomer solution during polymerization. The irregular white shapes on the surface are crystals of electrolyte which have formed on the surface during the drying of the polymer film. The crystal's composition was determined using the EG&G ORTEC X-ray Analysis attachment on the SEM. Large X-ray peaks were found for Li and Cl during the electron bombardment of the crystals. Figure III.6 is the edge view of the PPY film. Note the crystals of electrolyte on the edge of the film. These crystals appear to be on the surface of the edge, but closer views of the edges of other polymer films (eg. Figure III.20) indicate that the crystals have grown within the film. If the polymer is fully oxidized we would not expect to find $LiClO_4$ in the polymer film, but work by J.H. Kaufman et al. [121] suggests that during reduction the mobile Li cation moves into the film to balance the charge. As some reduction of the polymer may occur even if the polymer is just standing in solution [122] it is possible that some reduction of the polymer

Figure III.1 Electronmicrograph of Polypyrrole polymerized on a Pt Electrode

Figure III.2 Electronmicrograph of Poly(2,2'-Bithiophene) polymerized on a Pt Electrode

Figure III.3 Electronmicrograph of the copolymer polymerized on a Pt Electrode

Figure III.4 Electronmicrograph of the copolymer polymerized on a Pt Electrode

Figure III.5 Electronmicrograph of the Surface of a Polypyrrole Film

Figure III.6 Electronmicrograph of the Edge of a Polypyrrole Film

Figure.III.1

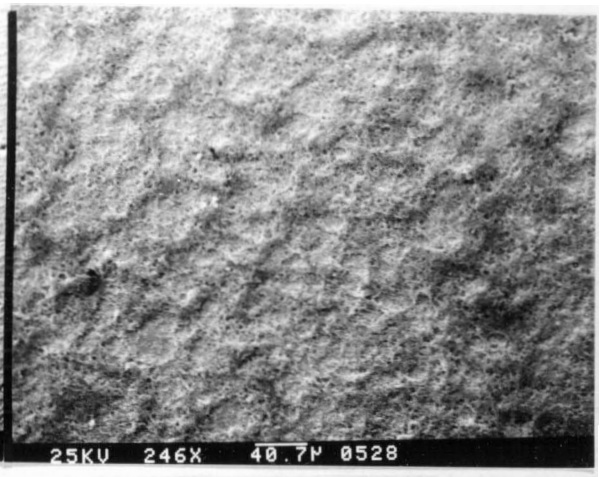

Figure.III.2

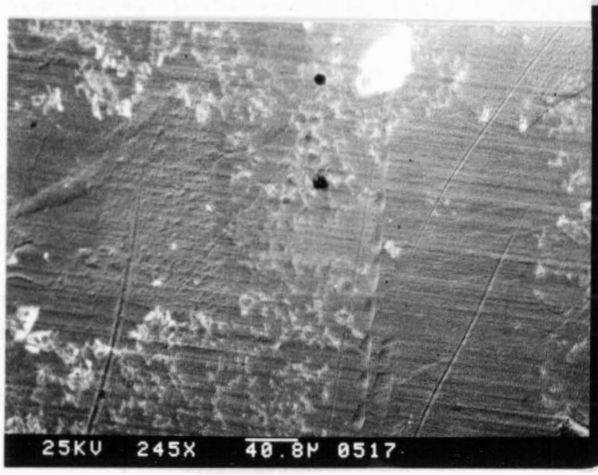

Figure.III.3

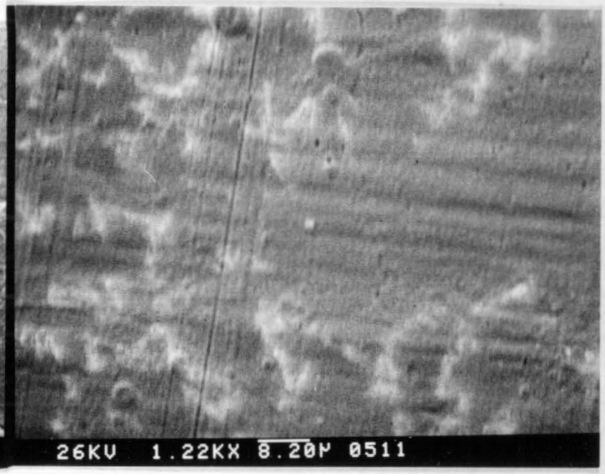

Figure.III.4

Electrode facing surface

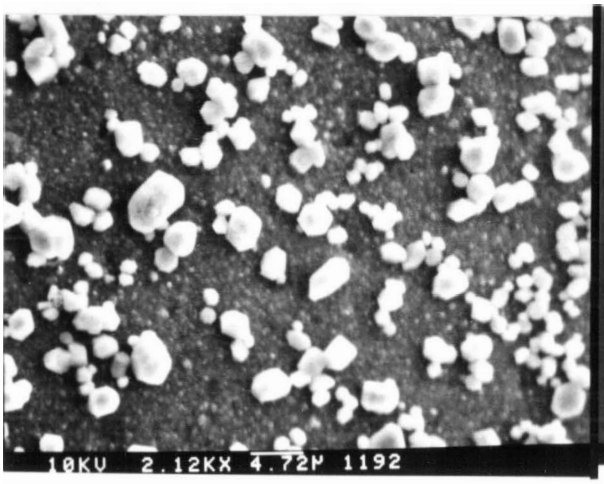

Figure.III.5

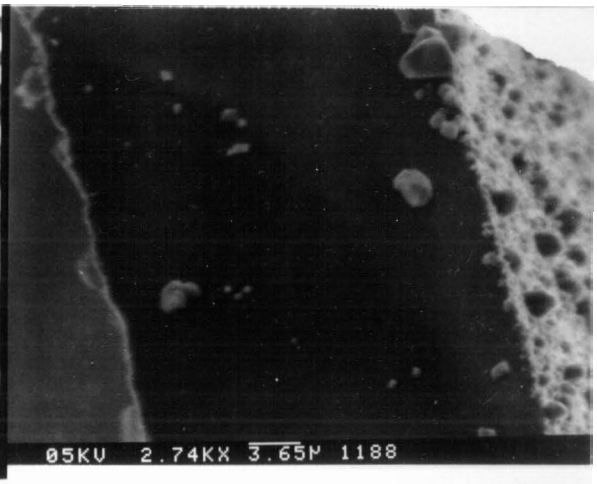

Figure.III.6

occured before the electrolyte solution was removed from the polymer's surface. Thus the SEM of $LiClO_4$ crystals formed within a polymer film during drying is the first hard evidence to support Kaufman's theory.

The thickness of the film, appears to be approximately 27.4 μm ± 0.4 μm using this view, which is not aligned for exact measurements. Figure III.8 is a high magnification (20,600 X) view of the surface of the PPY film. This view shows that the film is extremely smooth compared to the other conducting polymers.

Table III.1 Composition of Samples Analyzed

Sample #	Percent PY in the Monomer	Mole Percent PY in the Polymer	Film Thickness in microns
1.3 V			
CO01	100.00	100.00	27.4
CO02	0.00	0.00	36.3
CO10	4.97	59.45	32.2
1.4 V			
06-CO-86	24.95	83.17	
07-CO-86	19.95	78.24	24.5
08-CO-86	14.96	74.74	27.8
11-CO-86	0.00	0.00	77.4
14-CO-86	49.87	97.20	

Figures III.7,9,10 are the pictograms of sample # CO2 (PBT polymerized at 1.3 V). Figure II.7 is a view of the surface facing the electrolyte during polymerization. The surface morphology of PBT appears much more irregular than that of PPY polymerized under the same conditions. The surface structures of the film resemble those of pillow lavas and cumulus clouds indicating an almost radial growth of the polymer from single

points along the film. Small crystals of electrolyte can be seen dispersed around the surface of the polymer.

Figure III.9 is the edge view for the PBT film. The surface facing the electrode is much smoother than that facing the electrolyte. Fiberous texture lines can be seen starting on the electrode surface of the polymer and traveling about two thirds the way through the polymer film. Figure III.10 is a close up of this layering showing how fine the texture is. According to M. Ito et. al. these layers stacked perpendicular to the electrode are due to the alignment of the polymer chains. As this directionality seems to extend only two thirds the way through the film, growth in the area of the electrode during polymerization may change the charge density on the electrode surface enough to cause a reorientation in the direction of growth of the polymer chains.

Figures III.7.11-14, are three different photographs of sample # CO10 (a 50:50, BT:PY copolymer polymerized at 1.3 V). Figure III.11 is a view of the surface facing the electrolyte during polymerization. Close inspection of this surface (Figure III.12) shows that the surface is coated with electrolyte crystals and none of the polymer surface can be seen. Figure III.13, the edge view for the polymer film, shows the large coating of crystals on the surface facing the electrolyte and a few crystals in the interior of the polymer. The edge view shows a polymer which appears quite granular in nature. Although these structures are relatively large (200 nm), both the electrode facing surface and the electrolyte facing surface are relatively smooth compared to the surfaces of PBT in Figure III.9. Close

Figure III.7 Electronmicrograph of the Surface of a Poly(2,2'-Bithiophene) Film

Figure III.8 Electronmicrograph of the Surface of a Polypyrrole Film

Figure III.9 Electronmicrograph of the Edge of a Poly(2,2'-Bithiophene) Film

Figure III.10 Electronmicrograph of the Edge of a Poly(2,2'-Bithiophene) Film

Figure III.11 Electronmicrograph of the Surface of a Copolymer Film

Figure III.12 Electronmicrograph of the Surface of a Copolymer Film

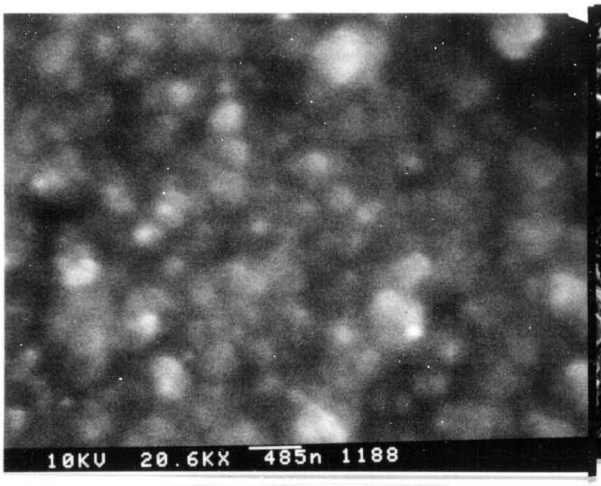

Figure.III.8

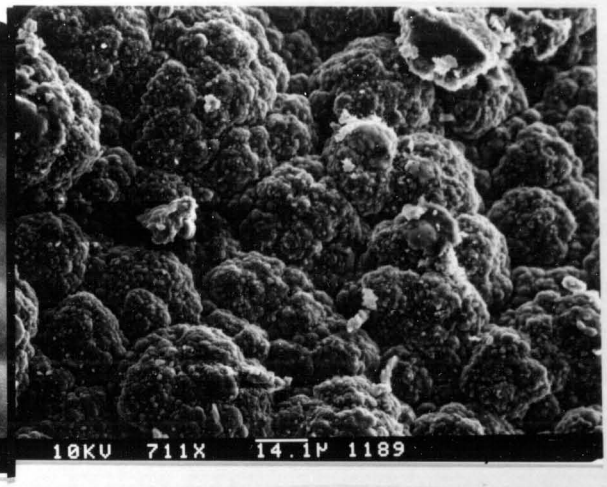

Figure.III.7

Electrode facing surface

Electrode facing surface

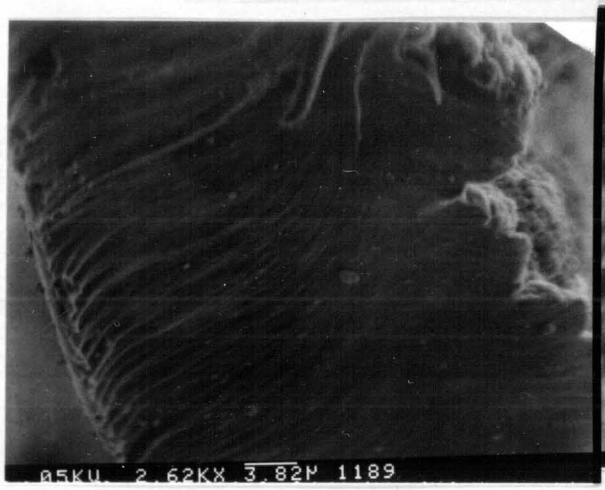

Figure.III.9

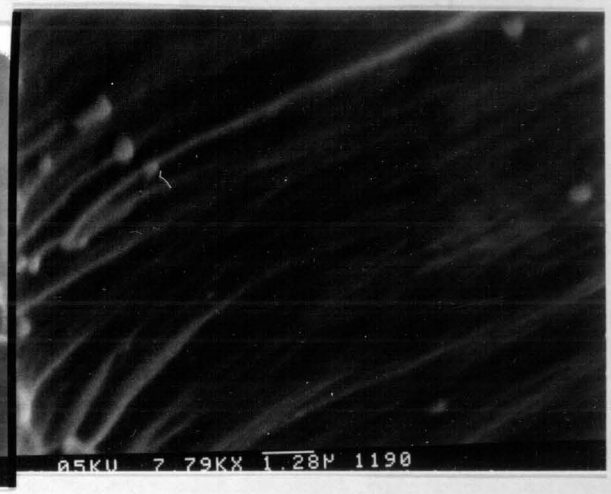

Figure.III.10

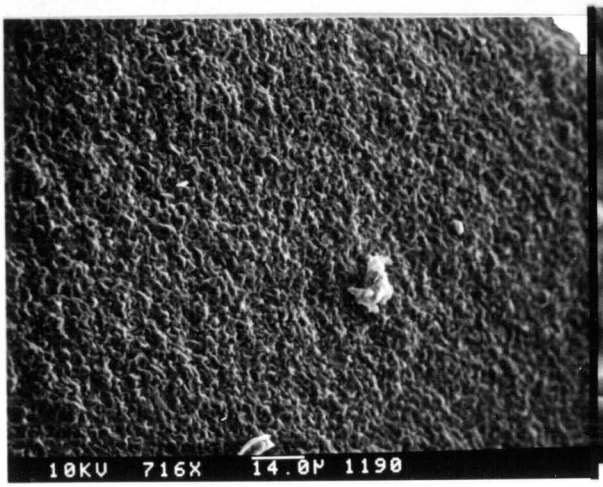

Figure.III.11

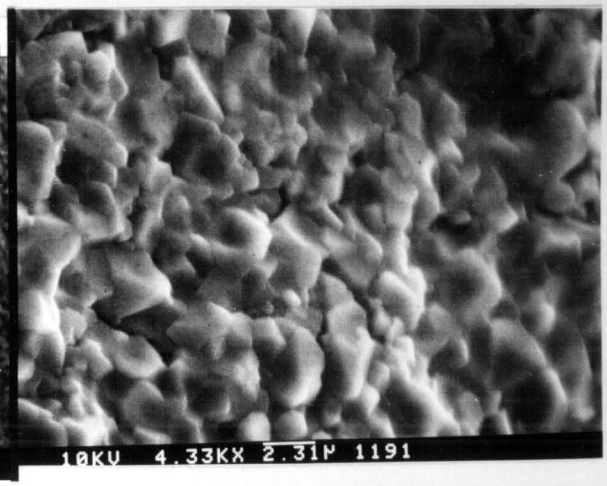

Figure.III.12

inspection of the film (Figure III.14) does not show whether the granules represent two phases of the polymer or a porous structure. The layering on the edge would indicate that some ordering of the polymer chains occurs when the current density on the electrode is high. The thickness of the polymer is approximately 20 percent greater than the other polymers measured, indicating that the polymer may be somewhat porous.

Figures III.15-18 are pictograms of copolymers of varying composition polymerized at 1.4 V. All the samples show a similar surface morphology and each has a few crystals of electrolyte on the surface. The surface morphology of PBT (Figure III.22) polymerized under the same conditions is considerably more textured than the copolymers. The surface of PBT is similar to that of PBT polymerized at 1.3 V (Figure III.5).

The edge views of sample # 07-CO-86 and 08-CO-86, figures III.19 and III.21 are quite similar in appearance. Both show a layered structure along the electrode facing surface and electrolyte crystals with in the polymer. A close up view (Figure III.20) of sample # 07-CO-86 shows the fine layering along the surface edge of the polymer.

Figure II.23 is the edge view of PBT showing the extremely porous nature of the polymer. Unlike the other polymers photographed, PBT, polymerized at 1.4 V has only a relatively thin continuous layer ($\approx$10 μm) on the surface facing the electrode and the greater volume of the polymer is an extremely porous layer. The porous structure is double the thickness of the other polymers measured although equal amounts of polymer were polymerized on the electrodes.

Figure III.13 Electronmicrograph of the Edge of a Copolymer Film

Figure III.14 Electronmicrograph of the Edge of a Copolymer Film

Figure III.15 Electronmicrograph of a Surface of a Copolymer Film

Figure III.16 Electronmicrograph of a Surface of a Copolymer Film

Figure III.17 Electronmicrograph of a Surface of a Copolymer Film

Figure III.18 Electronmicrograph of a Surface of a Copolymer Film

Electrode facing surface →

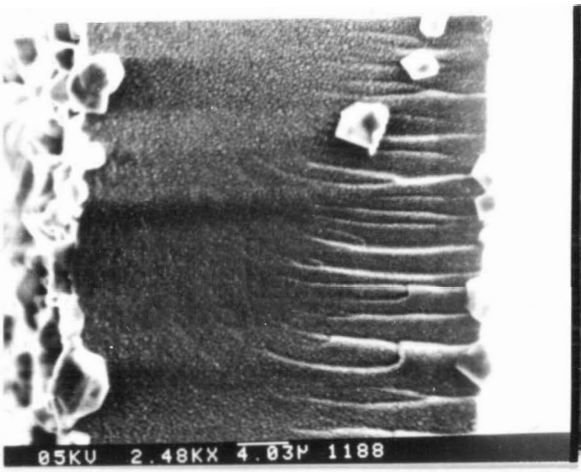

Figure.III.13

Electrode facing surface →

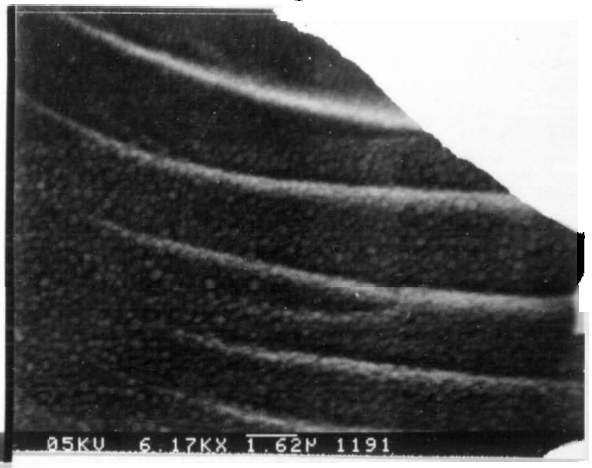

Figure.III.14

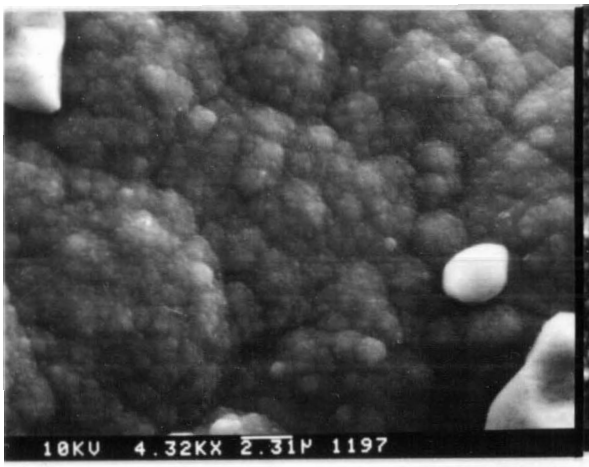

Figure.III.15

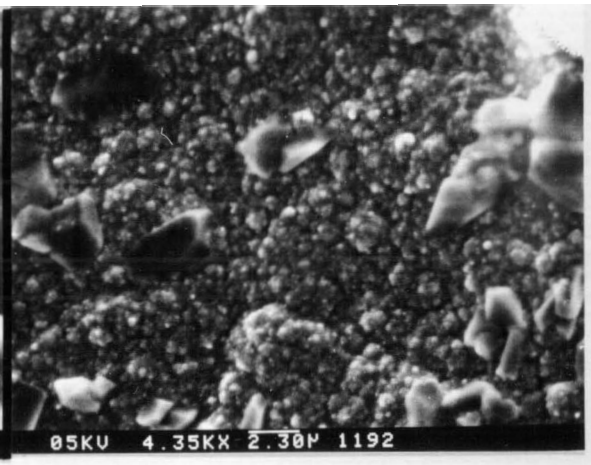

Figure.III.16

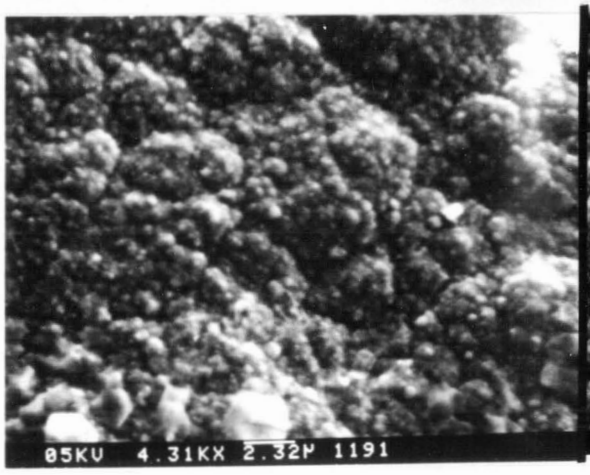

Figure.III.17

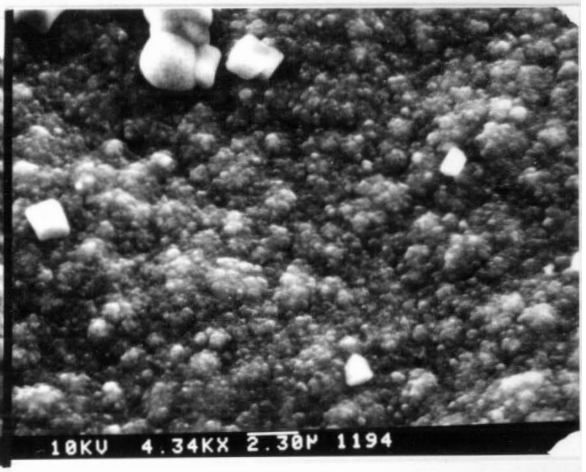

Figure.III.18

Figure III.19 Electronmicrograph of the Edge of a Copolymer Film

Figure III.20 Electronmicrograph of the Edge of a Copolymer Film

Figure III.21 Electronmicrograph of the Edge of a Coploymer Film

Figure III.22 Electronmicrograph of a Surface of a Poly(2,2'-Bithiophene) Film

Figure III.23 Electronmicrograph of the Edge of a Poly(2,2'-Bithiophene) Film

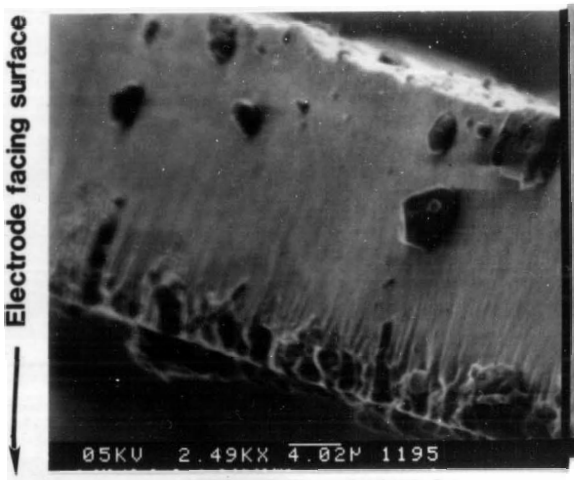

Figure.III.19

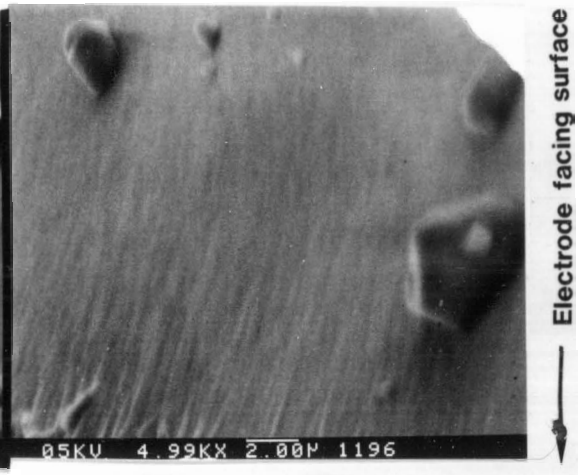

Figure.III.20

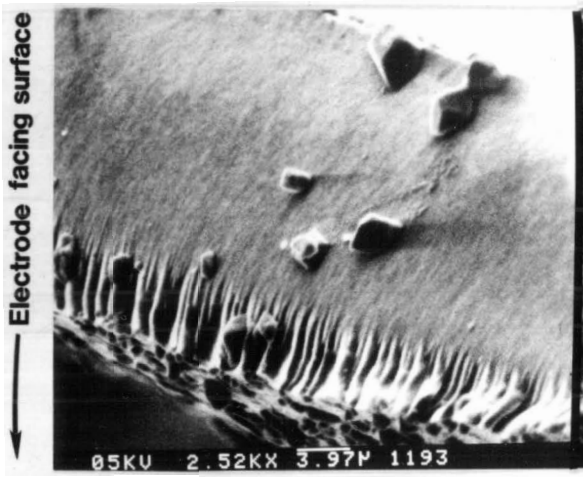

Figure.III.21

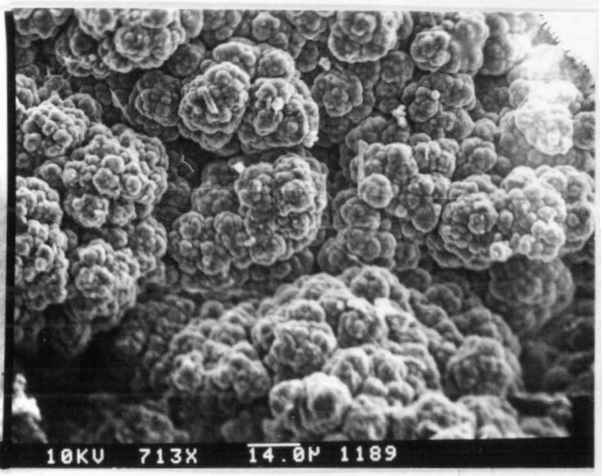

Figure.III.22

Electrode facing surface

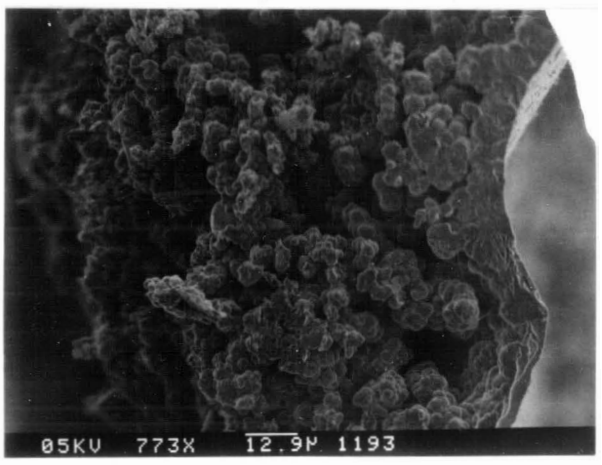

Figure.III.23

Section III.4 Conclusions

Many more questions are raised by pictographs in this chapter than are answered. This chapter has shown that electrolyte contamination can be a significant factor in the analysis of the copolymers composition. It is also shown that the surface morphologies of the copolymers are significantly different than the homopolymers, although a comparison of the change in morphology with composition was not attempted.

Many of the polymers showed evidence of layering perpendicular to the surface on the edge near the electrode facing surface, but the orientation of the polymers decreased as the polymer grew on the electrode. This decrease in orientation could be due to the decrease in current density on the electrode surface, as a result of the growth of polymer increasing the electrode area. No conclusions could be drawn from these observations. Current densities will need to be varied significantly (500 %) [50] and the electrode areas kept constant for the copolymer structure to be compared to Ito's results.

It is shown that the thickness of the polymer films can be accurately measured using the SEM. These thickness values are important for the calculation of the polymer's conductivities although the thickness measurements made here were not used for conductivity calculation in this thesis.

CHAPTER IV MEASUREMENT OF ELECTRICAL CONDUCTIVITY

Section IV.1 Introduction

As stated in section I.3 the charge carrying species in doped PPY and PBT is thought to be the bipolaron. This theory is still controversal but the fact is, these polymers conduct electricity. Measurement of conductance in films can be done using various methods. Most of the techniques were first developed for the semiconductor industry by companies such as Bell Telephone [101] and Phillips Electronics [102]. The technique most commonly used for thin films of conducting polymers is the four point probe technique. This technique uses four probes or interface connections evenly spaced in a line (see Figure IV.1) on the surface of the film. A constant current is applied to the outer two electrodes and the voltage drop is measured between the inner two electrodes. The conductivity is calculated using these two measurements along with the dimensions of the film and the distances between the probes [106].

The conductivity of these polymers is affected by a number of variables. The type of dopant used [10,100] and the degree of anion doping [100] have both been shown to affect the conductivity of the polymer. In general the greater the percentage of doping anions in the polymer the greater the conductivity. For most polymers there is a finite number of doping anions that can be incorporated into the polymer, approximately one anion to four heterocyclic rings, therefore there is a maximum conductance value for each polymer-dopant system.

Figure.IV.1 FOUR POINT PROBE DIAGRAM APPARATUS

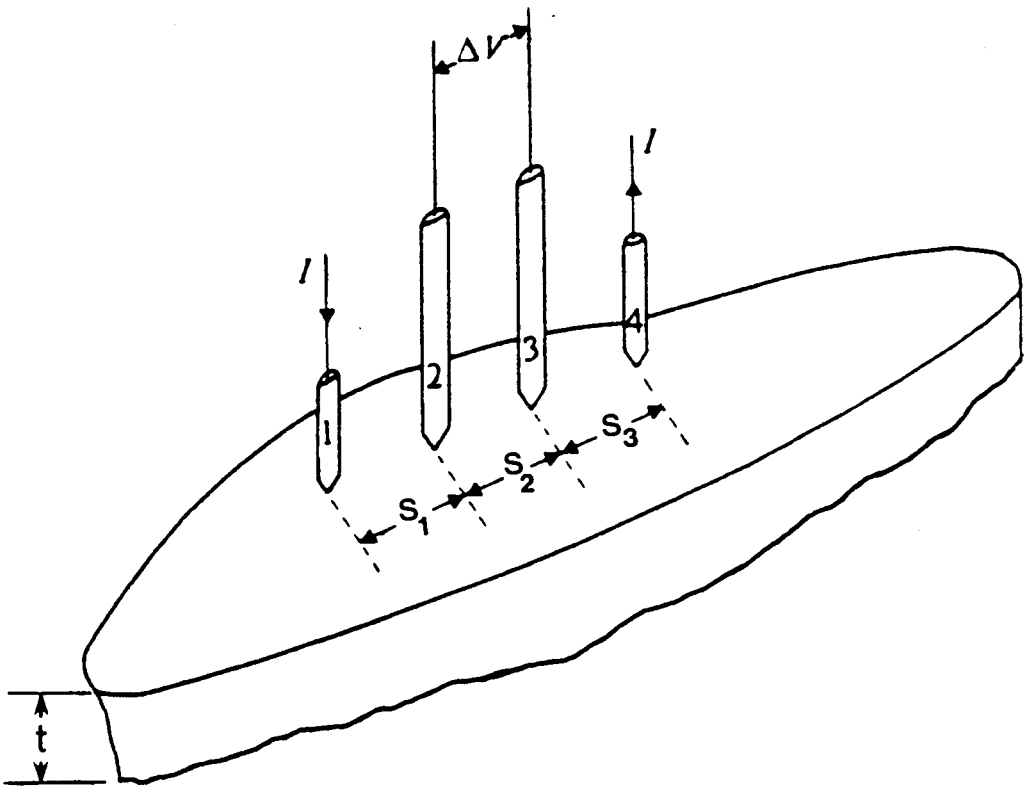

Figure.IV.1

Although there is no direct correlation between the conductivity of the polymer film and the size of the anion, generally polymers doped with very large anions such as potassium poly(vinylsulfate) and soduim poly(styrenesulfonate) [105] have lower conductivities than polymers doped with halides or other relatively small anions. The conductivity appears to be adversely affected when the anion is large enough to influence the ordering of the chains within the polymer substrate.

The conductivities of the polymers have been shown to be temperature dependant [103]. The conductivity of the polymers increases with the temperature in the range from 100 K to 400 K. This is opposite to the trend found for metals and similar to that of n-type semi-conductors. The conductivity of the films are also affected by the temperature of the polymerization mixture [122]. Polymers [104] polymerized at temperatures below 30°C (in PC) were found to be approximately 4 times as conductive as those polymerized at 50°C.

The length of the polymer chain affects the conductivity of the films. The longer the polymer chains in the film the higher the conduction. As mentioned in Sections I.3 and III.1 Kaneto et al. [40] found that the films conductivity was anisotropic, thus the conduction between chains is much more difficult than along the chain. The shorter the chain the greater the number of times the polaron or bipolaron must jump between the chains and the lower the conductivity.

The conductivities of the polymer films are enhanced by stretching. M. Ogasawara et al. [104] stretched PPY films up to 2.2 times their original length and found that conductivities

increase by a factor of 3. Wide angle X ray diffraction patterns of these stretched PPYs indicated that the polymer chains are roughly ordered in the direction that was stretched, consequently increasing the conductivity of the film.

B. Lundberg et al. [105] found that the conductivity of PPY was dependent on the pressure applied to the film. Films were placed in a hydrostatic pressure apparatus and pressures up to 2.5 gigapascal were applied. The conductivities were measured using the four-point probe method. Lundberg found that the conductivity increased with increasing pressure and fit this data to a variable range hopping model, to show that the major effect of pressure is to reduce the distance between hopping sites.

Various methods have been used to polymerize copolymers with PY and thiophene units in the chain [71,72,78,80]. Inganas et al. [71] polymerized terthiophene (TT) and pyrrole together and found that the conductivity was intermediate between those of the homopolymers, but the conductivity of polyterthiophene (PTT) is significantly lower than PPY (between 1000 and 100,000 times) and the composition of these copolymers were not given, therefore this result may be specific to only the sample tested and not the copolymers in general.

S. Naitoh et al. [72] electropolymerized a dimer containing a PY and a thiophene ring joined at the α position and found that the conductivity of the copolymer was much higher than that of similarly prepared PPY and polythiophene. As this copolymer is an even mixture of both monomer units these results are far more significant.

G.G. McLeod et al. [80] polymerized a trimer, 2,5-di-(-2-thienyl)-pyrrole to form a copolymer that would approximate an alternating copolymer of PY and BT. Conductivity measurements of the films was found to be difficult due to the irregularity of the films surfaces and thus values are given only for measurements of films at low doping levels.

Section IV.2 Experimental

IV.2.1 Sample Preparation

Similar problems to those encountered by McLeod et al. were encountered for copolymer of PY and BT. The surface morphology of continuous films of PPY and PBT, as shown in the electron micrographs of chapter III, are significantly different. Obtaining uniform polymer films of PPY and PBT, polymerized in the same solvent system, with sufficient film strength to allow the removal from the electrodes for conductivity measurements was very difficult. The system that worked well for one homopolymer tended to work poorly for the other. After many experiments with many different solvent systems the $LiClO_4$/PC system was found by chance during the polymerization experiments for Chapter II. Conductivity measurements were made on the films polymerized for the composition work at 1.3 V in the $LiClO_4$/PC system.

The samples were initially polymerized for the experiments in chapter II. Samples were polymerized at 1.3 V in the $LiClO_4$/PC solvent system using the apparatus and techniques described in sections II.2.2 and II.2.3. After the initial drying of the polymer films for 24 hours at reduced pressure the films were lifted from the electrodes and mounted on the tacky side of a "3M

Postit". The "Postit" was used because the sticky polymer on its surface would not transfer glue to the samples, which were needed for further analysis.

IV.2.2 Conductance Measurements

The four point probe apparatus was constructed from a machinist's surface gauge. The arm from the gauge was removed and replaced with a steel rod, to which was fastened a plastic plate. Four holes were drilled into the plate so that 4 small brass screws could be threaded into the holes and four more holes were drilled so that steel spring wire fastened under the screws could wind through the holes to the end of the plastic plate. The wires were then bent so that they were all of equal distance apart and the points of the wires were in a line below the edge of the plastic sheet. The rod can easily be lowered so that the points can contact a polymer film and the pressure on the points can be adjusted easily using a tension knob on the surface gauge.

The current was passed through the outer two electrodes using a Hewlett Packard 6215A voltage and current regulator and monitored using a Fluke multimeter model 8000 A. The potential between the center two electrodes was measured using a Fluke multimeter model 8840A.

The contacts the probes made with the films were checked using a simple current doubling test. The current through the film was doubled from an original reading and the voltage was measured between the inner two electrodes. If the voltage readings were linear with the current then the contacts were considered good.

Current and voltage readings were taken at various points near the center of the film. These multiple readings were then averaged to give an approximate value.

IV.2.3 Measurement of the Films Dimensions

While the measurements for the conductance of the film were being taken, the dimensions of the film's surface were mapped, with the positions and spacings of the probes noted (Figure IV.2). These dimensions were later used in the calculations of the conductivity.

After the current and voltage measurements had been made on each sample film a small piece in the center of the film was cut out. The pieces were then mounted on edge on glass microscope slides using Parafin wax. Measurements of the thickness of the films were then made using a Ziess light microscope which had an eye piece with a calibrated scale etched on it. Multiple measurements were made and the average was recorded with the error.

Section IV.3 Results and Discussion

IV.3.1 Calculations of Conductivity

The calculation of the conductivity from the current and voltage measurements made using a four point probe is a difficult proceedure. Corrections must be made using the dimensions of the film and the distances of the spacings between the probes. The geometry of the four-point resistivity measurements is given in figure IV.1. The potentials at probes 2 and 3 are given by the equations:

Figure.IV.2 Dimensions of Film

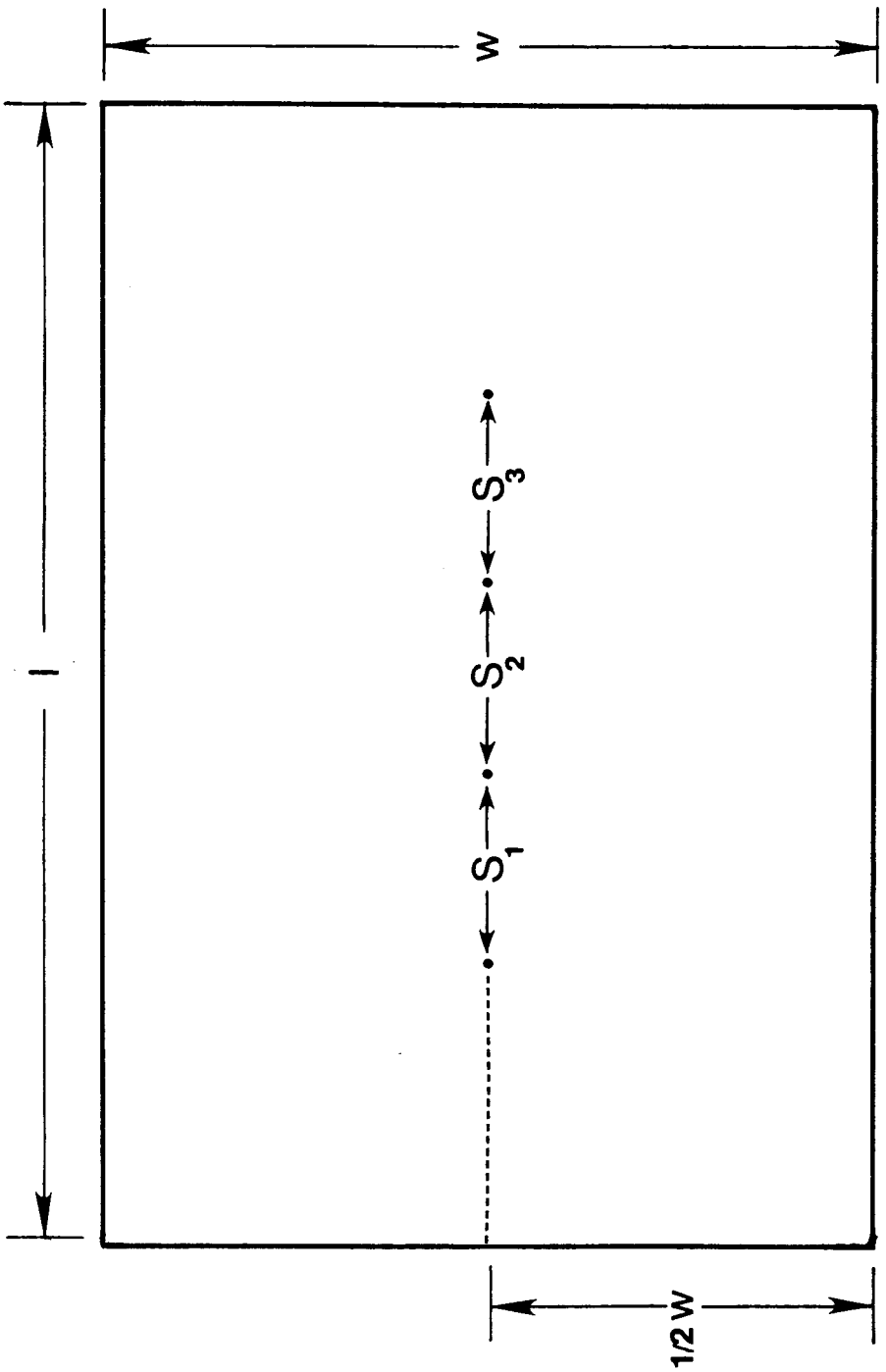

Figure.IV.2

$$V_2 = \frac{q}{S_1} - \frac{q}{S_2 + S_3} \qquad [4.1]$$

$$V_3 = \frac{q}{S_1 + S_2} - \frac{q}{S_3} \qquad [4.2]$$

where q is the strength of a source corresponding to the current I. The potential difference V between probes 2 and 3 is

$$V = q\left[\frac{1}{S_1} + \frac{1}{S_3} - \frac{1}{S_2 + S_3} - \frac{1}{S_1 + S_2}\right] \qquad [4.3]$$

the probe spacings are made to be equal then $S_1 = S_2 = S_3 = s$ and equation 4.3 simplifies to $V = q/s$.

If one considers the points on the probes to be hemispherical surfaces of infinitesimal radius r one sees that

$$I = \frac{1}{\Gamma} \times \text{area} \times E = \frac{1}{\Gamma}\, 2\, r^2\, \frac{q}{r^2}$$

or

$$q = I\Gamma/2 \qquad [4.4]$$

where Γ is the resistivity and $E = q/r^2$ is the magnitude of the electric field. Therefore

$$\Gamma = 2\, s(\, V/I) \qquad [4.5]$$

When the four-point probe is applied to a solid that is not approximately semi-infinite, a potential difference will still be observed when a current flows, so we will define an "apparent resistivity" Γ_o by

$$\Gamma_o = 2\, s(\, V/I) \qquad [4.6]$$

The true resistivity is given by

$$\Gamma = \Gamma_o/C.D. \qquad [4.7]$$

where C.D.

TABLE IV.1
Potential, Current and Dimension measurements for polymer films and calculated correction factors C for conductivity calculations.

Sample no.	Film Thickness in microns	V (mV)	I (mA)	w/s	l/w	C
CO01	39.6±2.4	10.9	5.65	6.75	0.873	3.76
		12.0	5.65	6.75		3.76
		6.7	3.57	6.75		3.76
CO03	40.0±3.3	30.0	7.90	6.73	1.070	3.76
		63.2	14.80	7.00		3.79
		82.7	19.68	6.45		3.73
CO04	36.0±1.0	3.2	0.32	6.88	1.070	3.78
		10.7	1.87	6.61		3.74
		9.6	1.66	6.61		3.74
		4.1	0.62	6.37		3.70
CO05	28.0±1.0	17.1	0.99	6.25	1.020	3.69
		37.5	2.01	6.25		3.69
		67.0	5.81	6.25		3.69
CO06	27.5±1.0	57.5	4.11	6.50	1.058	3.72
		45.3	3.09	6.00		3.65
		62.1	4.01	6.29		3.69
CO07	29.6±1.7	2.7	0.13	6.46	0.966	3.72
		5.2	0.29	7.00		3.79
		3.9	0.16	7.00		3.79
CO08	39.2±1.2	4.1	0.07	7.64	0.933	3.89
		4.7	0.07	6.46		3.72
		6.0	0.05	7.64		3.89
CO02	46.0±2.0	47.7	11.50	8.73	0.906	4.04
		74.4	17.01	8.73		4.04
		70.4	16.09	8.73		4.04
		63.4	14.71	8.73		4.04
		47.9	11.50	7.62		3.88

For thin slices C.D. is calculated from the formula

$$C.D. = s/t\ [2\ln 2 + N(s/2t) - N(s/t)] \qquad [4.8]$$

where t is the thickness of the film and N is a complicated function given in tables in reference [101]. If the slice thickness t is less than half the probe spacings s, C.D. = (2ln2)s/t and equations 4.6 and 4.7 give

$$\Gamma = t(V/I)\ln 2 = 4.53t(V/I) \quad (\text{for } w << 1/2s) \qquad [4.9]$$

Equation 4.9 gives the value for the bulk resistivity Γ_v. The sheet resistivity (Γ_s) is equal to the bulk resistivity divided by the thickness of the film t. ($\Gamma_s = \Gamma_v/t$)

Table IV.2
Correction Factor C for the calculation of the sheet resistivity measured with collinear four-point probes placed on a symmetry axis (after F.M. Smits [107])

w/s	Square C for l/w = 1	Rectangle C for l/w = 2	Rectangle C for l/w = 3	Rectangle C for l/w ≥ 4
1.0			0.9988	0.9994
1.5		1.4788	1.4893	1.4893
2.0		1.9454	1.9475	1.9475
3.0	2.4575	2.7000	2.7005	2.7005
4.0	3.1137	3.2246	3.2248	3.2248
5.0	3.5098	3.5749	3.5750	3.5750
10.0	4.2209	4.2357	4.2357	4.2357
20.0	4.4516	4.4553	4.4553	4.4553
∞	4.5324	4.5324	4.5324	4.5324

The calculations of the bulk resistivities and the sheet resistivities for the polymer samples were done using equations 4.10 and 4.11 taken for "Laboratory Notes on Electrical and

Galvanomagnetic Measurements" [108] by H.H. Wielder and Table IV.2.

$$\Gamma_v = (V/I)t * C(w/s,l/w) \quad [4.10]$$

$$\Gamma_s = (V/I) * C(w/s,l/w) \quad [4.11]$$

The w/s and l/w ratios for the samples, used in the determination of the correction factor C, are listed on Table IV.1. The C values listed on Table IV.1 were determined by extrapolating between the values given on Table IV.2. The resistivity values were calculated using these C values and the V and I data for the samples and the results are listed on Table IV.3. The conductivity values listed on Table IV.3 are the reciprocal of the bulk resistivity values Γ_v. Note that the conductivity of homopolymers (CO01 and CO02) are greater than most of the copolymers. When the conductivity values are plotted against the percent BT units in the copolymer samples (Figure IV.3) one can see an almost exponential decrease in the conductivity with increasing BT units in the polymer. As this graph is plotted to only about 10 percent BT units in the samples, and the conductivity of PBT is much higher than the high percentage copolymers, we would expect that there would be a minimum conductivity value for some intermediate composition and that the conductivity would increase with increasing percent BT in the copolymers after this minimum value.

The results are different than those found by Naitoh et al. [72] or Inganas et al. [71] as the conductivity of the copolymer is lower than that both of the homopolymers. The results from the copolymerization of terthiophene and Pyrrole [71] are meaningless

Figure.IV.3 CONDUCTIVITY VERSUS COMPOSITION GRAPH

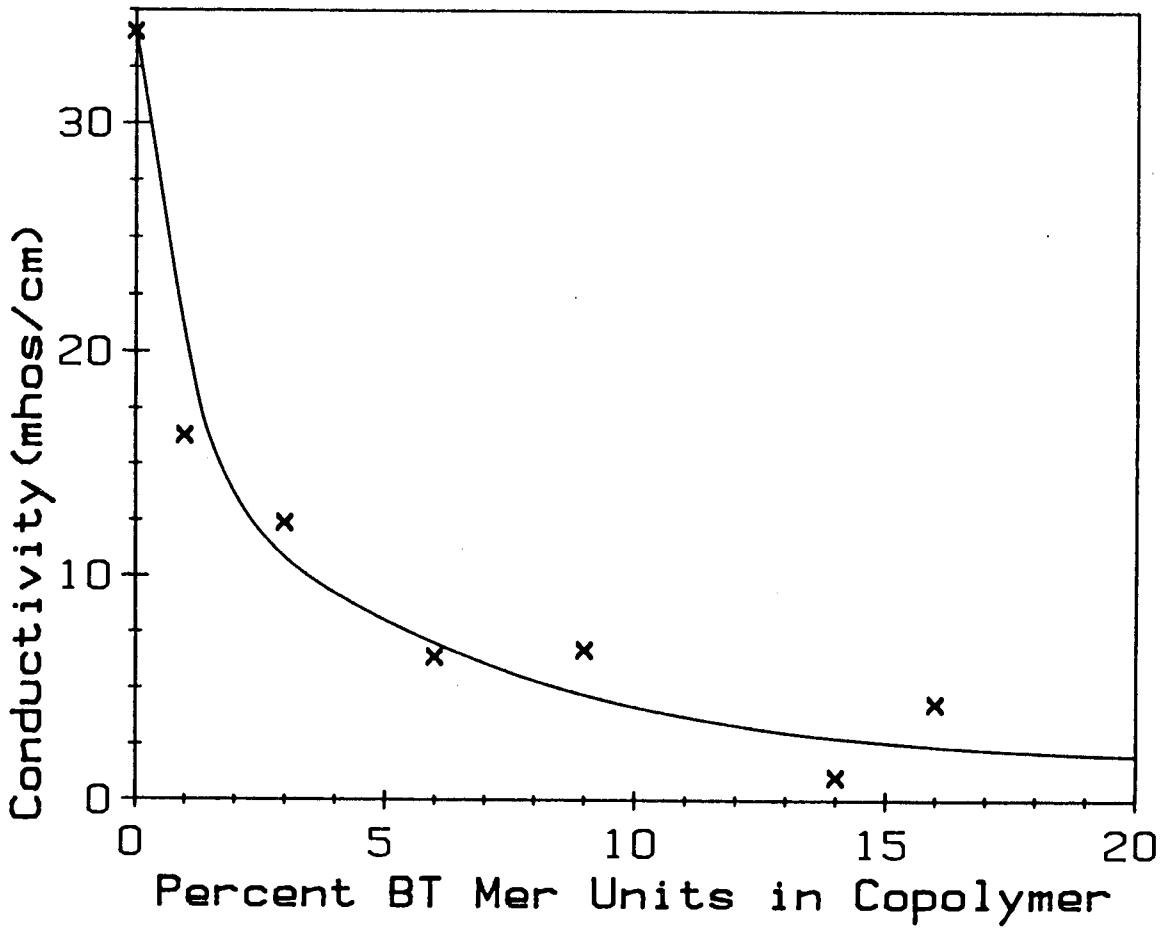
Conductivity (mhos/cm)
30
20
10
0
0
5
10
15
20
Percent BT Mer Units in Copolymer

Figure.IV.3

as the composition of the copolymers are not given. For example the conductivity of sample #CO03 could be classed as an intermediate between the two homopolymers, but when viewed in the context of the conductivity vs composition curve (Figure IV.3) one realizes that it is part of a trend and that one conductivity value for a copolymer can not determine anything without the compositions and conductivities of a number of different samples.

The reason for the copolymer's decrease in conductivity in comparison to the homopolymers is uncertain, more work will have to be done to confirm the results and theoretical studies must be done to determine the electronic and orbital configurations of the copolymers. Copolymerization may create electronic defects along the chain which will decrease the conductivity. J. Roncali et al.[34] observed that the conductivity of thiophene ring polymers decreased in the order PT > PBT > PTT and postulated that the average chain length of the polymers decreased as the monomer's reactivity decreased. Similarly the conductivity of the copolymers may simply be caused by a reduction of the average chain length due to the interaction of the two monomers.

TABLE IV.3
Resistivity and Conductivity

no.	Data V (mV)	Data I (mA)	C	Sheet Γ_s	Bulk Γ_v R	Cond. $\Omega^{-1}cm^{-1}$	Ave. Cond.	% BT in poly
C001	10.9	5.65	3.76	7.25	0.029	34.82	34.08	0
	12.0	5.65	3.76	7.98	0.032	31.63		
	6.7	3.57	3.76	7.05	0.028	35.80		
C003	30.0	7.90	3.76	14.28	0.057	17.51	16.30	1
	63.2	14.80	3.79	16.18	0.065	15.45		
	82.7	19.68	3.73	15.67	0.063	15.95		
C004	3.2	0.32	3.78	37.80	0.136	7.35	12.39	3
	10.7	1.87	3.74	21.40	0.077	12.98		
	9.6	1.66	3.74	21.63	0.078	12.84		
	4.1	0.62	3.70	24.47	0.088	11.35		
C005	17.1	0.99	3.69	64.02	0.179	5.58	6.39	6
	37.5	2.01	3.69	68.71	0.192	5.20		
	67.0	5.81	3.69	42.52	0.119	8.40		
C006	57.5	4.11	3.72	52.09	0.143	6.98	6.71	9
	45.3	3.09	3.65	53.54	0.147	6.79		
	62.1	4.01	3.69	57.20	0.157	6.36		
C007	2.7	0.13	3.72	77.30	0.229	4.37	4.33	16
	5.2	0.29	3.79	68.03	0.201	4.97		
	3.9	0.16	3.79	92.48	0.274	3.65		
C008	4.1	0.07	3.89	227.57	0.892	1.12	1.07	14
	4.7	0.07	3.72	249.89	0.980	1.02		
	6.0	0.05	3.89	466.24	1.828	0.55		
C002	47.7	11.50	4.04	16.76	0.077	12.97	12.70	100
	74.4	17.01	4.04	17.67	0.081	12.30		
	70.4	16.09	4.04	17.68	0.081	12.30		
	63.4	14.71	4.04	17.41	0.080	12.48		
	47.9	11.50	3.88	16.16	0.074	13.45		

Section IV.4 Conclusion

This chapter has shown that the conductivity of the copolymer is significantly less than the conductivity of PPY or PBT. It has also shown that the conductivity of the copolymer is dependent on its composition.

CHAPTER V DETERMINATION OF OXIDATION POTENTIAL BY CYCLIC VOLTAMMETRY

Section V.1 Introduction and Theory

Cyclic voltammetry is one of the most important electroanalytical techniques. Most electrochemical systems are initially tested using this technique to determine the redox potentials of the components in the system. Its ease of measurement and versatility have resulted in extensive use of cyclic voltammetry in many diverse fields of research [110]. Unfortunately, despite the power, flexibility and increasing application of the technique, it is not generally well understood in comparison with other instrumental methods such as spectroscopy and chromatography. Few instrumental analysis courses or texts even mention this technique. Thus, although it is not essential to the comprehension of the data, some review of the basics of cyclic voltammetry are required.

In cyclic stationary-electrode voltammetry the potential of a small electrode immersed in an unstirred solution is varied linearly with time, from a value where no electrode reaction occurs to a value higher or lower than the point where the reaction of interest takes place. The direction of the potential sweep is then reversed and the electrolysis of the products may occur. Cycling of the electrode potential enables a rapid search for redox couples within a system. Once located, a couple can be characterized by the potential of the current peaks on the cyclic voltammogram and by changes in the waveshape caused by variations in scan rate.

Figure V.1.a depicts a typical potential-time signal for

cyclic voltammetry. The potential is scanned from +0.25 to +0.75 volts (line A). At point B the direction of potential scan is reversed. Line C is the negative potential scan from +0.75 to +0.25 and point D is the termination of the first cycle. The dotted line depicts the a second cycle of any number which may be taken.

A typical cyclic voltammogram of a reversible system is shown in Figure V.1.b. At the beginning of the scan no current flows. During the scan from +0.25 to +0.75 volts the applied potential becomes sufficiently positive at +0.4 V to cause oxidation of the species in solution at the electrode surface. This oxidation results in an anodic current, which increases rapidly until the surface concentration of the species at the electrode substantially diminished, causing the current to peak at A. The current then decays after peak A as the solution surrounding the electrode is depleted of the species. At point B the scan direction is reversed and the product of the oxidation in the forward scan is reduced and a cathodic peak is observed.

The important parameters of a cyclic voltammogram are labeled on Figure V.1.b: i_{pc} and i_{pa} are the magnitudes of the cathodic and anodic peak currents, and E_{pc} and E_{pa} are the potentials at which these peaks occur.

If one considers the reduction of species S_o in solution:

$$S_o + ne \text{ --------> } S_r \qquad [5.1]$$

and if the product of reaction 5.1, S_r, is oxidizable the reaction is fully electrochemically reversible, and the Nernstian equation gives the relationship between the electrode potential E and the

Figure.V.1 CYCLIC VOLTAMMETRY DIAGRAMS
a) Applied Potential Program
b) Typical Cyclic Voltammogram

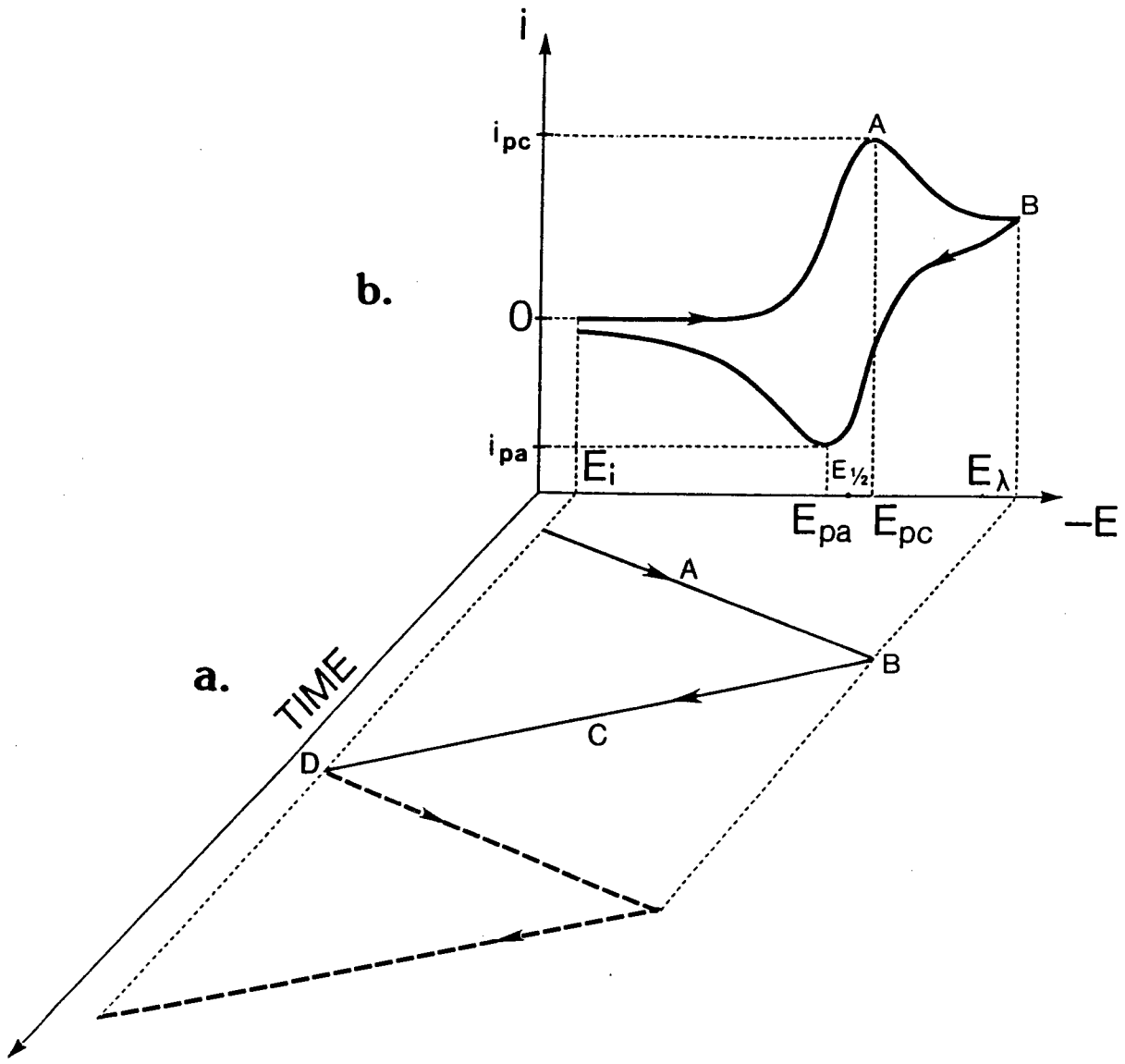

Figure.V.1

solution composition in the vicinity of the electrode surface:

$$E = E_o' + RT/nF \ln ([S_r]/[S_o]) \quad [5.2]$$

where E^{o}' is the formal potential of the S_r/S_o redox couple, R is the gas constant, T is the temperature, F is the Faraday constant, n is the number of electrons involved in reaction 5.1 and $[S_r]$ and $[S_o]$ are the concentrations of the species at the electrode surface. For the case of single electron transfer at 25° C equation, 5.2 can be rewritten as:

$$E = E_o' + 0.059 \log ([S_r]/[S_o]) \quad [5.3]$$

Therefore, to be termed fully reversible, the reaction must be fast enough to so that the concentrations of the oxidized and reduced species are in equilibrium with one another near the surface of the electrode [109]. Many systems show a reversible nature at slow potential scan rates, but at higher rates the E_{pc} and E_{pa} potentials will shift farther apart and are then categorized as quasi-reversible.

Another characteristic of the reversible system is the dependence of the peak height on the square root of the scan rate. The peak current i_p is related to the experiment by the Randles-Servick equation [112,113]. At 25° the peak current is:

$$i_p = (2.69 \times 10^5) n^{3/2} A D_o^{1/2} v^{1/2} C \quad [5.4]$$

where A is the electrode area, C the bulk concentration of the species, D_o the species diffusion coefficient and v the scan rate of the potential. The peak current for a quasi-reversible system is not proportional to $v^{1/2}$ except when the peaks are so widely

separated that the system is more appropriately described as totally irreversible. For a redox species absorbed onto the electrode, such as a conducting polymer films, the peak current has been found to be proportional to the scan rate [114,116]. This is because the electroactive film is grafted onto the electrode so that the redox species does not have to diffuse to and away from the electrode.

The positions of the E_{pc} and E_{pa} peaks, relative to the formal potential E^{o}' were calculated by Nicholson and Shain and are given by [115]:

$$E_{pc} = E_{1/2} - 28.5/n \text{ mV (at } 25^{o}C) \quad [5.4]$$

$$E_{pa} = E_{1/2} + 28.5/n \text{ mV} \quad [5.5]$$

where

$$E = E_{o}' + 0.059 \log(D_{o}/D_{r}) \quad [5.6]$$

$E_{1/2}$ is the half-wave potential which corresponds to the value on a polarographic curve where the current is equal to one-half of the limiting current. D_r and D_o are the diffusion coefficients of the reduced and oxidized species. Naturally, usually D_r and D_o are almost the same as the oxidized and reduced forms are normally very close to the same molecular structure and therefore $E_{1/2}$ is approximately equal to E^{o}'. This allows the determination of the $E_{1/2}$ from the voltammograms as shown in Figure V.1.b. $E_{1/2}$ is important because it is characteristic for a given substance and may be used as a qualitative identification.

The oxidation and reduction of conducting polymers films is more complex than simple reversible redox reactions: anions must

diffuse in and out of the films to balance the charge during the oxidization and reduction. As with species absorbed onto the electrode, the peak current i_p is normally proportional to the scan rate of the potential v. The rate of anion diffusion is affected by a number of factors including the thickness of the film, the swelling of the film by the solvent and the relative size of the anion. Thus the behavior of the films can be reversible, quasi-reversible or irreversible depending on the conditions of measurement. Many anodic and cathodic peaks are very broad due to the slow diffusion of the anions and therefore E_{pa} and E_{pc} are very difficult to define.

Conducting polymers, such as PT and PBT, have multiple reduction peaks due to the rearrangement of the polymer lattice structure as the anion is removed for the polymer (Figure V.2) [116]. This makes it difficult to determine the $E_{1/2}$ from the cyclic voltammogram and other methods must be used to determine the $E_{1/2}$ potentials. Only the E_{pa} peaks can be determined from the voltammograms and they are somewhat dependent on the scan rate and other factors.

In these experiments two different redox systems were examined: 1) the oxidation potentials of BT and PY were determined for the solvent systems used in the copolymerization in chapter II and 2) the oxidation potentials of the copolymer films were determined.

Section V.2 Experimential

V.2.1 Purifications

The same purification techniques used in section II.2.1 were

Figure.V.2 CYCLIC VOLTAMMOGRAM OF POLY(2,2'-BITHIOPHENE)
Scan rate 50 mV/s, in 0.1 M TBAP/ACN

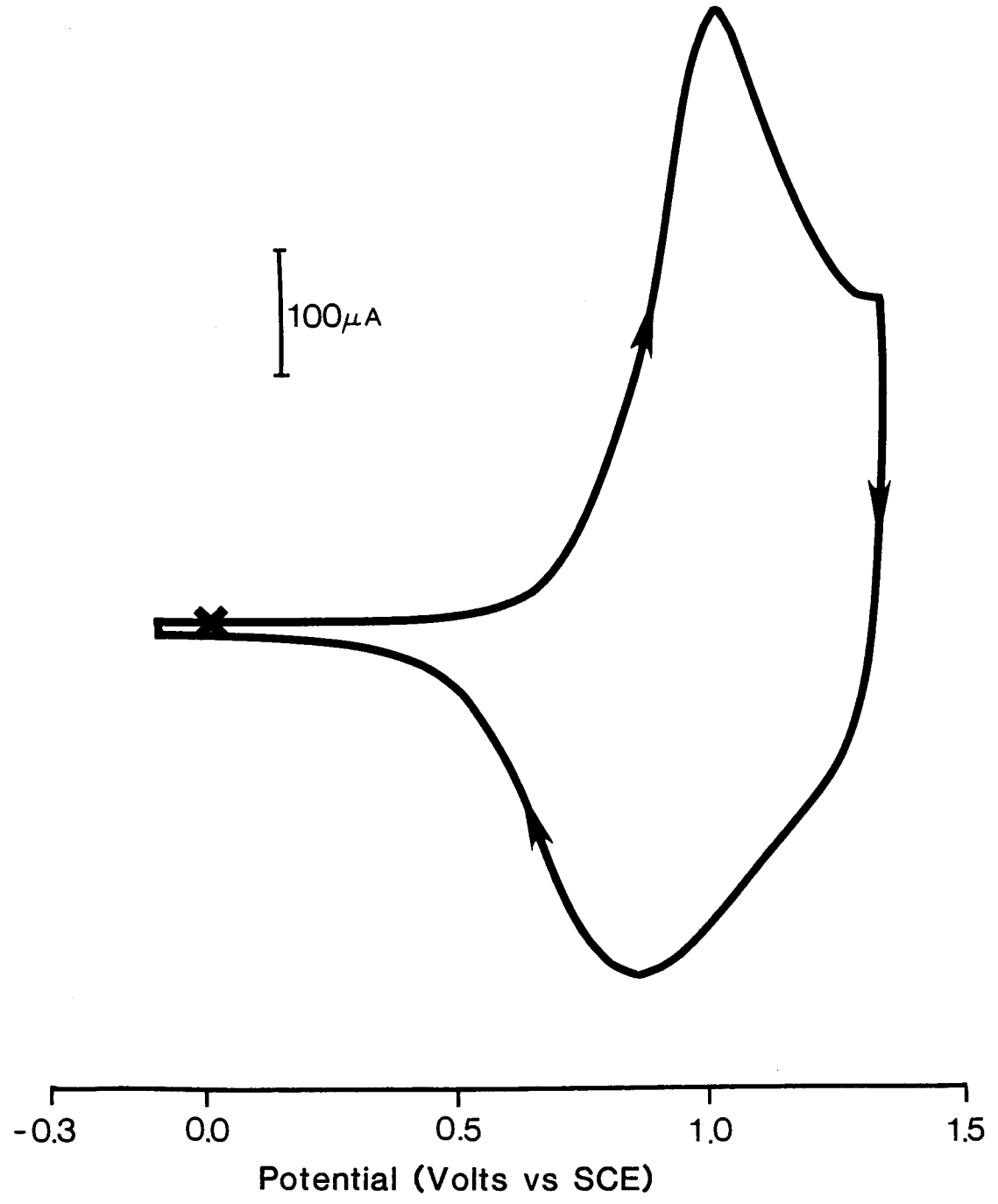

Figure.V.2

Figure.V.3 DIAGRAM OF CYCLIC VOLTAMMETRY CELL

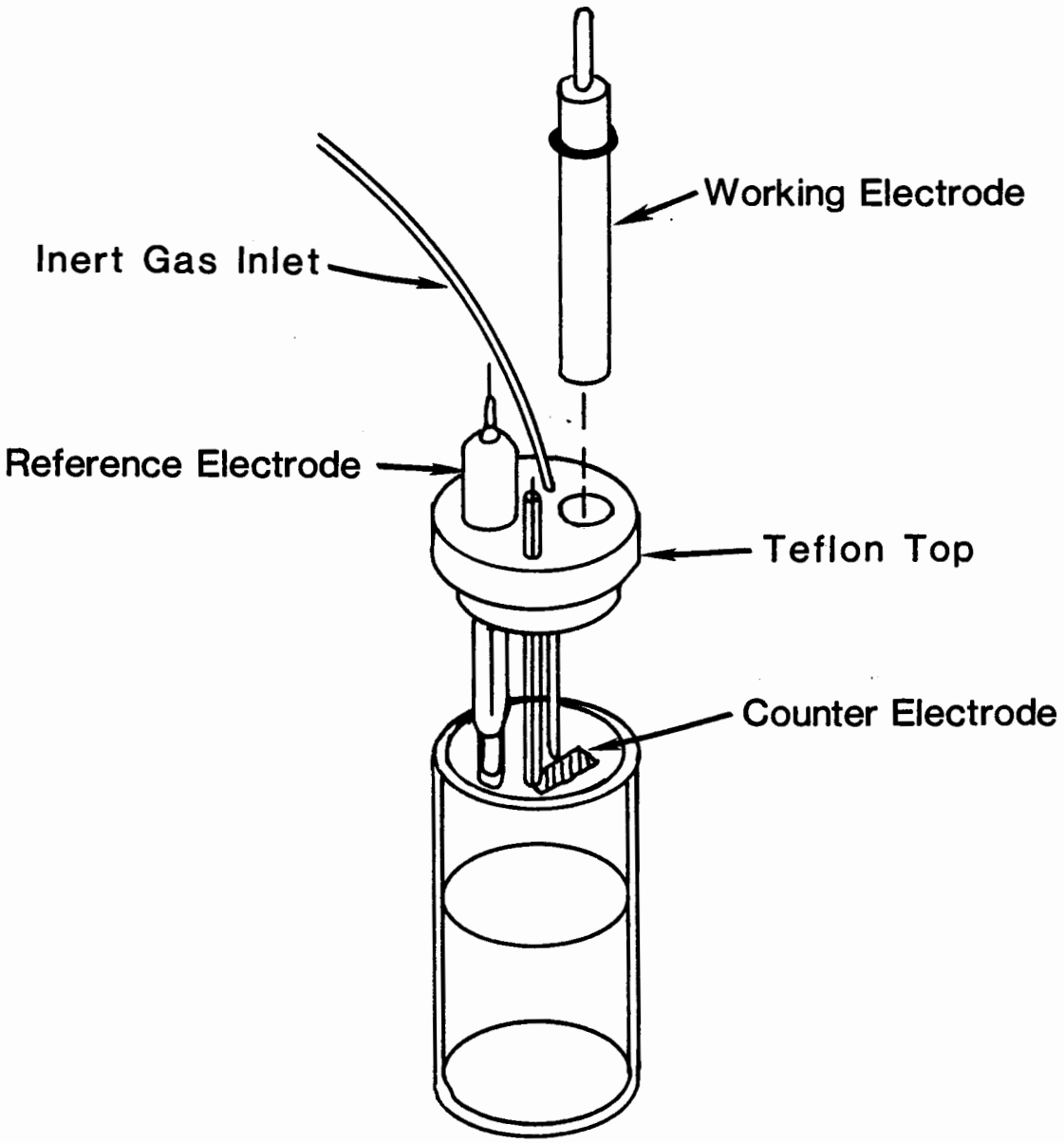
Working Electrode
Inert Gas Inlet
Reference Electrode
Teflon Top
Counter Electrode

Figure.V.3

used for the TBAP, BT, PY, and ACN used in this chapter. The Tetrabutylammonium tetrafluoroborate (TBAF) used as an electrolyte was dried under reduced pressure for 48 hours to remove water.

V.2.2 Apparatus

Three identical single compartment cells, as diagrammed in Figure V.3, were manufactured in the S.F.U. shops. Air tight tops were machined from "Teflon" with all inlets and outlets sealed with silicone rubber "O" rings.

The working electrodes were small polished Pt electrodes with a circular areas of 0.227 cm^2. The counter electrodes were made from a sheet of Pt. One square cm of Pt was spot welded onto Pt wire and a 4 mm diameter "pyrex" glass tube was sealed onto the Pt wire to form an electrode shaft. A Fisher Scientific SCE was used as the reference electrode. The reference electrode was separated from the working compartment by a Luggin capillary and KCl salt bridge.

V.2.3 Polymerization

The working electrodes were polished before each polymerization to clean the electrode and remove the polymer films from previous polymerizations. Fine polishing solution (> 0.05 μm) was used for the cleaning. After the polishing the electrode was ultrasonically cleaned in baths of concentrated HNO_3 and concentrated KOH. After rinsing, the electrode was conditioned by cycling the electrode between 0.0 and 1.5 V in 0.5 M H_2SO_4, washed with distilled H_2O and the dried in an oven at 90°C.

Solutions containing 0.1 M TBAP or TBAF and 0.01 M concentrations of the monomers in acetonitrile were bubbled with Ar gas before the polymerizations of the films. An Ar atmosphere was maintained in the cell throughout the reaction to prevent oxidation of the monomers.

The working electrode was stepped to a selected value vs the SCE reference using a PAR 170 electrochemistry system for all the reactions except the bilayer films. Bilayer films were polymerized using a EG&G PAR 173 potentiostat combined with the EG&G PAR 179 reversible coulometer so that the thickness of the layers of the two polymers could be estimated.

After the polymerizations the electrodes, with the polymers in their reduced form were removed from the cell, washed with clean solvent and placed in a previously prepared cell containing only the electrolyte (0.1 M TBAP or TBAF) in an Ar atmosphere.

V.2.4 Cyclic Voltammograms

With the polymer coated electrodes immersed in the electrolyte solution, cyclic voltammograms were taken using the PAR 170 electrochemistry system. The potential scan on the electrode was monitored using a SCE reference. The scan rates ranged from 5 mV/s to 500 mV/s.

The voltammograms were recorded on the PAR 170 X-Y recorder and an Allen 720M X-Y recorder.

Section V.3 Results and Discussion

V.3.1 Cyclic Voltammetry of the Monomers

At the beginning of this research the oxidation potentials

Figure.V.4 SUCCESSIVE CYCLIC VOLTAMMOGRAMS OF BITHIOPHENE AND POLY(2,2'-BITHIOPHENE)
Polished Pt electrode was initially bare.
Bithiophene is polymerized in successive scans.
Scan rate 50 mV/s, in 0.1 M TBAP/ACN [33]

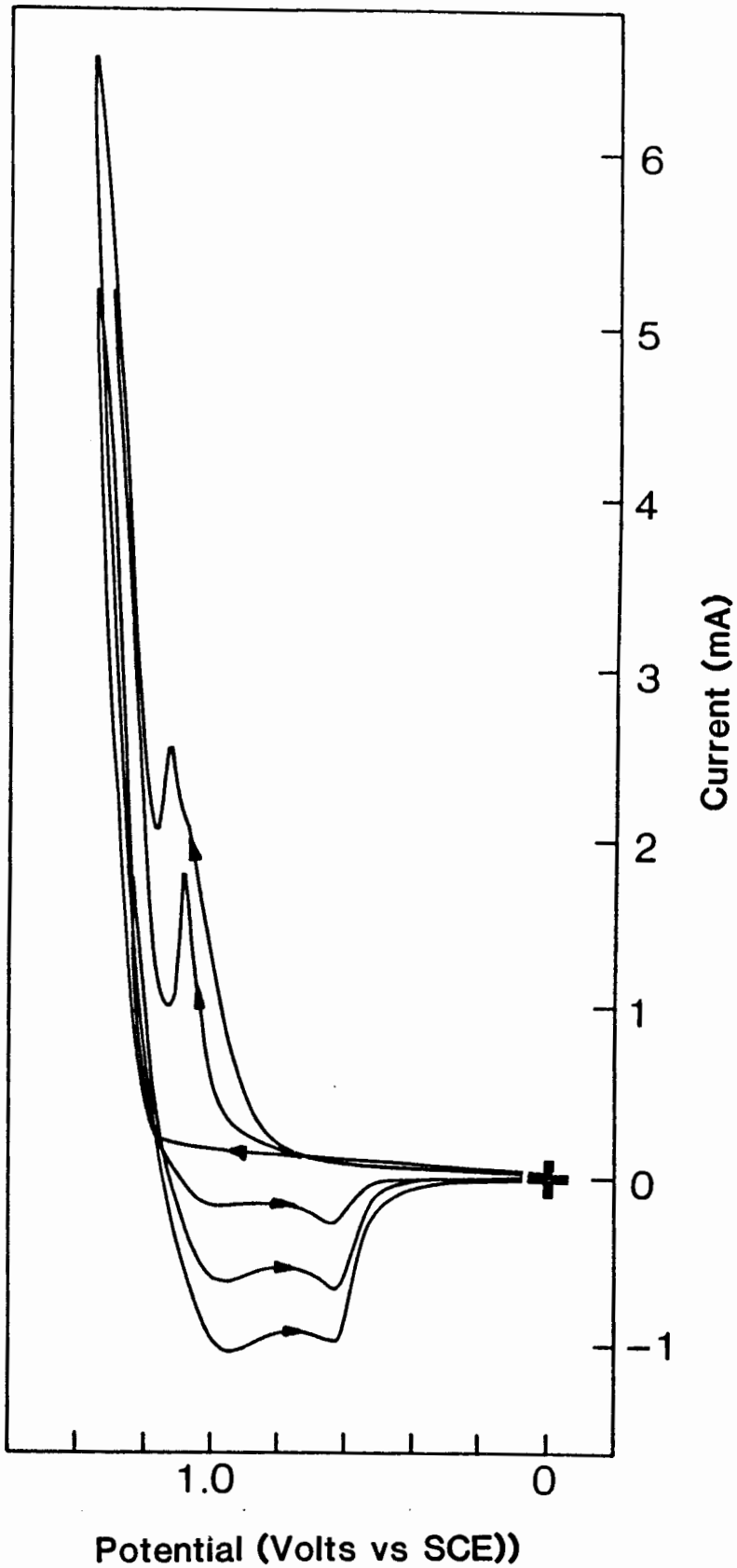

Figure.V.4

of PY and BT had not been established. Values for the oxidation potentials were published in the literature, but different values were reported for BT and PY. As we were not certain of the E_{pa} potentials for the monomers, it was necessary to determine them, before other experiments could be done.

The monomers are not a reversible species. They are oxidized to form polymer, thus the $E_{1/2}$ value can not be determined for the monomer using cyclic voltammetry. Only the E_{pa} peak can be estimated for a particular system. The initial cathodic scan (Figure V.4) shows a reduction peak for the polymer which is significantly smaller than the oxidative peak for the monomer. Only a small fraction of the polymer can be reduced (1 electron in 4 monomer ring units) compared with the oxidation of the monomer (2 1/4 electrons per monomer unit). On successive scans a second oxidative peak at lower potential than that of the monomer oxidation grows as increasing amounts of polymer are reoxidized on each scan.

Figure V.5 is a voltammogram of a single scan at 50 mV/s of BT in a TBAP/ACN solution. The E_{pa} peak for the monomer appears at +1.30 V vs SCE. The other E_{pa} peak (+0.98 V) on the voltammogram is for the oxidation of a small amount of PBT that was on the electrode.

Figure V.6 is a voltammogram of PY in a TBAP/ACN solution and the monomer E_{pa} peak is at approximately +1.1 V vs SCE. The oxidation peak for PY in this solvent system is not as distinct as BT. The peak appears as only a break in the curve rather than a distinct peak due to the relatively slow scan rate.

The E_{pa} potentials were also recorded for BT and PY in the

$LiClO_4$/PC solvent system. The E_{pa} potentials for the momomers in this solvent system were the same as those recorded for the TBAP/ACN solvent system +1.3 V and +1.1 V.

The monomer's E_{pa} potentials determined in this section were used as electrode potentials for the oxidation of BT and PY in the other chapters.

V.3.2 Cyclic Voltammograms of the Polymers and Copolymers

Figure V.7 is the voltammogram of a copolymer polymerized from a 50:50 mixture of BT and PY. Note that there are 3 oxidation peaks for the copolymer, one at +0.15 V, one at +0.54 V and one at +1.0 V. When compared to similarly prepared homopolymers scans in Figure V.8 one can see that two of the copolymers peaks are at similar oxidation potentials to those of the homopolymers. Only the peak at +0.54 V is completely unique to the copolymer. Naitoh et. al. [72] reported that the oxidation potential of poly(2,2'-thienylpyrrole), obtain by cyclic voltammetry, was 0.50 V. This polymer consists of alternating pyrrole and thiophene units and thus the peak at +0.54 V in the copolymer seems to result from alternating units within the copolymer.

The peaks corresponding to the oxidation potentials of PPY and PBT could be due to concurrent homopolymer formation within the copolymer matrix, but this is unlikely as the PPY formation must be minimal judging from the small size of the peak in relation to the other peaks and from the copolymerization study (Chapter 2) we would expect PY to react much more quickly

Figure.V.5 CYCLIC VOLTAMMOGRAM OF BITHIOPHENE
Scan rate 50 mV/s, in 0.1 M TBAP/ACN

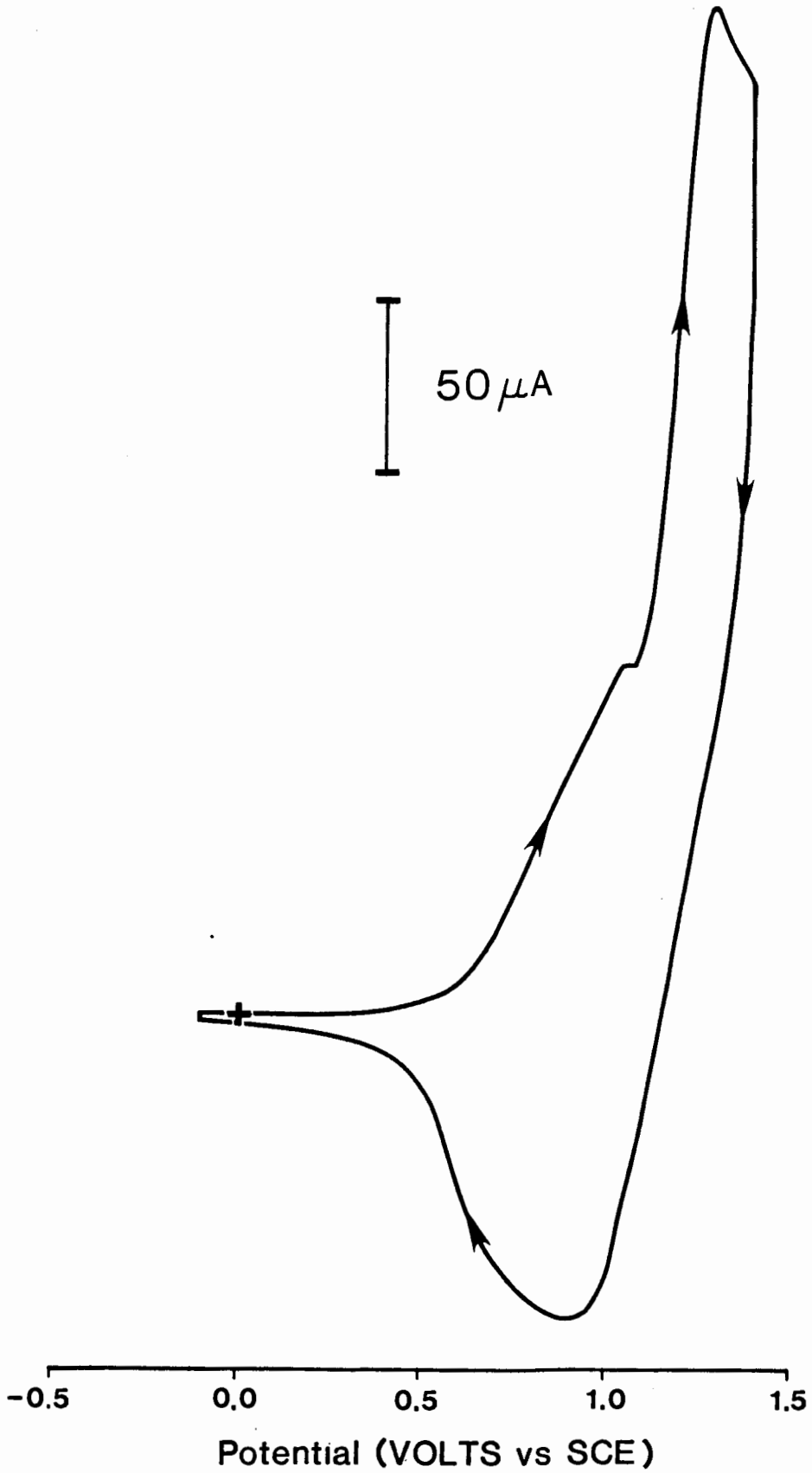

Figure.V.5

Figure.V.6 CYCLIC VOLTAMMOGRAM OF PYRROLE
Scan rate 20 mV/s, in 0.1 M TBAP/ACN

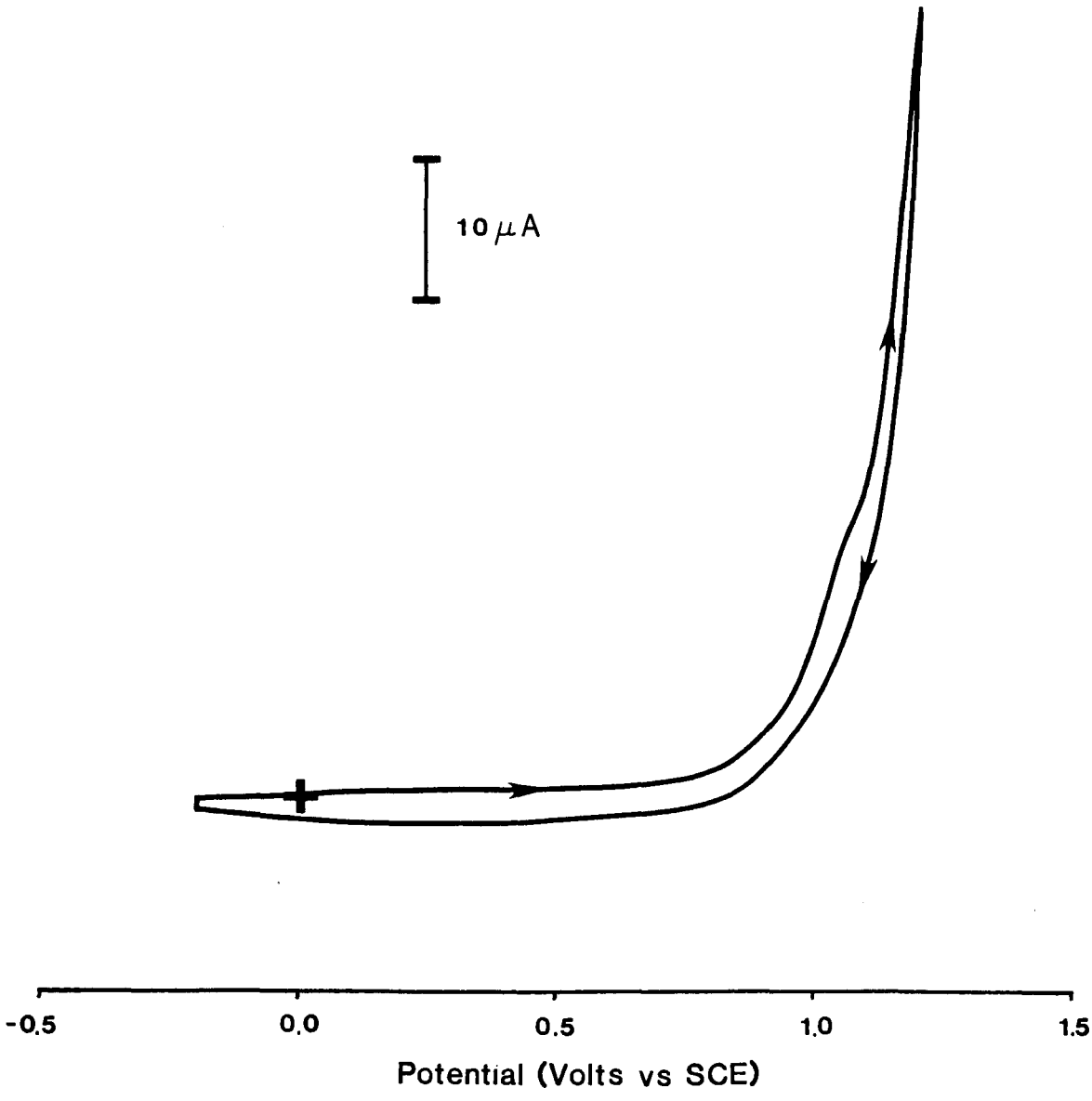

Figure.V.6

Figure.V.7 CYCLIC VOLTAMMOGRAM OF A COPOLYMER POLYMERIZED FROM AN EQUAL MOLAR MONOMER MIXTURE
Scan rate 50 mV/s, in 0.1 M TBAP/ACN

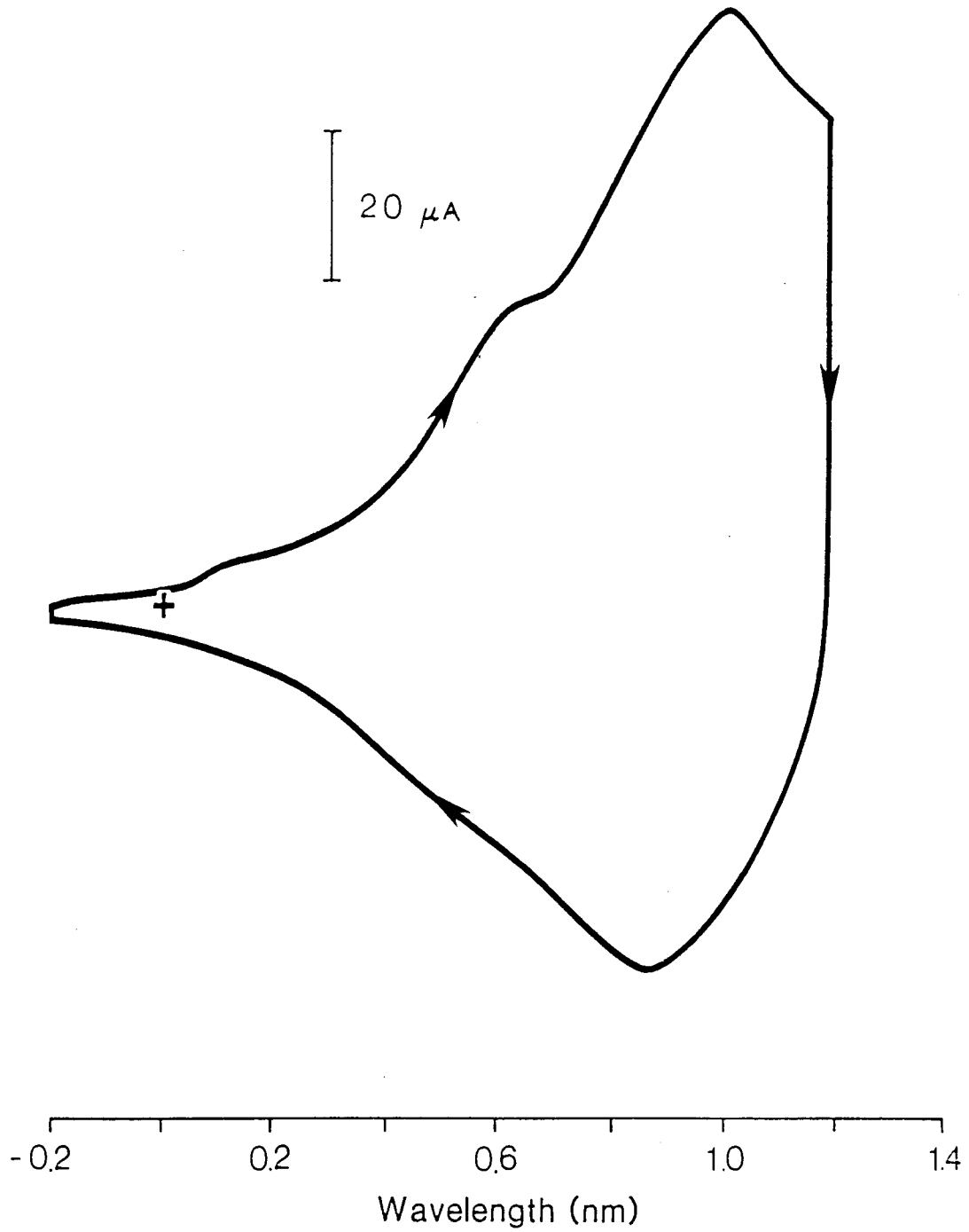

Figure.V.7

Figure.V.8 COMPARISON OF CYCLIC VOLTAMMOGRAMS OF POLY(2,2'-BITHIOPHENE), POLYPYRROLE AND A COPOLYMER
A) PPY, Scan rate 50 mV/s, in 0.1 M TBAP/ACN
B) A Copolymer, Scan rate 50 mV/s, in 0.1 M TBAP/ACN
C) PBT, Scan rate 50 mV/s, in 0.1 M TBAP/ACN

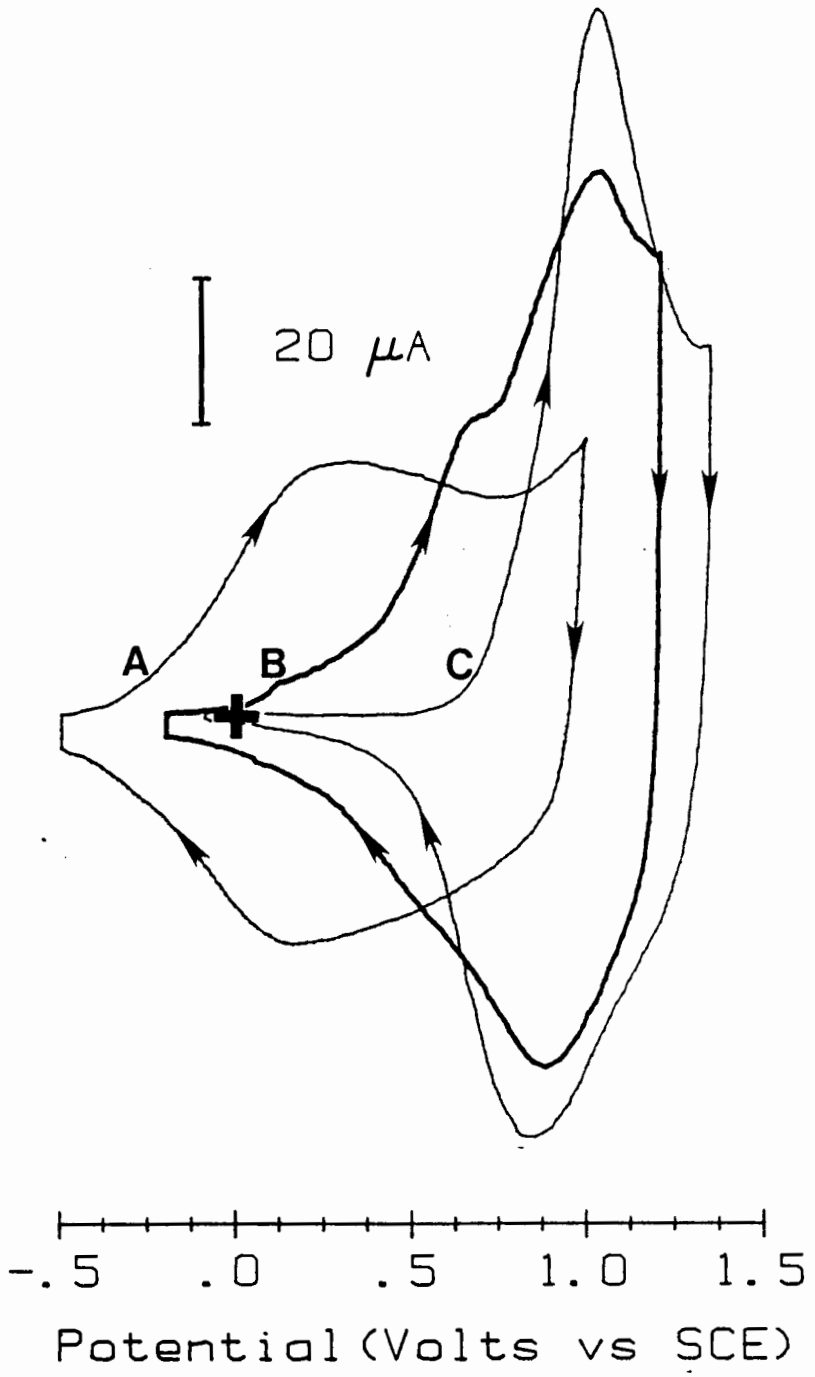

Figure.V.8

to form polymer. Even when the reaction mixture is enriched with PY, the peak corresponding to PY in the copolymer is much smaller than the others (Figure V.9).

The voltammograms of the bilayer films in Section V.3.3 show that the peak heights are representative of the amounts of PPY and PBT on the electrode, therefore we would expect the peaks in the copolymer to be representative of the number of oxidizable sequences of each of the three types within the polymer. The ratio of the peak heights for the BT and PY sequences can easily be explained using sequence probability. For example;if one considers one oxidizable unit in the copolymer chain to be 4 heterocylic rings, then the probability of 2 BT mer units polymerizing in sequence to form one oxidizable unit is much greater than the probability of 4 PY mer units polymerizing in sequence. For example the number fraction of sequences of PY 4 units long (N_{PY}) is equal to the probability that any particular sequence of PY units is 4 units long [67]:

$$N_{PY} = P^3_{PYPY} P_{PYBT} \qquad [5.7]$$

where P_{PYPY} is the probalility that a growing chain carrying a terminal PY adds a PY monomer unit:

$$P_{PYPY} = \frac{r_1}{r_1 + [BT]/[PY]} \qquad [5.8]$$

and P_{PYBT} is the probability that the same growing chain adds to BT. $P_{PYBT} = (1-P_{PYPY})$. r_1 is the reactivity ratio for PY.

The number fraction of sequences of thiophene 4 units long (N_{BT}) is equal to the probability that any particular sequence of BT units is 2 units long:

Figure.V.9 CYCLIC VOLTAMMOGRAM OF A COPOLYMER POLYMERIZED FROM A PYRROLE RICH MONOMER MIXTURE
Monomer mixture 80 % pyrrole, 20 % 2,2'-bithiophene, scan rate 50 mV/s, in 0.1 M TBAP/ACN

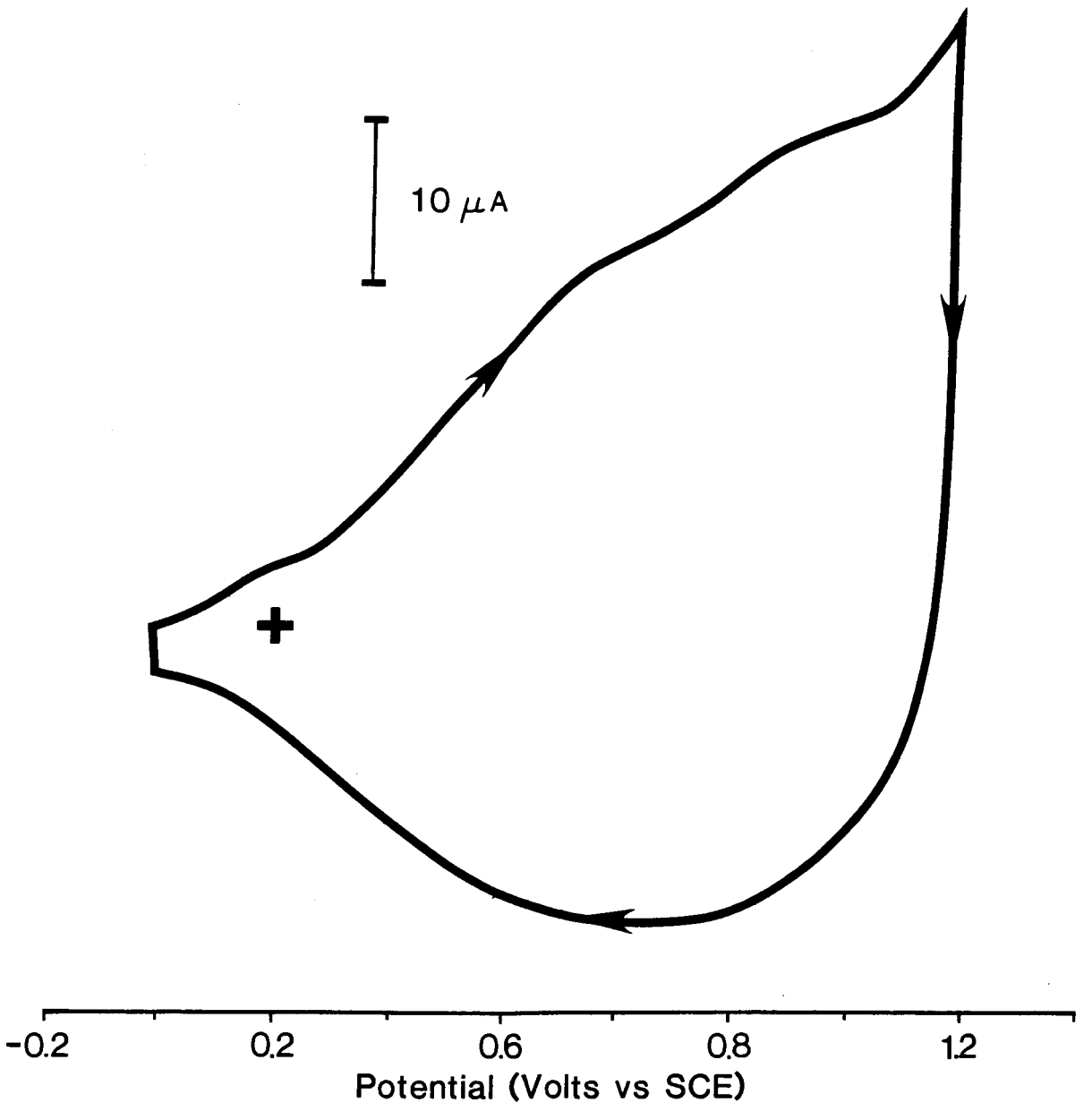

Figure.V.9

$$N_{BT} = P_{BTBT}P_{BTPY} \quad [5.9]$$

where P_{BTBT} is:

$$P_{BTBT} = \frac{r_2}{r_2 + [PY]/[BT]} \quad [5.10]$$

and $P_{BTPY} = (1-P_{BTBT})$. This means that for a equal molar monomer solution where the reactivity ratios r_1 and r_2 are 5.1 and 0.31 respectively, there will be approximately three times as many oxidizable units of BT than there are of PY (N_{PY}=0.07 and N_{BT}=0.24). This ratio should be reflected in the heights of the oxidation peaks of the copolymer.

Figure V.10 is a series of voltammograms for a copolymer taken at various scan rates. This figure shows that the peak currents are proportional to the scan rate indicating that the polymer is a species absorbed onto the electrode [114]. Both PPY and PBT also show this relationship.

Figure V.10 also shows that the oxidation peak position of the copolymer varies with the scan rate above 50 mV/s. For a simple redox system this would indicate that the system was quasi-reversible but for an absorbed species like the copolymer this is not necessarily the case as anions must diffuse into the film and are therefore diffusion controlled. Both PBT and PPY showed similar effects with scan rate.

It was considered that the +0.54 V peak could be some effect created by the perchlorate anion. Thus anion acting as a dissolved and absorbed species [125] during the oxidation of the copolymer. J.K. Kaufman et al. [121] suggested that the anion remained in the film and the mobile cation (Li^+) moved in and out of the film during oxidation and reduction. These observations were supported

Figure.V.10 CYCLIC VOLTAMMOGRAMS OF A COPOLYMER POLYMERIZED FROM A 2,2'-BITHIOPHENE RICH MONOMER MIXTURE
Monomer mixture 20 % pyrrole, 80 % 2,2'-bithiophene in 0.1 M TBAP/ACN Scan rates: A) 10 mV/s, B) 20 mV/s, C) 50 mV/s and D) 100 mV/s

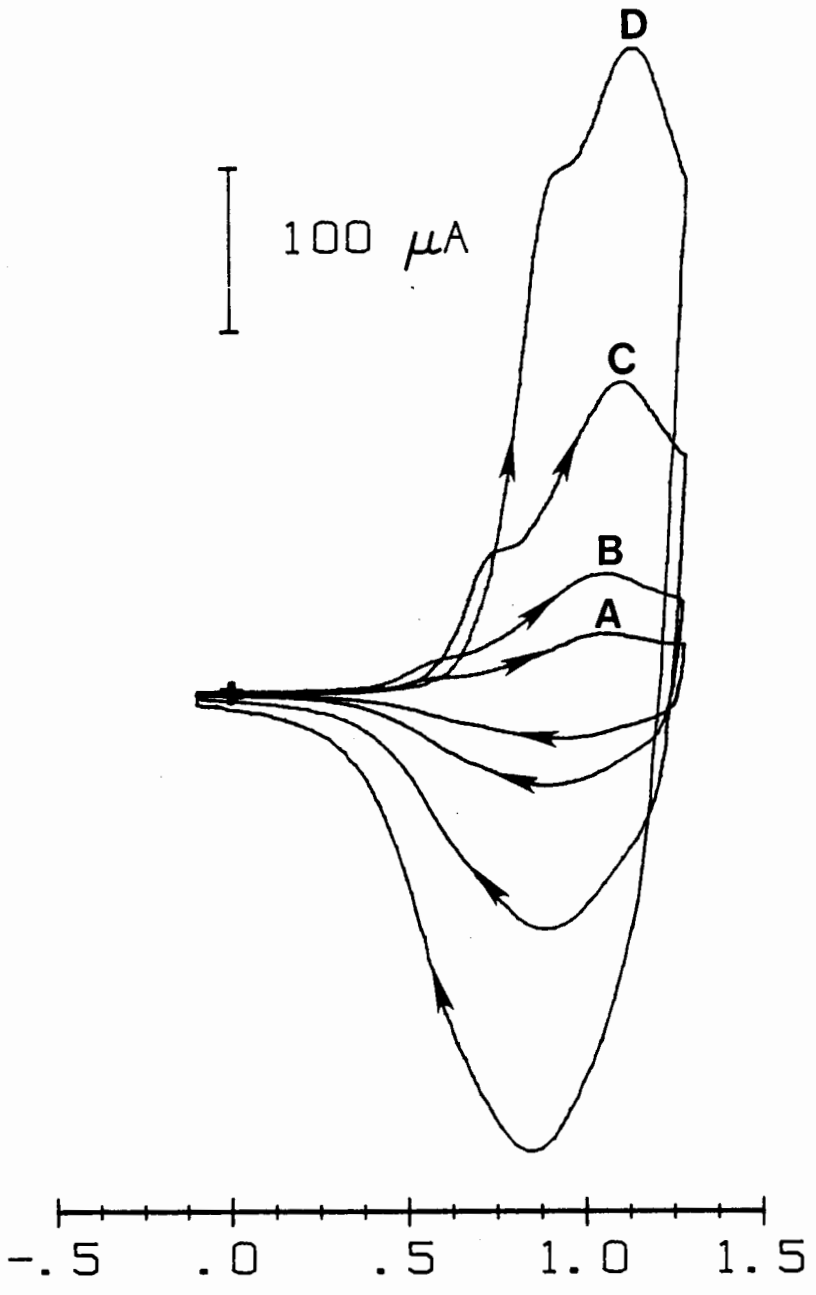

Figure.V.10

by scanning electron micrographs in Chapter III. Although the cation in this case is much larger than the Li cation used in the earlier experiments some of the cation may diffuse into the polymer and give the effect of an absorbed and dissolved species.

For these reasons the supporting electrolyte TBAP was exchanged for TBAF for a set of experiments. In retrospect it would have been more effective to change the cation used rather than the anion, if the +0.54 V peak is caused by the electrolyte any change in electrolyte should cause some change in the voltammograms.

The copolymer was polymerized in a 0.1 M TBAF/ACN monomer solution and cyclic voltammograms were taken in a 0.1 M TBAF/ACN solution. The voltammograms of the copolymers doped with the tetrafluoroborate anion had three E_{pa} peaks at the characteristic positions of the perchlorate doped copolymer. For this reason the three E_{pa} peaks are considered to be a characteristic of the copolymer and not just an effect created by the anions diffusion into the copolymer films.

V.3.3 Cyclic Voltammograms of Bilayer films

Two different bilayer films were polymerized. One film with a layer of PPY next to the electrode and a layer of PBT covering (PY/BT) and the other film with a layer of PBT next to the electrode and a layer of PPY covering (BT/PY). The number of coulombs used in the polymerization of each layer were measured and the thickness of the layer was estimated using equation 5.7 formulated by E.M. Genies and J.M. Pernaut [37]:

$$t(cm) = \frac{M}{2.00\ FdA} \times Q(C) \qquad [5.7]$$

where t is the thickness of the polymer film in cm, M is the molecular weight of the monomer unit, d is the density, F is Faradays constant, A is the surface area of the film and Q is the charge passed to form the film.

The thickness values for the films are listed on Table V.1. These values were calculated assuming that the densities of the BT and PY films were 1.5, similar to those found by Genies [37].

TABLE V.1 Coulombic Measurements and Thicknesses for BT and PY Layers

Bilayer Films	no. of C for PY	Thickness of PY layer	no. of C for BT	Thickness of BT layer
PY/BT	4.8×10^{-4} C	4.7×10^{-6} cm	2.5×10^{-4} C	6.0×10^{-6} cm
BT/PY	5.4×10^{-4} C	5.2×10^{-6} cm	2.7×10^{-4} C	6.7×10^{-6} cm

Figure V.11 is a voltammogram for the BT/PY film. The oxidation peaks for the PPY and the PBT are clearly evident at their respective potentials. The coating of PBT under the PPY appears to have little or no effect on the oxidation of the PPY. The peak current was linear with the scan rate.

Figure V.12 are voltammograms for the PY/BT film. Figure V.12.a is a voltammogram taken at a scan rate of 100 mV/s showing one distinct E_{pa} peak at +1.10 V, but as the scan rate was decreased the peak's width broaden until at 10 mV/s (Figure (V.12.b) two peaks of approximately equal height separated from the one large peak. One peak is at the characteristic E_{pa} of PBT +0.98 V and the other is slightly lower at +0.80 V. This effect

Figure.V.11 CYCLIC VOLTAMMOGRAM OF A POLY(2,2'-BITHIOPHENE)-POLYPYRROLE BILAYER FILM
Scan rate 50 mV/s, in 0.1 M TBAP/ACN

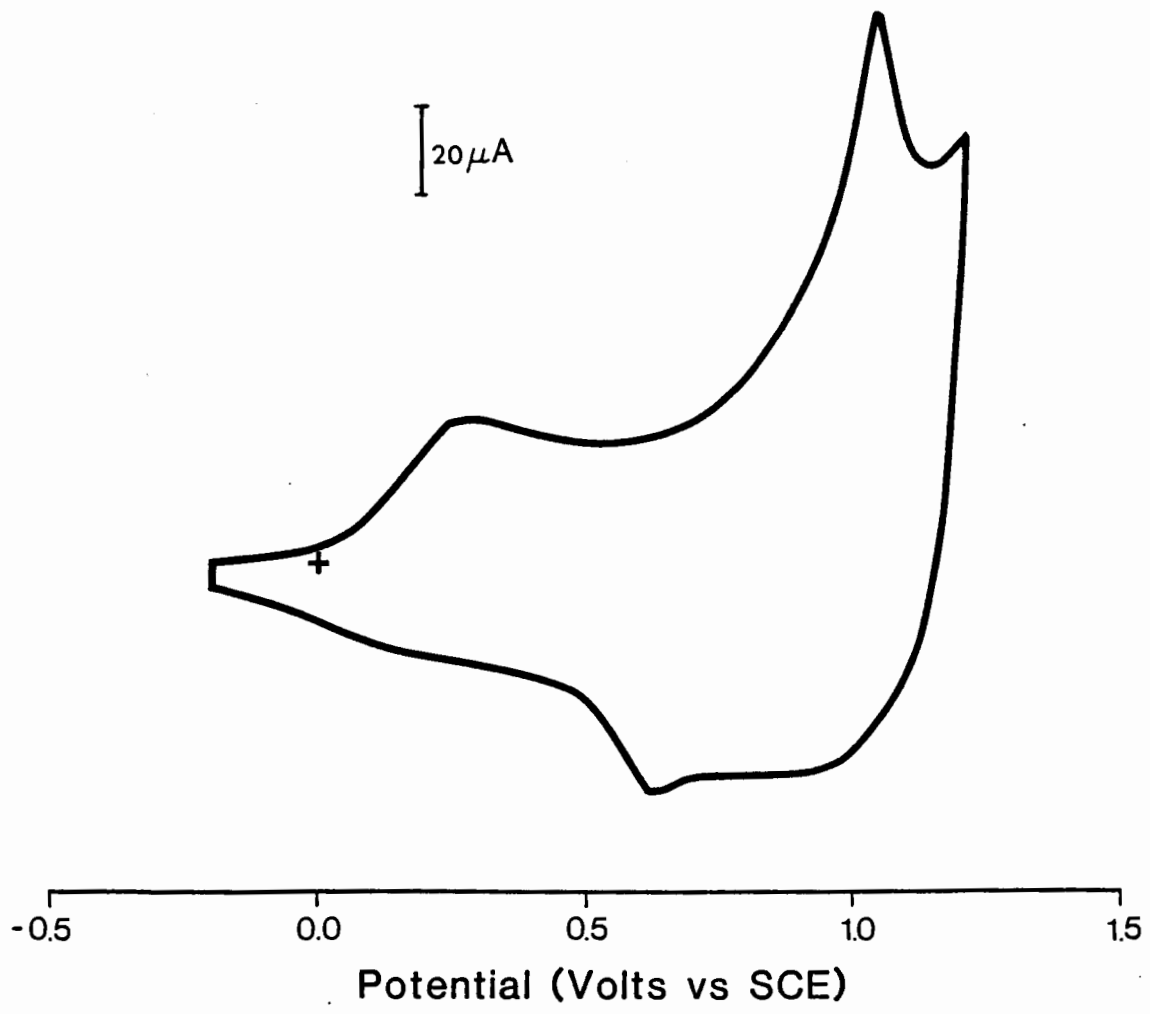

Figure.V.11

Figure.V.12 CYCLIC VOLTAMMOGRAMS OF A POLYPYRROLE-POLY(2,2'-BITHIOPHENE) BILAYER FILM
Scan rates a) 100 mV/s and b) 10 mV/s, in 0.1 M TBAP/ACN

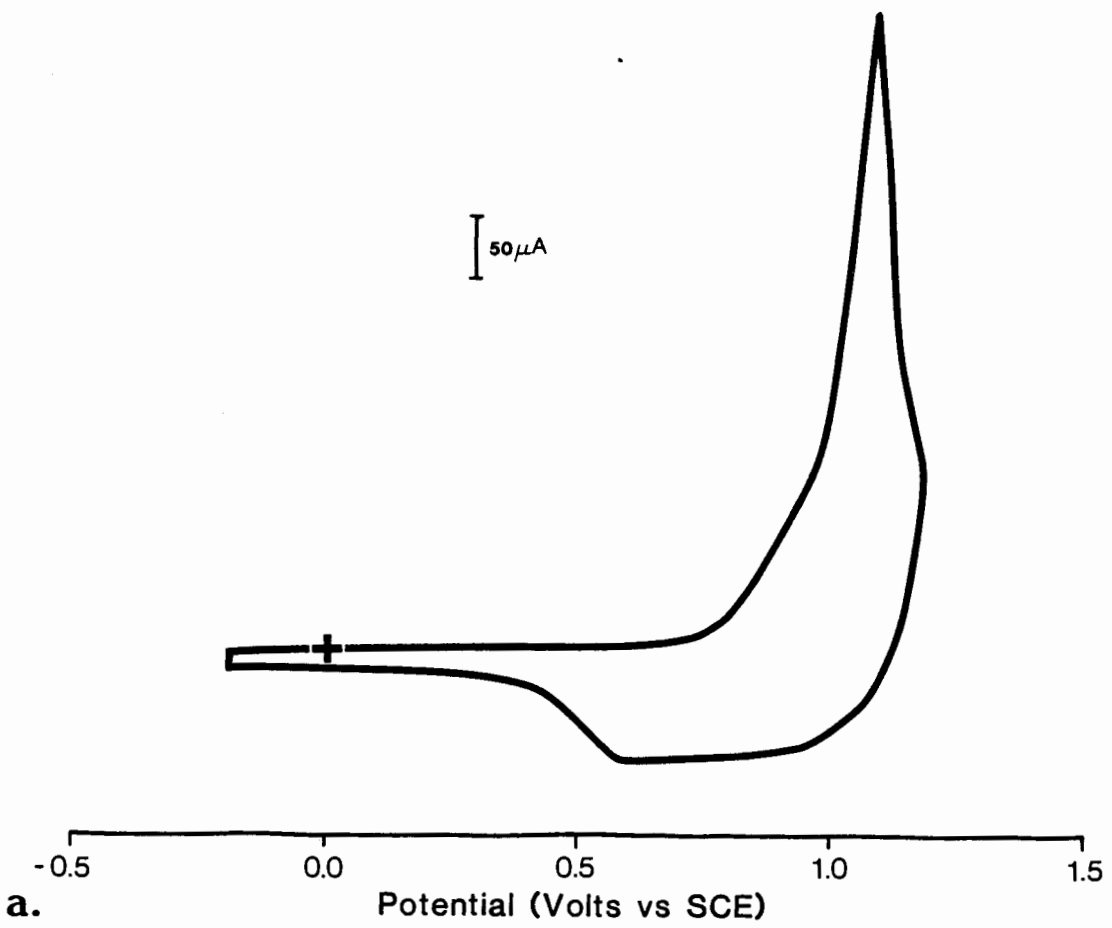
50μA
-0.5
0.0
0.5
1.0
1.5
a.
Potential (Volts vs SCE)

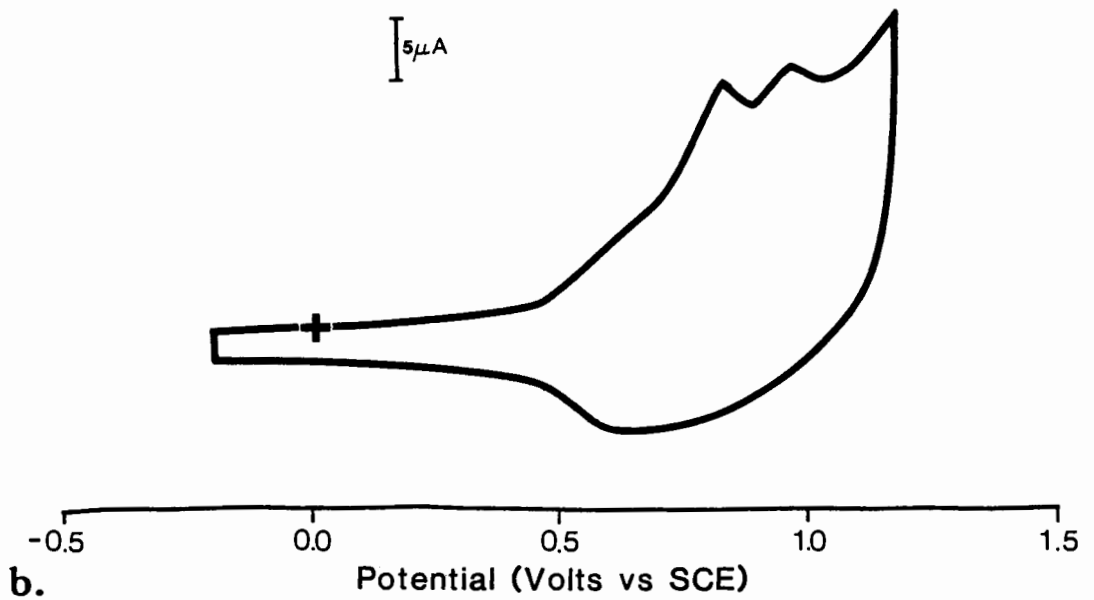
5μA
-0.5
0.0
0.5
1.0
1.5
b.
Potential (Volts vs SCE)

Figure.V.12

is caused by the suppression of PPY oxidation by the PBT coating [117]. The PBT must partially oxidize before the oxidation of PPY can occur. At high scan rates the anions do not have time to diffuse through the partially oxidized PBT film and thus one large sharp peak appears on the voltammogram as both films oxidize together. As the scan rate is decreased the anions have time to diffuse through the partially oxidized film and an E_{pa} peak appears for the PPY at a scan rate of 10 mV/s. When the scan rate is decreases to 5 mV/s the peak for the PBT remains at an oxidation potential of +0.98 but the PPY peak moves from +0.80 to +0.75 indicating that the oxidation of PPY is still diffusion controlled even at these low rates of scan.

The cyclic voltammograms of the bilayer films indicate that the film in contact with the electrolyte solution oxidizes before the film in contact with the electrode. In terms of electrochemical theory for these conducting polymers this is difficult to explain. The polymers in their reduced forms are good insulators. Conduction of electrons through the reduced film at the electrode surface to the film coating it is thought to be difficult.

In Figure.VII.5.A in chapter VII, a UV-Visible absorption vs potential plot for PBT, the slightly negative slope between -0.5 V and +0.75 V indicates that a small amount of polymer oxidation occurs in this range. Conversely Figure.VII.5.B shows that oxidation of PPY begins at -0.5 V and that the polymer is completely oxidized by +0.5 V. If anions diffuse through the outer polymer film and oxidize the polymer near the electrode first, then the PPY layer in the PY/BT bilayer film should show

some oxidation in the cyclic voltammograms (Figure.V.12) below +0.5 V at slow rates of scan. Conversely the PBT film in the BT/PY bilayer film (Figure.V.11) should be only slightly oxidized and the oxidation of the PPY layer should be affected by the PBT layer on which it was polymerized.

The cyclic voltammograms of the bilayer films indicate that some transfer of electrons through the reduced polymer film must occur for the polymer coating the surface of the polymer to be oxidized. As these are only one set of experiments much more work must be done to prove or disprove these results.

Comparing the copolymer results to these bilayer films one can see that the polymerization of the two homopolymers together does not give rise to the +0.54 V E_{pa} peak found in the voltammogram of the copolymer. The peak heights of the two homopolymers in the bilayer films were proportional to the amounts of either polymer on the electrode, therefore the oxidation peaks in the copolymer should be representative of the number of oxidizable sequences of the three types in the copolymer.

Section V.4 Conclusions

This chapter has shown that the copolymer of PY and BT has three E_{pa} peaks. Two of the peaks are at similar potentials to those of the homopolymers, but the peak at +0.54 V is new and characteristic of only the copolymer.

Two bilayer films were polymerized with PPY and PBT layers of equal thicknesses. The cyclic voltammograms of these bilayers indicated that the peak currents are proportional to the number

of oxidizable polymer units. The bilayers also indicated that the oxidation of the films occurs first at the surface of the polymer film and then spreads through the bulk of the film.

CHAPTER VI THE IN SITU MEASUREMENT OF THE UV-VISIBLE ABSORPTION SPECTRUM OF CONDUCTING COPOLYMERS

Section VI.1 Introduction

One of the most interesting physical properties of PBT and PPY is their absorption of light in the UV-visible spectra. The peak absorbance of the polymers shift as the films are doped or undoped. In the neutral or undoped state the polymers' peak absorbance of light is in the 350-450 nm range of the spectrum and in the doped or oxidized state the polymers' peak absorbances range from 650-800 nm. For PPY this means that thin films have a vivid orange colour in the reduced state and a purplish blue in the oxidized. PBT's colours change from a bright red to a dark green-blue. The shade and hue of the doped polymers are somewhat affected by the doping anion and the polymerization parameters. The colours are most vivid when polymerized on polished Pt or on a Pt mirror.

The discovery that these polymers change colour has led to a number of suggested applications, such as electrochromic display devices [118]. The polymer's abilities could be easily used to create displays similar to liquid crystal displays, however the switching time for the polymers is currently prohibitive. Chemical doping of the polymers could allow the polymers to be used as a litmus type test for certain chemicals [119]. The polymers change colour when the films are in contact with chemicals which can oxidize or reduce it, indicating the presence of the chemicals in solution. Different types of conducting polymers could be used together in an array to give

sensitivities to a large number of different chemicals.

The absorption peaks in the 350-450 nm range of the reduced polymers can be identified as resulting from a π-π^* transition of the double C bonds in the extended conjugation of the polymer chain [120]. The identification of the peaks in the oxidized spectra are much more difficult and must rely on conductivity theory. For highly oxidized PPY there are two intense peaks and one minor peak in the range of 200-2400 nm. Three of these peaks are in the visible range (1200-350 nm). The peaks responsible for the intense colour are caused by the transitions between the valence band and the antibonding polaron state and between the valence band and the bonding polaron state [39]. The other peak is the π-π^* transition, which is reduced considerably in intensity in comparison to the reduced spectrum. At low levels of doping a fourth peak appears in between the peaks for the valence band-bonding and valence band-antibonding transitions. This peak is due to the formation of a polaron rather than bipolarons at low levels of doping and results from the transition between the bonding and antibonding polaron states. Oxidized PT (or PBT) has the same three peaks in the oxidized form as PPY but does not show the same polaron formation at low levels of doping [43].

For this study the absorbance of PPY, PBT, their copolymers and a bilayer film, formed by the polymerization of layers of PPY and PBT of equal thickness, were examined in the 750-350 nm range. The polymers were examined at various levels of doping and the oxidized and reduced forms of the polymers were compared.

Section VI.2 Experimental

VI.2.1 Purifications

The same purification techniques used in section II.2.1 were used for the purification of TBAP, PY, BT and ACN in this chapter.

VI.2.2 Apparatus

An H cell was constructed that was similar to that diagrammed in Figure II.3 in size and dimensions, except that the bottom of one of the compartments was extended and a "Vycor" glass spectrometer cuvette was attached (see Figure VI.1). The cell used the same "Teflon" air tight tops sealed with silicone rubber "O" ring as were used on the H cells in Figure II.3.

The cell was fitted with two saturated calomel reference electrodes (Fisher Scientific). The SCE's were separated from the working compartment by a Luggin capillary and a KCl salt bridge (see Figure VI.1)

The working electrodes were constructed from a sheet of In doped SnO_2-coated glass. This coating is optically clear and does not absorb in the 750-190 nm range but the glass on which it is coated cuts off all transmission through it below 340 nm. Thus the absorption spectra from 340 nm to 190 nm cannot be recorded. For this reason a "Vycor" cuvette was used rather than a Quartz cuvette. The glass was cut into 0.9 cm by 2.0 cm pieces using a diamond saw. Wires were connected to the pieces of glass by spotting the edges of the glass with an In-Ga amalgam and then gluing the wires over the spots with conducting silver dag (Acheson). Adhesion to the wires was improved through the coating

Figure.VI.1 DIAGRAM OF SPECTROPHOTOMETRIC ELECTROCHEMICAL CELL

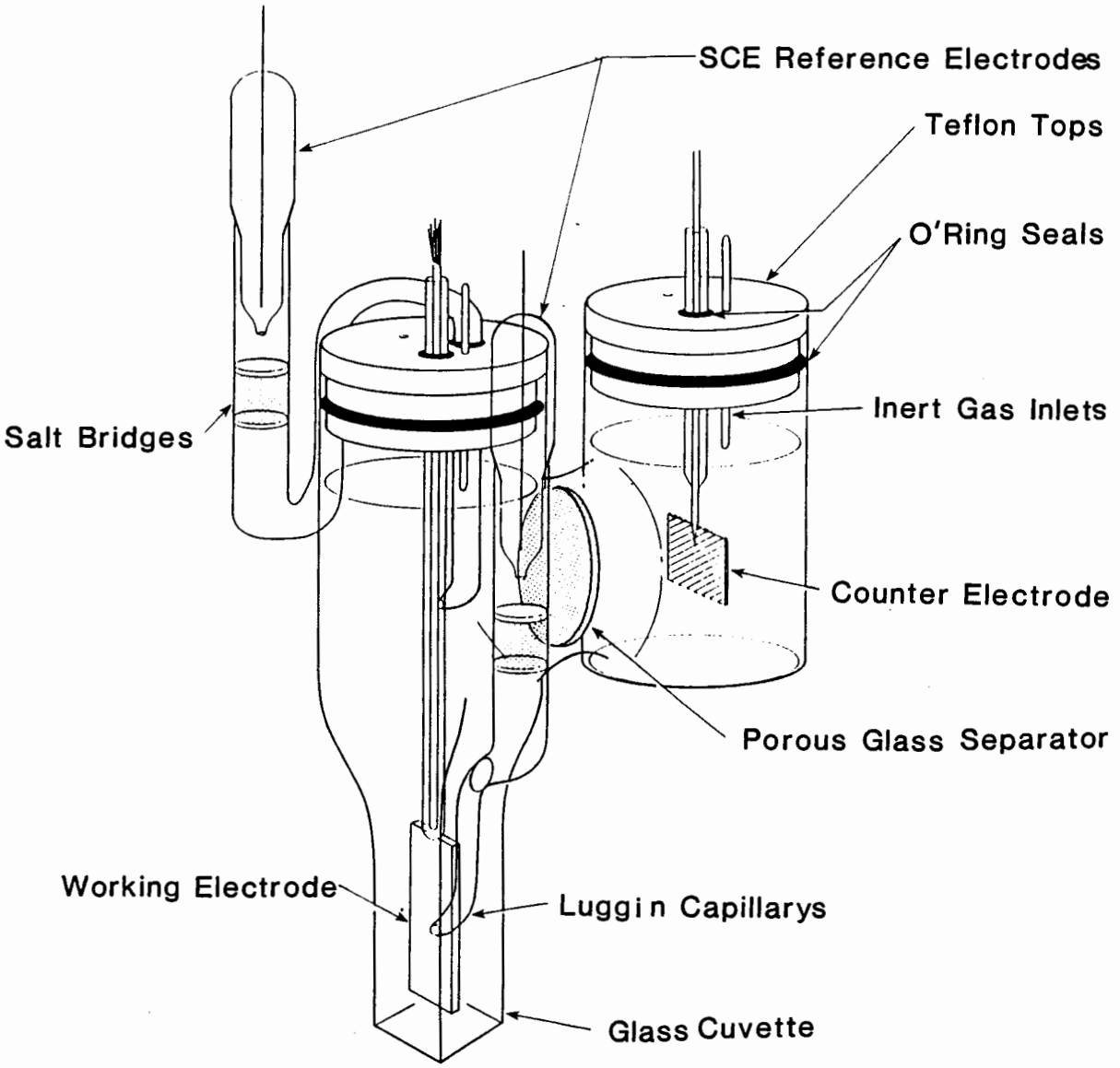
SCE Reference Electrodes
Teflon Tops
O'Ring Seals
Salt Bridges
Inert Gas Inlets
Counter Electrode
Porous Glass Separator
Working Electrode
Luggin Capillarys
Glass Cuvette

Figure.VI.1

of the silver dag with 24 hour epoxy (Conap Easypoxi). The electrode wires were covered with 4.0 mm diameter "Pyrex" glass tubing to form electrode shafts and one end was sealed to the electrodes with the epoxy.

The counter electrodes were constructed from Pt sheet. A 4 cm^2 piece of thin Pt sheet was spot welded to a Pt wire. The Pt wire was covered with a 4 mm "Pyrex" glass tube and the end of the tube near the electrode was sealed with a torch to the Pt wire.

The absorbance measurements were made using a Perkin-Elmer model 190 UV-visible spectrophotometer connected to a Perkin-Elmer R100A chart recorder.

VI.3 Polymerization

Before polymerization each part of the cell was carefully washed and then dried in a 90°C oven for 4 hrs. to remove water from the surface of the cell. The cell was flushed with Ar before being charged with 75 ml of monomer solution. The monomer solutions were mixed in 100 ml volumetric flasks and contained a 0.1 M concentration of TBAP and 0.01 M concentration of one or both the monomers in ACN. The TBAP/ACN solutions were bubbled with Ar before the monomers were added to the solution to reduce the change of oxidation of the monomers. An Ar atmosphere was maintained in the polymerization cell during polymerization and subsequent spectrophotometric measurements.

The working electrode was maintained at a selected value by a PAR 170 potentiostat for all the reactions except the bilayer films which were polymerized using the EG&G PAR 173, so the

thickness of the layers could be estimated using the integral EG&G PAR 179 reversible coulometer. For the polymerization of PBT and the copolymer the electrode potential was set at +1.3 V vs SCE, and for the polymerization of PPY the potential was set at +1.0 V vs SCE.

The polymers were polymerized on the electrode with the electrode near the capillary in the upper part of the compartment. A small amount of each polymer was polymerized and then reduced. In the reduced form the polymer coated electrode was moved down into the cuvette and the absorbance of the polymer was measured with the spectrophotometer. If the absorbance of the polymer was sufficient, the monomer solution was removed from the cell by suction, the cell was rinsed with clean O_2 free electrolyte solution (0.1 M TBAP in ACN) and then refilled with the electrolyte solution, but if the absorbance was insufficient then the electrode was moved back to the upper position and more momomer was polymerized on the electrode.

For the bilayer film, a layer of PBT was polymerized on the electrode first and the thickness was calculated from the coulometric measurements. The PBT's absorbance was measured, then the BT solution was suctioned from the cell, the cell was flushed with clean O_2 free electrolyte solution and then filled with a PY solution. Next a layer of PPY was polymerized on top of the PBT and the thickness was calculated using the coulometer. Again the monomer solution was suctioned from the cell and the cell was flushed with electrolyte, but this time the cell was filled with electrolyte solution for spectrophotometric measurements.

VI.4 Spectrophotometric Measurements

Once the monomer solution had been removed and replaced with electrolyte solution, measurement of the polymer's visible absorbance spectra could begin. The potential on the electrode was set so that the polymer was fully reduced and was allowed to remain at this potential for 15-20 minutes so that all anions were removed from the polymer. After this waiting time the polymer's visible absorbance spectrum (350-750 nm) was taken at a scan rate of 60 nm/s. The potential on the electrode was then stepped up by +0.20 V and the electrode was allowed to equilibrate again for 15-20 minutes. The absorbance spectrum was taken again and this procedure was repeated until a voltage of +1.4 V (vs SCE) was reached.

Section VI.3 Results and Discussion

In Figure VI.2 the absorption spectra for the copolymer polymerized for a 50:50 BT:PY monomer solution are plotted together to show the evolution of the absorbance peaks with the changing potential. The π-π^* transition peak at 445 nm is visible even in the oxidized form although it is some what masked by valence band-antibonding polaron band transition at approximately 700 nm.

Figures like VI.2 were made for the homopolymers and the bilayer film to help characterize the peaks. The plots of absorbance vs potential (Figure VII.5) were used to determine the potentials for the fully oxidized and neutral spectra of the copolymer and the homopolymers. The fully oxidized spectra were taken at the potential given for the minimum absorbance of these

Figure.VI.2 UV-VISIBLE ABSORPTION SPECTRA FOR A COPOLYMER FILM

Spectra for a copolymer film recorded in situ on a In doped SnO_2-coated glass electrode at potentials ranging from -0.2 V to 1.4 V versus a SCE. The electrolyte used was TBAP in ACN. The spectra are plotted with the potential on the electrode increasing with absorption. The spectrum plotted with the minimum absorption is for -0.2 V and spectra of increasing absorption are recorded at 0.2 V potential intervals. The spectra's absorptions are offset so that the spectra do not overlap.

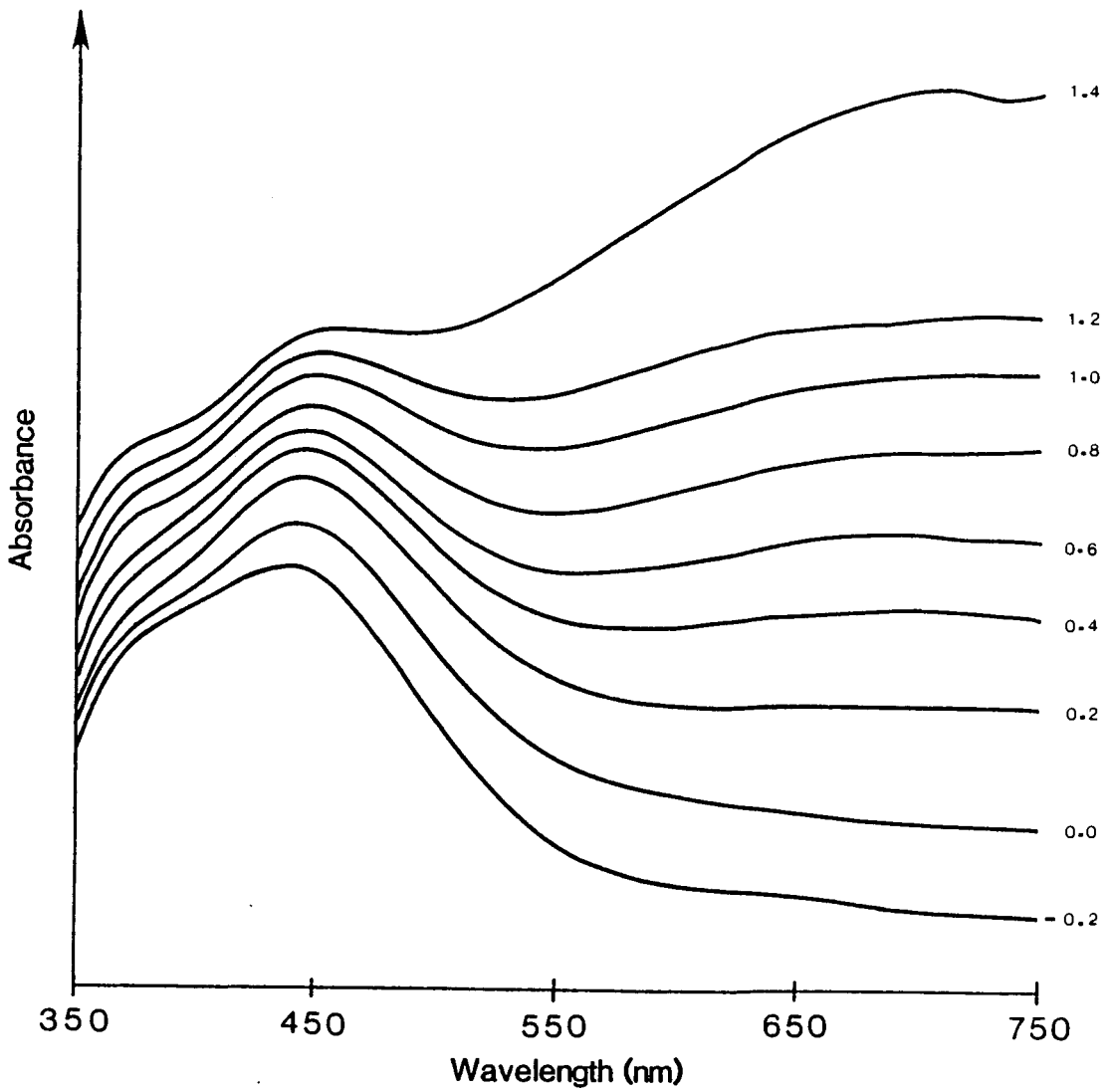
Absorbance
1.4
1.2
1.0
0.8
0.6
0.4
0.2
0.0
0.2
350
450
550
650
750
Wavelength (nm)

Figure.VI.2

curves and the neutral spectra were taken at the potential given for the maximum absorbance at low potentials for these curves. The spectra for the neutral forms of PPY, PBT, the copolymer and the bilayer film are plotted together in Figure VI.3. The major peak in each spectra is from the π-π^* transition. The peak for the copolymer (spectrum B) appears at a wavelength between those for PBT (spectrum A) and PPY (spectrum D). The copolymer's peak is not symmetrical like PBT's, but has an irregular shape that looks almost as if it is comprised of two peaks. The peak of poly(thienylpyrrole) polymerized by Naitoh et al. [72] has a similar shape and position (440 nm), but the polymer is composed only of pyrrole and thiophene rings. Thus this peak must be from a single copolymer and can not be comprised of two separate peaks. The bilayer film, Figure VI.3.C, should give a spectrum representative of equal amounts of the homopolymers polymerized together in a mixture, as layers of PBT and PPY of equal thicknesses were polymerized on the electrode. The bilayer appears have a greater absorbance in the PPY area than the PBT area as the spectrum has a large peak in the 360 nm range which is similar to PPY's. The peak however is much broader than PPY's indicating that some absorption is present for the PBT. Note that the position of the peak does not shift as with the copolymer but the two peaks simply merge to form one broad peak.

The spectra for the oxidized forms of PPY, PBT, the copolymer and the bilayer film are plotted together on Figure VI.4. The interpretation of the spectrum for the copolymer (Spectrum B) is difficult. Only one of the two peaks (700 nm) appears in the spectra for poly(thienylpyrrole) [72]. For Figure

Figure.VI.3 UV-VISIBLE ABSORPTION SPECTRA FOR REDUCED POLYMER FILMS

Spectra for reduced polymer films recorded in situ on In doped SnO_2-coated glass electrodes in a 0.1 M TBAP/ACN solution. Spectra are recorded for:

A) PBT
B) The Copolymer
C) a Bilayer film with layers of PPY and PBT
D) PPY

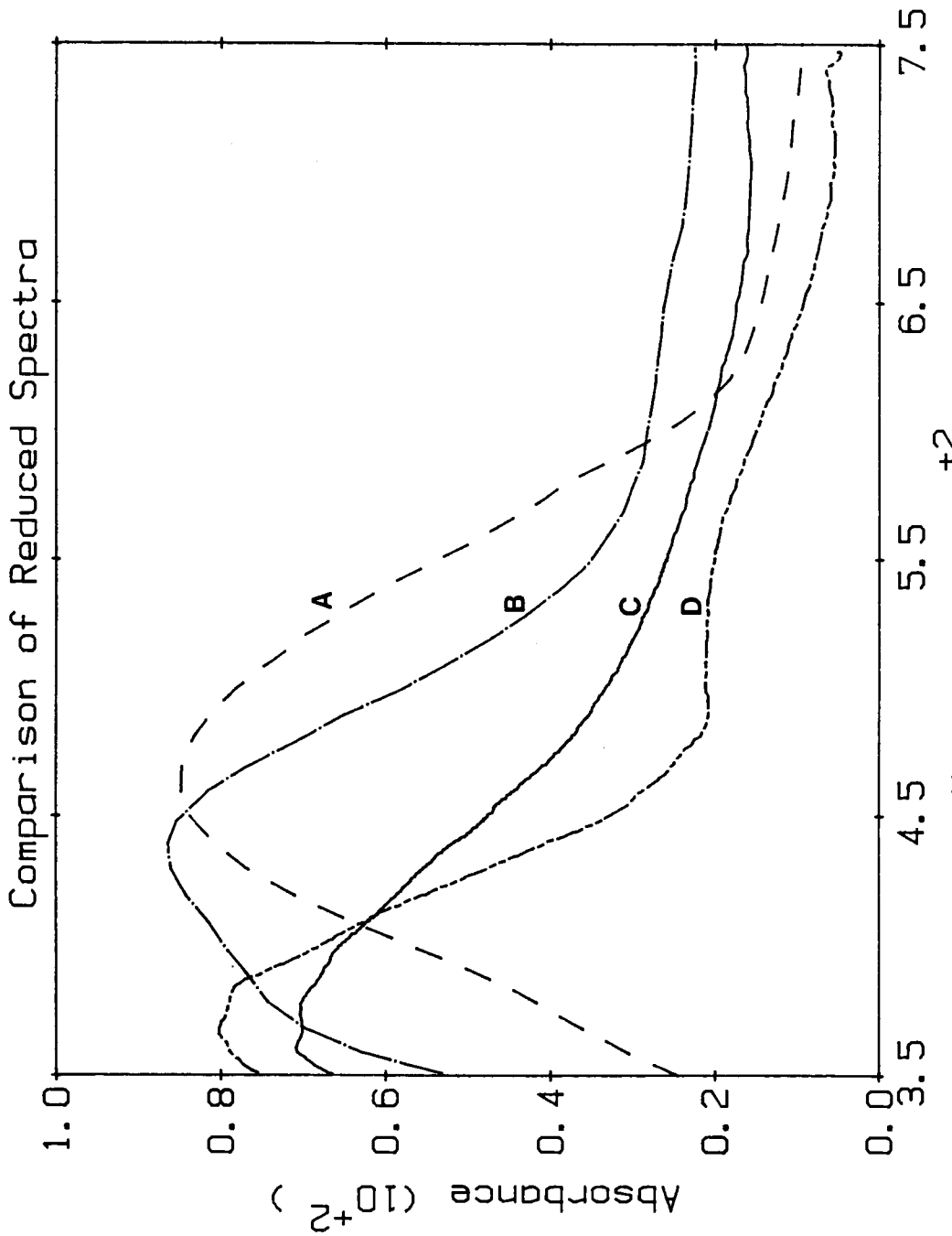
Comparison of Reduced Spectra
Absorbance (10^{+2})
1.0
0.8
0.6
0.4
0.2
0.0
3.5
4.5
5.5
6.5
7.5
Wavelength (10^{+2} nm)
A
B
C
D

Figure.VI.3

Figure.VI.4 UV-VISIBLE ABSORPTION SPECTRA FOR OXIDIZED POLYMER FILMS

Spectra for oxidized polymer films recorded in situ on In doped SnO_2-coated glass electrodes in a 0.1 M TBAP/ACN solution. Spectra are recorded for:

A) PBT
B) The Copolymer
C) PPY
D) A Bilayer Film with layers of PPY and PBT

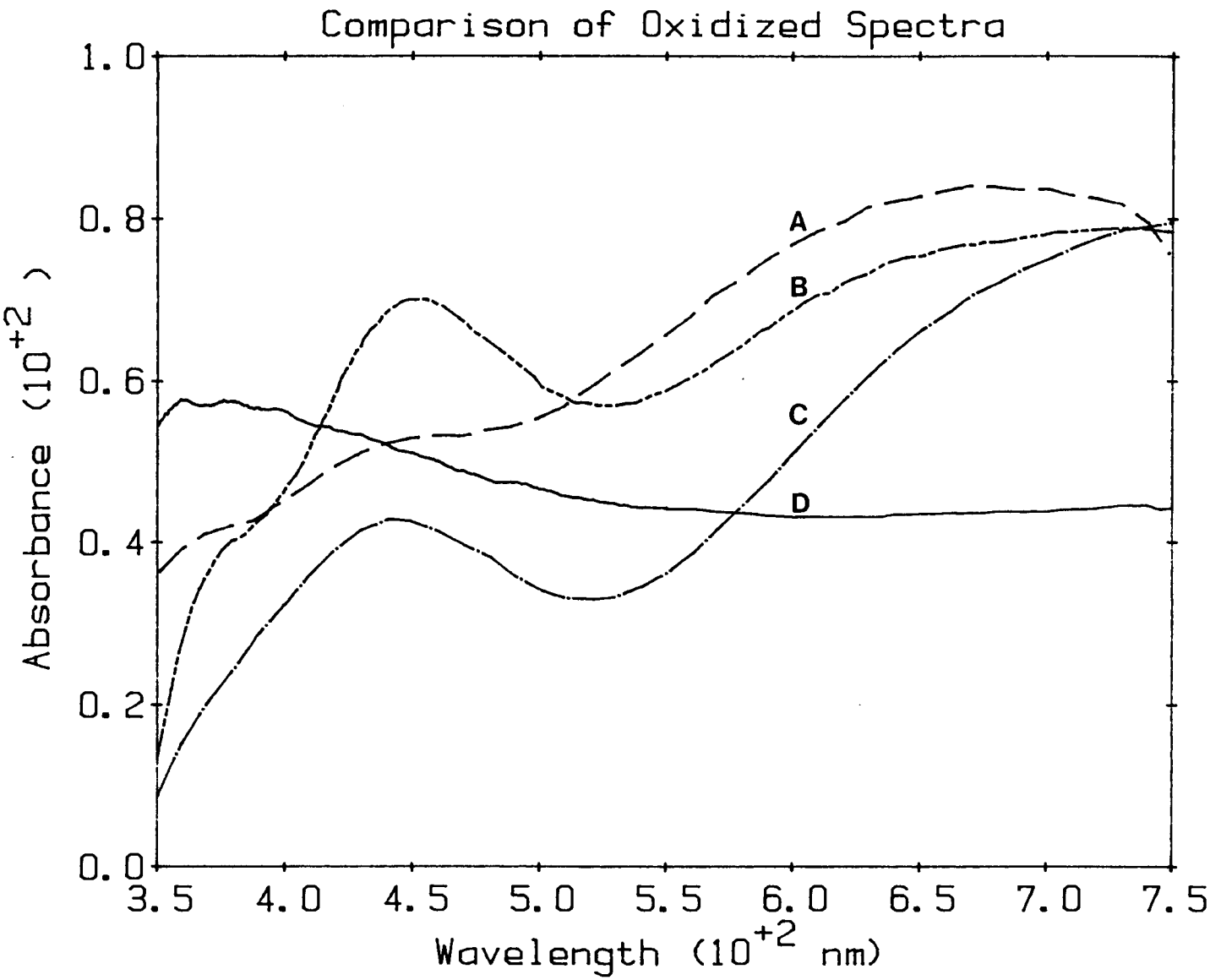
Comparison of Oxidized Spectra
1.0
0.8
0.6
0.4
0.2
0.0
Absorbance (10^{+2})
A
B
C
D
3.5
4.0
4.5
5.0
5.5
6.0
6.5
7.0
7.5
Wavelength (10^{+2} nm)

Figure.VI.4

VI.2 the peak ranging from 450-375 nm was defined as resulting from the π-π^* transition and the peak at 700 nm from the Valence band-antibonding transition. The reason that the π-π^* peak in our copolymer remains close to the 450 nm wavelength during oxidation while the poly(thienylpyrrole) copolymer's peak shifts to a shorter wavelength is unclear. Naitoh et al. do not give a plot of the spectra at various electrode potentials like Figure VI.2 so we can only speculate that his film may have been oxidized irreversibly or that the fact that he is using HSO_4^- as the anion may be affected the film's spectra.

The spectrum for oxidized PBT is given in Figure VI.4 as spectrum A. According to Heeger [43] the peak at approximately 650 nm is from the valence band-antibonding polaron state transition and the small peak at about 440 nm is from the π-π^* transition.

Line C is the spectrum for the oxidized PPY film. Bredas et al. [39] defined the peak at 450 nm as from the valence band-antibonding polaron state transition and the peak > 750 nm as the valence band-bonding polaron state transition.

Thus the valence band-antibonding transition peak of the copolymer is at a longer wavelength than either of the homopolymers. The peak for the π-π^* transition is proportionally larger than the PBT's possibly due to the shift of the valence band-antibonding transition peak to higher wavelengths.

The spectrum for the oxidized form of the bilayer film appears very featureless. The peak from the π-π^* transition is visible at approxiately 370 nm, but little else can be defined.

Note that the spectrum is significantly different from that of the oxidized copolymer, which has two clearly definable peaks.

Two of the three possible peaks have been defined for copolymer, but unfortunately the valence band-bonding transition peak has not been found. Thus the polaron band gap can not be calculated. Further experiments must be done to determine in situ UV-visible absorption spectra in the range from 750-2400 nm to define the other peak.

Section VI.4 Conclusion

In this chapter the visible absorption spectra of the copolymer have been measured and compared to the spectra of the homopolymers. The spectra of the copolymer have been shown to be significantly different than the spectra of the homopolymers and similar to poly(thienylpyrrole) spectra, a copolymer polymerized by Naitoh et al. The copolymer's peaks have been defined using polaron band gap theory although the band gap for the copolymer was not defined.

CHAPTER VII DETERMINATION OF OXIDATION POTENTIAL USING IN SITU SPECTROPHOTOMETRIC MEASUREMENTS

Section VII.1 Introduction and Theory

Much of the theory and introduction for the UV-visible spectra of these conducting polymers can be taken from the preceding chapter. Only the method for the determination of the oxidation potentials from the spectra will be outlined here.

In "The Determination of Oxidation Potentials by Cyclic Voltammetry" (Chapter V) only the anodic peak potentials (E_{pa}) were determined for the copolymer films at specific potential scan rates. The species specific $E_{1/2}$ value could not be determined as the polymers did not act as normal reversible species during reduction. For this reason other techniques were considered to enable the $E_{1/2}$ to be determined.

A method has been developed from the Nernst Equation [123,124] which uses the spectra of redox couples at equilibrium taken at various potentials, similar to the data displayed in Figure VI.2., to determine the $E_{1/2}$ and the electron stoichiometries of the redox couple. This method was modified to determine these values for these conducting polymers.

Section VI.2 Experimential

VI.2.1 Purifications

The same purification techniques used in section II.2.1 were used for the TBAP, BT, PY and ACN used in this chapter.

VI.2.2 Apparatus

The cell and all of the equipment were identical to that

used in Chapter VI except for slight modifications to the working electrodes.

The working electrodes were constructed from a sheet of In-doped SnO_2-coated glass, using the same methods as outlined in Chapter VI, but before the wires were attached a layer of Au was applied along the sides of the glass electrodes to aid in conduction of electricity around the electrode surface. The layer of gold was coated on the edges of the glass by masking the middle of the electrode and condensing a thin layer of gold on the electrodes in a vacuum evaporator. After the layer of gold was applied, the masking on the center portion of the electrode was removed and wires were attached using the same procedure as outlined in Section VI.2.2. The center of the electrode was then remasked and a layer of Conap epoxy was applied to cover the layer of gold on the edges of the electrode. Before the epoxy had fully hardened, the masking in the center of the electrode was removed to leave a clear window in the center of the electrode on which the polymers were coated.

VII.2.3 Polymerizations

Before polymerization each part of the cell was carefully washed and dried in a 90° C oven for 12 hrs. to remove water from the surface of the cell, and monomer solutions were mixed containing 0.1 M concentrations of TBAP and 0.01 M concentrations of one or both the monomers. Care was taken to remove O_2 from the solutions by bubbling them with Ar gas before the addition of the monomers. After the cell was assembled and flushed with Ar, it was charged with 75 ml of the monomer solution. An Ar atmosphere

was maintained in the cell during polymerization and subsequent spectrophotometric measurements.

The potential on the working electrode was applied on the working electrode with a PAR 170 Potentiostat for the polymerizations and subsequent spectropotential measurements. For the polymerization of PBT and the copolymer the electrode potential was set at +1.3 V vs SCE and for the polymerization of PPY the potential was set at +1.0 V vs SCE.

The polymerizations of the polymer films were done with the electrode near the capillary in the upper part of the working compartment. A small amount of polymer was polymerized and then reduced to -0.50 V vs SCE. In the reduced form the polymer coated electrodes were moved down into the cuvette and the absorption spectra were taken for the polymers at wavelenghths from 350 to 750 nm. If the peak absorbance was not great enough for accurate photodetection then the electrode moved back up and more polymer was polymerized on the electrode. Once the absorbance was sufficient, the monomer solution was suctioned from the cell, the cell was rinsed with clean O_2 free electrolyte solution (0.1 M TBAP in ACN) and filled with the same electrolyte solution.

VII.4 Spectropotentiometric Measurements

After the monomer solution had been removed and replaced with clean electrolyte the electrode was moved into the cuvette for spectrophotometric measurements. The Perkin-Elmer 190 spectrophotometer was set to measure the absorbance at a single

Figure VII.1: UV-VISIBLE ABSORPTION SPECTRA FOR A COPOLYMER FILM

Spectra for a copolymer film recorded in situ on a In doped SnO_2-coated glass electrode at potentials ranging from -0.2 V to 1.4 V. The electrolyte used was TBAP in ACN.

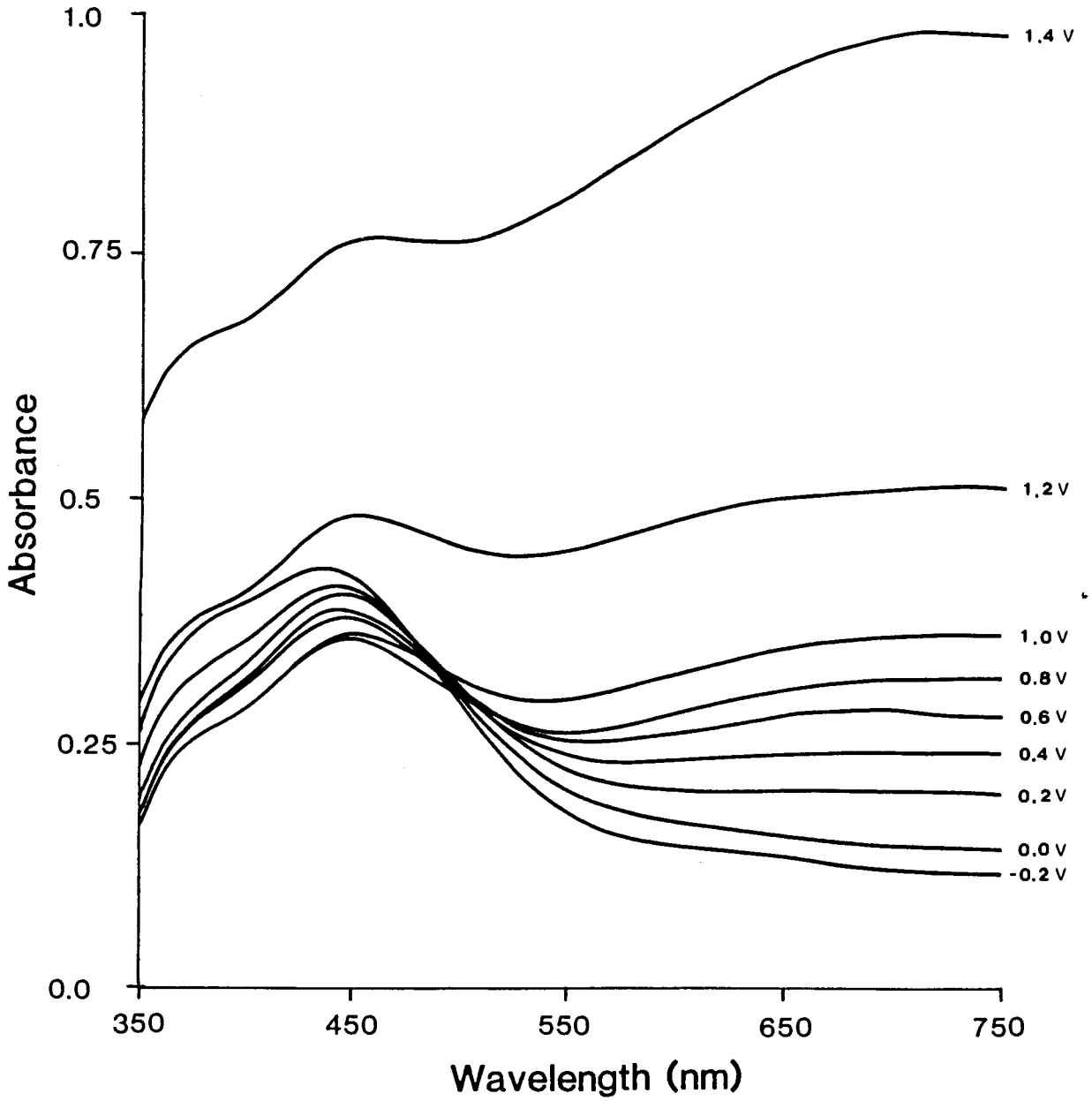
1.0
0.75
0.5
0.25
0.0
Absorbance
350
450
550
650
750
Wavelength (nm)
1.4 V
1.2 V
1.0 V
0.8 V
0.6 V
0.4 V
0.2 V
0.0 V
-0.2 V

Figure.VII.1

wavelength and the potential was slowly scanned by the potentiostat. The film's absorbance vs time was recorded on a Perkin-Elmer R100A chart recorder. The potential on the electrode was monitored using a Fluke 8840A multimeter and the accuracy of the potential ramp was monitored using a Cole-Palmer R100A chart recorder. The initial potential on all of the polymers was -0.50 V vs SCE but the final potential varied with the polymer being measured. The potential scan rate was very slow (0.2 mV/s) so that the redox couple was essentially at equilibrium at all times. The scans took 2 to 3 hours to complete.

Section VII.3 Results and Discussion

Initially the data from Chapter VI was used to calculate the E_o' (or $E_{1/2}$) values for the polymers. Figure VII.1 is the absorption spectra of the copolymer film for various electrode potentials. Figure VII.1 is essentially the same data as that displayed in Figure VI.2 execpt that the spectra in Figure VI.2 were offset so that the spectra did not overlap. Other figures similar to Figure VII.1 were constructed for the spectra of PPY and PBT. Each spectrum was recorded 15 min after the potential was applied to the electrode so that the polymer redox couple was at equilibrium with the electrode. The absorbances at a single wavelength for the various electrode potentials were taken from these plots and used for the calculation of the formal oxidation potential E_o'.

The calculations used the Nernst equation. The Nernst equation relates the electrode potential to a redox couple in the form:

$$E = E_o' - \frac{RT}{nF} \ln \frac{[S_o]}{[S_r]} \qquad [7.1]$$

where $[S_o]$ and $[S_r]$ are the concentrations of the oxidized and reduced species, R is the gas constant, T is the temperature, F is the Faraday constant, n is the number of electrons involved in the reaction and E_o' is the formal potential. E_o' is equal to $E_{1/2}$ for systems where the diffusion of the oxidized and reduced species are equivalent.

The spectrophotometric absorption A of a redox couple taken from the spectra of the polymer at various levels of doping as in Figure VII.1 is equated to the concentrations of the oxidized and reduced species using the relationship [123]:

$$\frac{[S_o]}{[S_r]} = \frac{(A_{red} - A)}{(A - A_{ox})} \qquad [7.2]$$

Where A_{red} and A_{ox} are the absorbances of the polymer in the reduced form and oxidized form.

For a redox couple at 294°K equation 7.1 simplifies to:

$$E = E_{1/2} - 0.0253/n \ln \frac{(A_{red} - A)}{(A - A_{ox})} \qquad [7.3]$$

The absorbance values taken from Figure VII.1 and the other similar spectra for PPY and PBT were used to calculate $\ln [(A_{red}-A)/(A-A_{ox})]$. The potentials on the electrodes were plotted against these calculated ln values, to give straight lines with slopes equal to 0.0253/n and intercepts equal to E_o' (or $E_{1/2}$).

This method worked in principle but as these experiments were not designed for this type of analysis some of these plots had only three points. The selection of the A_{red} and A_{ox} values

was also difficult because the absorption of the polymer films continues to increase as the film becomes irreversibly oxidized. The effects of irreversible oxidation can be seen in Figure VII.1 by the increase in absorption at low wavelengths in the oxidized +1.4 V spectrum.

To correct for these errors modifications to the procedure were made. Rather than take spectra for a few potentials after allowing the polymer film to equilibrate for 15 mins, the spectrophotometer was set at a specific wavelength of interest and the potential was scanned very slowly (0.2 mV/s) from -0.5 V to the point were irreversible oxidation occurs. As the potential on the polymer coated electrode is increased from -0.5 V the absorption of the π-π^* transition peak decreases to the point were irreversible oxidation of the polymer occurs and then starts to increase, but the absorption of valence band-antibonding polaron state transition peak increases and continues to increase during irreversible oxidation. Thus the potential where the polymer oxidation ends and irreversible oxidation begins is difficult to define using the valence band-polaron antibonding transition peak. For this reason the absorption wavelength of the spectrophotometer was centered on the π-π^* transition peak of the reduced polymer. The exact wavelengths, which were chosen using Figures VII.2-4, are marked on these figures. The wavelengths were chosen for the difference in absorption between the reduced and oxidized spectra and not necessarily on the absorption maxima in the reduced state.

Figure VII.2: OXIDIZED AND REDUCED SPECTRA FOR POLYPYRROLE

Spectra for a polypyrrole film recorded in situ on a In doped SnO_2-coated glass electrode. The dotted line at 360 nm denotes the wavelength used for spectropotentiometric study of polypyrrole.

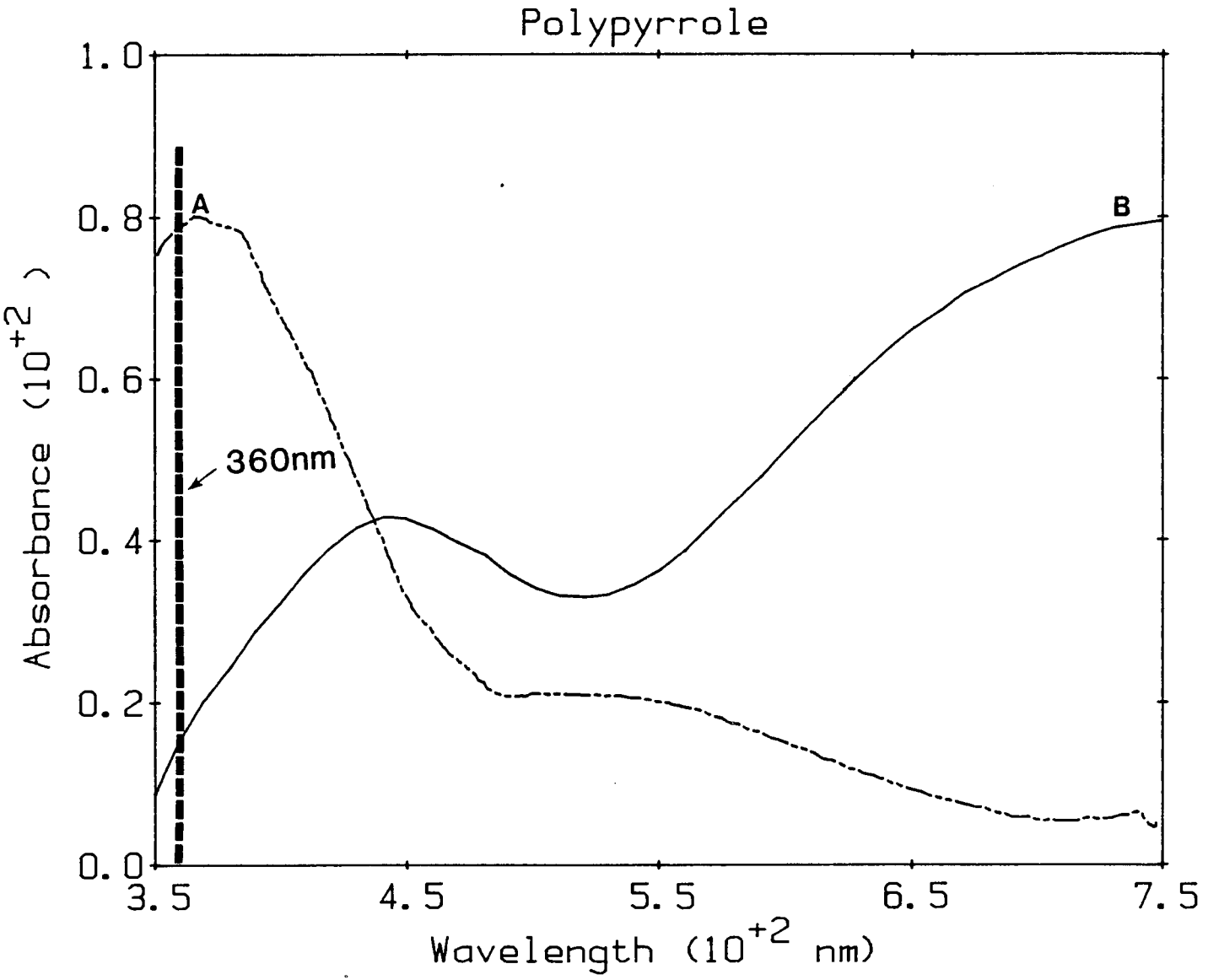

Figure.VII.2

Figure VII.3: OXIDIZED AND REDUCED SPECTRA FOR POLY(2,2'-BITHIOPHENE)

Spectra for a poly(2,2'-bithiophene) film recorded in situ on a In doped SnO_2-coated glass electrode. The dotted line at 450 nm denotes the wavelength used for spectropotentiometric study of poly(2,2'-bithiophene)

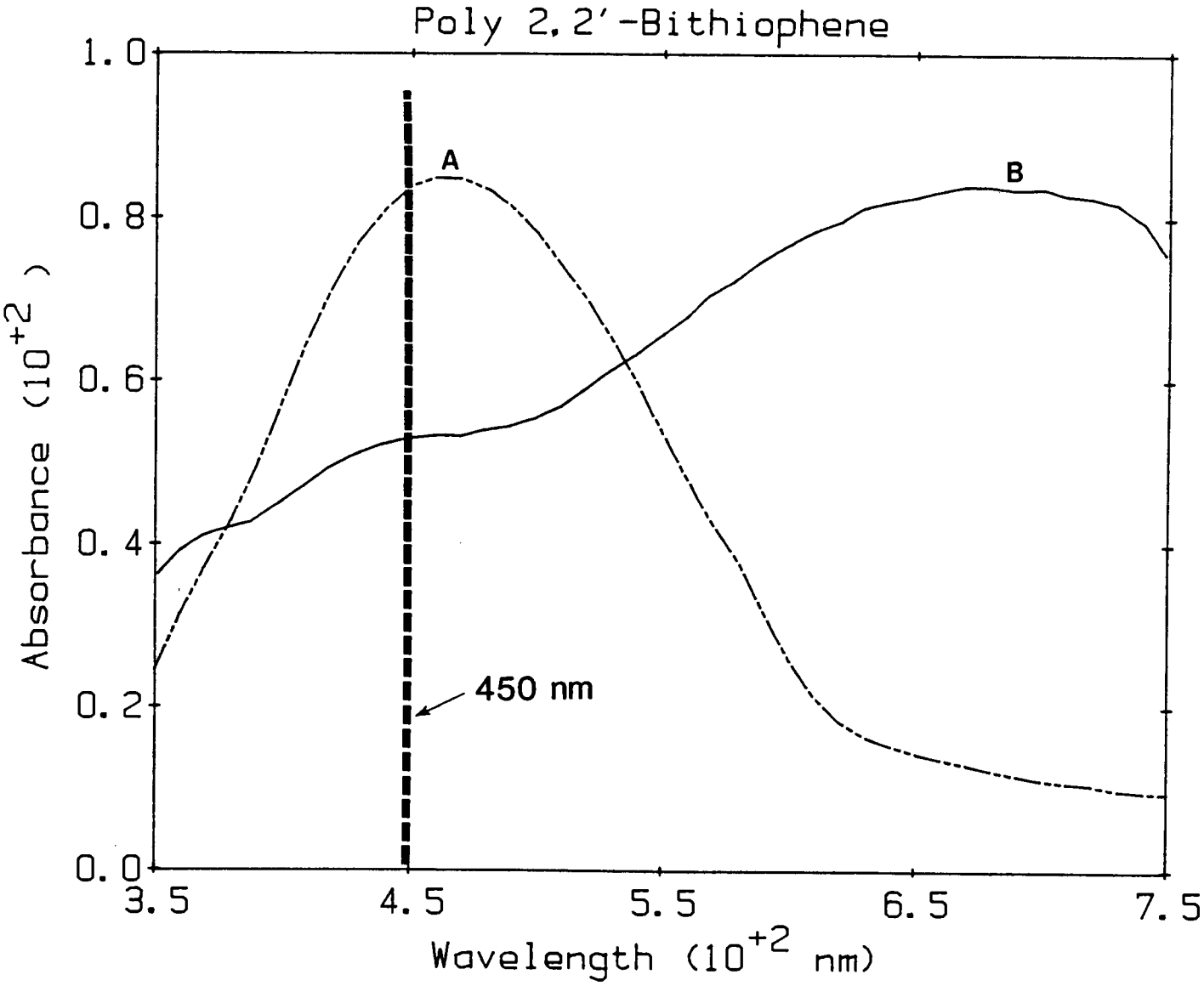
Poly 2,2'-Bithiophene
1.0
0.8
0.6
0.4
0.2
0.0
Absorbance (10^{+2})
A
B
450 nm
3.5
4.5
5.5
6.5
7.5
Wavelength (10^{+2} nm)

Figure.VII.3

Figure VII.4 OXIDIZED AND REDUCED SPECTRA FOR A COPOLYMER

Spectra for a Copolymer film recorded in situ on a In doped SnO_2-coated glass electrode. The dotted line at 390 nm denotes the wavelength used for spectropotentiometric study of the copolymer

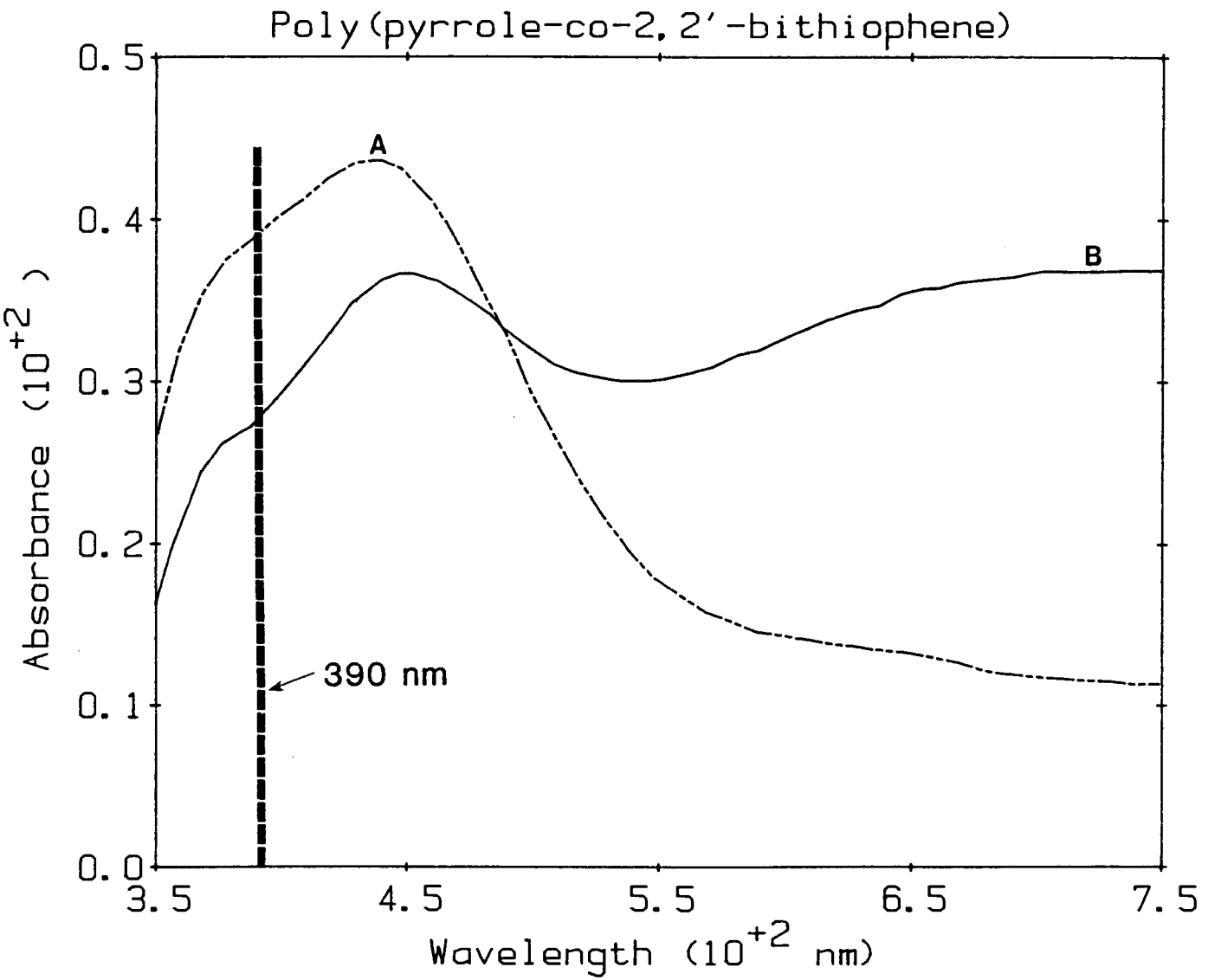
Poly(pyrrole-co-2,2'-bithiophene)
0.5
0.4
0.3
0.2
0.1
0.0
Absorbance (10^{+2})
A
B
390 nm
3.5
4.5
5.5
6.5
7.5
Wavelength (10^{+2} nm)

Figure.VII.4

Plots of absorbance at these wavelengths as a function of the potential are illustrated in Figure VII.5. Curve A shows that the oxidation of PBT begins at approximately +0.70 V and reaches a maximum at around +1.28 V before the oxidation becomes irreversible. The oxidation of PPY begins -0.50 V and reaches a maximum at +0.50 V (curve B). Curve C shows that the oxidation of the copolymer begins around +0.0 V and reaches its maximum at +1.10 V.

The Nernstian plot from curve A in Figure VII.5 for PBT is shown in Figure VII.6. For linearization, the standard Nernstain equation 7.3 had to be modified slightly as the decay of the π-π^* transition peak was observed rather that one of the peaks forming due to the valence band transitions.

$$E = E_{1/2} - 0.0253/n \ln \frac{(A - A_{ox})}{(A_{red} - A)} \qquad [7.4]$$

Values of absorbance A are taken at increasing applied voltage E. Using the absorbance values at 0.0 and +1.28 V as characteristic of the reduced and oxidized species for A_{red} and A_{ox} respectively in the log function, the slope of the Nernstian plot for PBT is 0.087, which yields a value for the number of electrons transferred in the oxidation step n = 0.30. This means that one electron is transferred in the oxidation of approximately 3.3 thiophene ring units. The intercept of this graph is equal to +1.03 volts, the standard oxidation potential for the redox couple in PBT (E_o').

Figure VII.7 is the Nernstian plot for PPY. The values for A_{red} and A_{ox} were taken from the absorbance values of the polymer

Figure VII.5 ABSORPTION VERSUS POTENTIAL PLOTS

Plots are recorded at the single wavelength denoted on Figures VII.2-4. The potential on the electrode are monitored vs a SCE reference electrode. The absorptions are recorded in situ for:

A) PBT
B) PPY
C) Copolymer

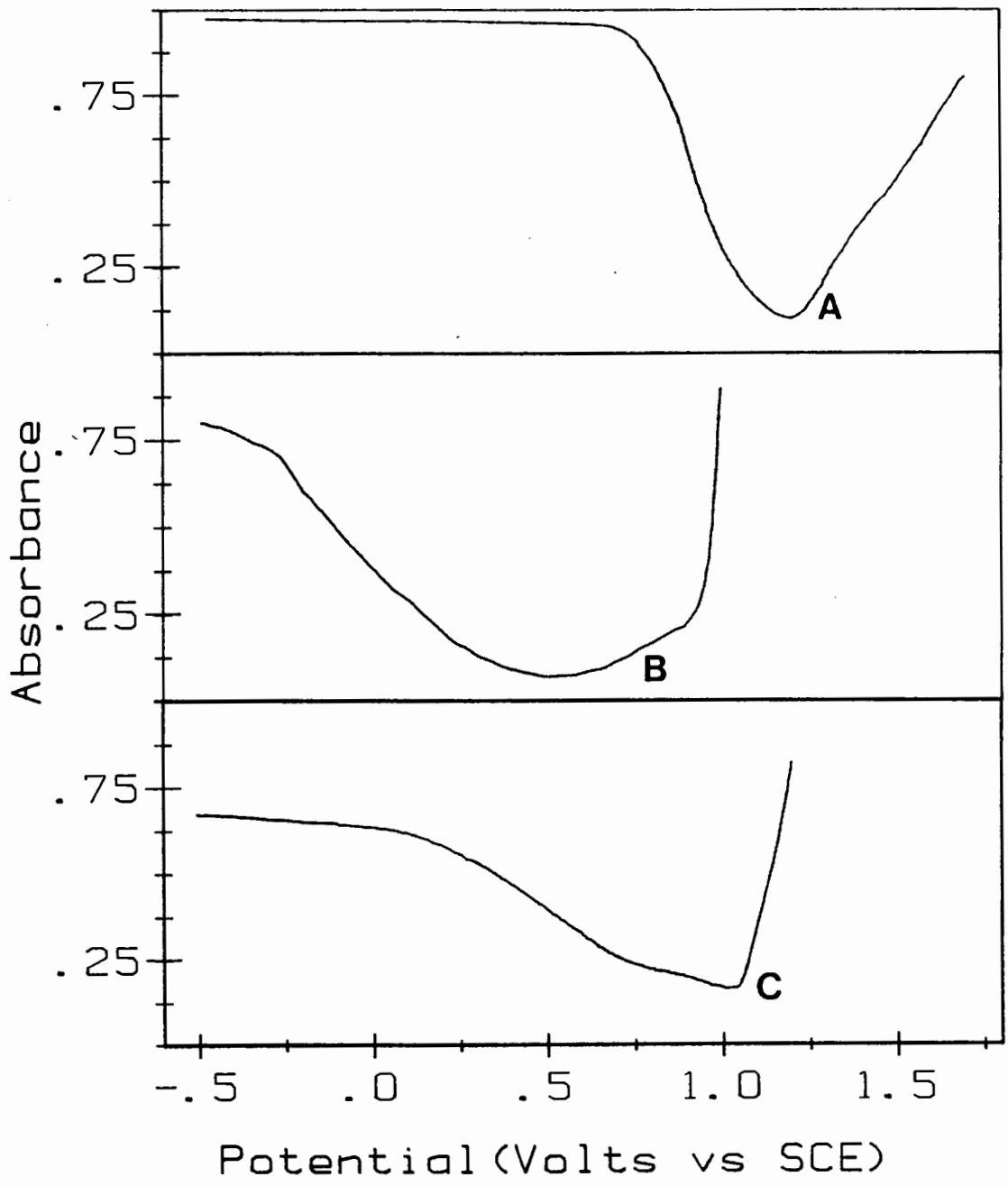
.75
.25
A
.75
.25
B
.75
.25
C
Absorbance
-.5
.0
.5
1.0
1.5
Potential (Volts vs SCE)

Figure.VII.5

Figure VII.6 NERNSTIAN PLOT FOR POLY(2,2'-BITHIOPHENE)

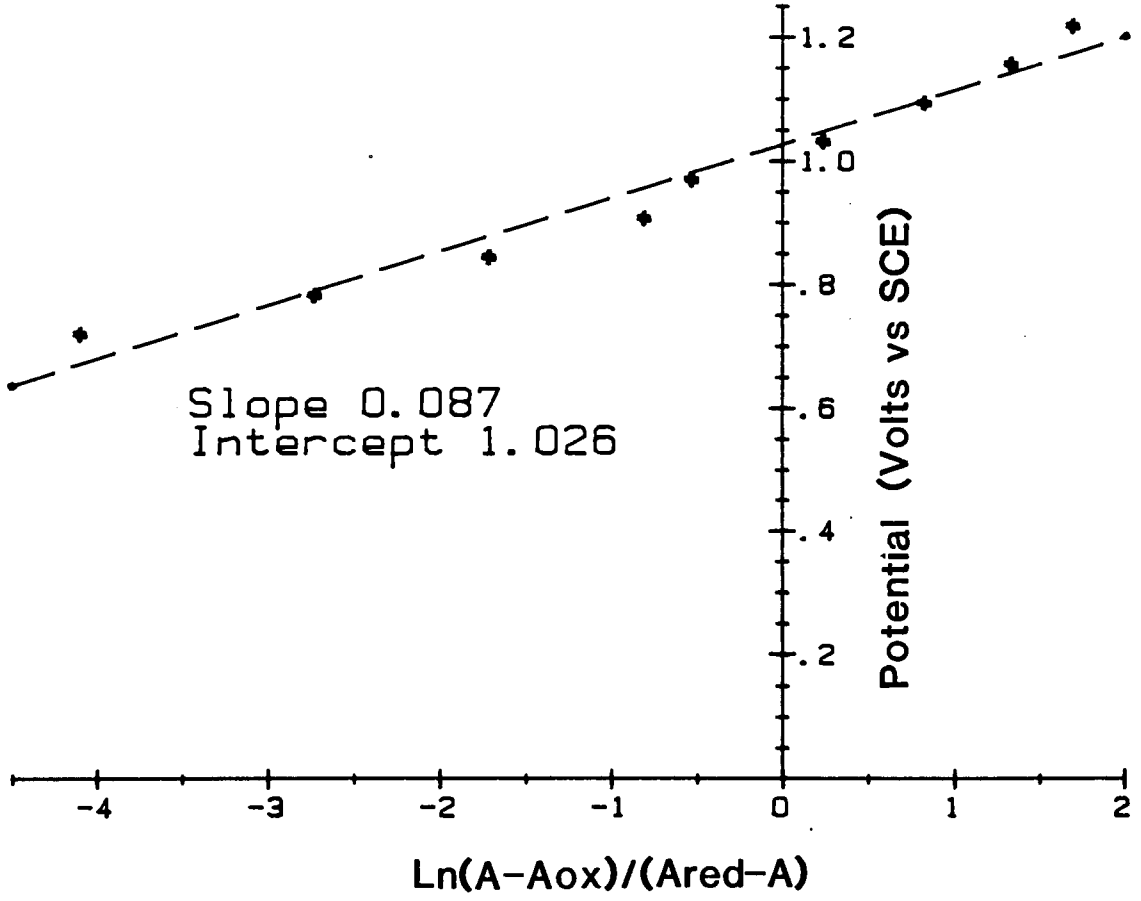
Slope 0.087
Intercept 1.026
1.2
1.0
.8
.6
.4
.2
Potential (Volts vs SCE)
-4
-3
-2
-1
0
1
2
Ln(A-Aox)/(Ared-A)

Figure.VII.6

at -0.50 V and +0.50 V respectively. The linear regression of the points on the Nernstian plot (Figure VII.7) yielded a slope of 0.136 and an intercept or standard oxidation potential E_o' of -0.043 V. The number of electrons transferred in the oxidation step n is 0.19, indicating that one electron is transferred in the oxidation of 5 PY units.

The plot of absorbance vs potential (Figure VII.5.C) was conducted on a copolymer prepared from a 50:50 monomer mixture. An expanded version of this plot is shown in Figure VII.8. The curve has two breaks in the slope (+0.30 V and +0.70 V) and three linear sections corresponding to the three oxidation peaks seen in the copolymer's cyclic voltammogram (Figure V.7). The first section is between the break at 0.0 V and the break at +0.30 V and is attributed to the oxidation of PY units in the copolymer chain. The second section (+0.30 V to +0.70) is for the oxidation of polymer chain sequences containing BT and PY units. The last section, between +0.70 V and +1.10 V, corresponds to the oxidation of BT units in the copolymer chain. The values for A_{red} and A_{ox} for the three species were set at the break point potentials on the curve as listed on Table VII.1.

Table VII.1

Polymer	A_{red} potential	A_{ox} potential	Slope	Intercept	n
PPY	-0.50	+0.50	1.14	-0.043	0.19
PBT	+0.70	+1.28	0.087	1.026	0.30
Copolymer					
PY units	0.00	+0.30	0.051	0.215	0.49
PY-BT	+0.30	+0.70	0.078	0.509	0.33
BT units	+0.70	+1.10	0.067	0.854	0.38

Figure VII.7 NERNSTIAN PLOT FOR POLYPYRROLE

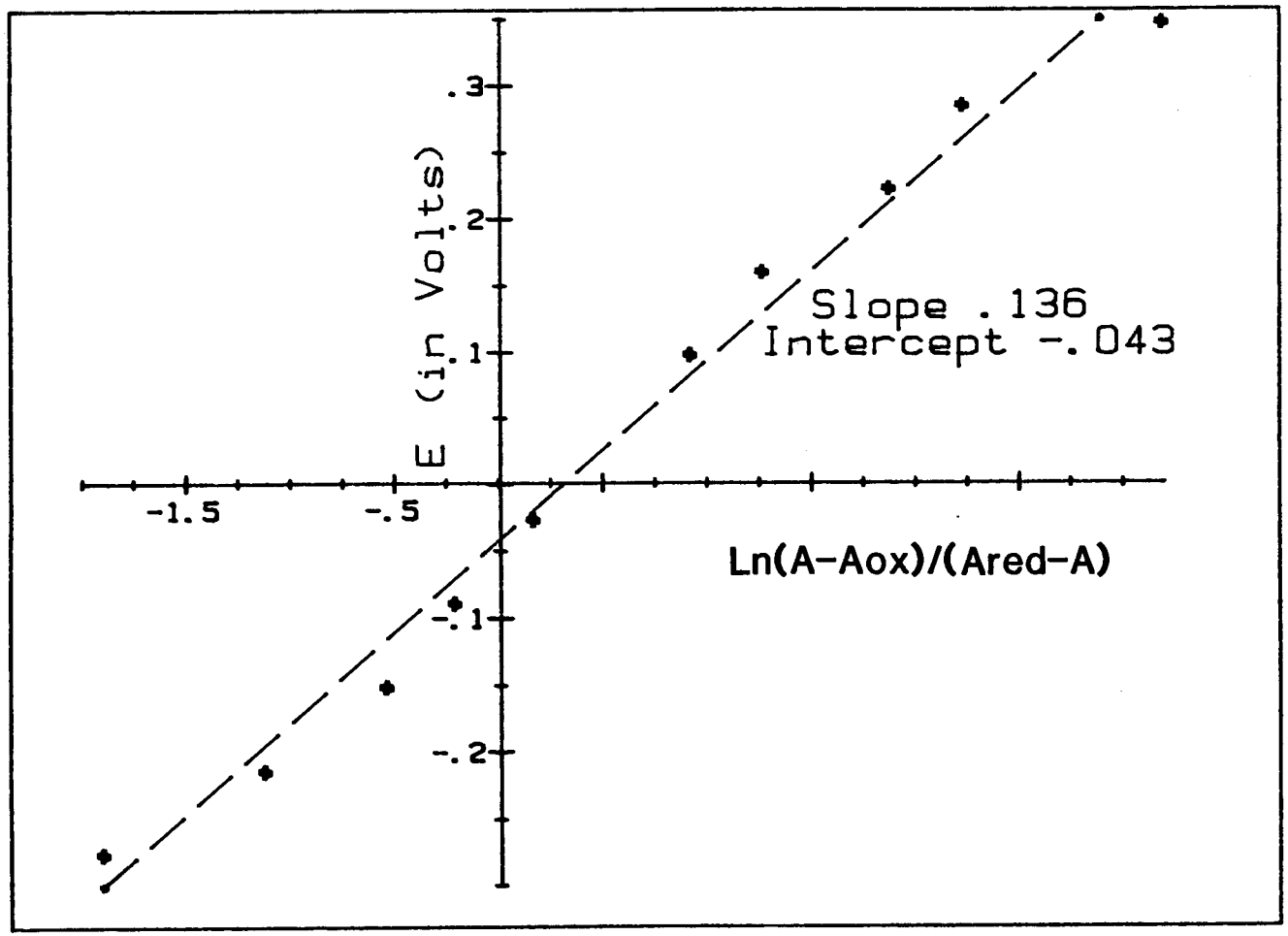

Figure.VII.7

Figure VII.8 ABSORPTION VERSUS POTENTIAL PLOT FOR THE COPOLYMER

The absorbance is plotted against the potential applied on the copolymer coated electrode monitored against a SCE reference electrode. Three regions of the plot which were used for analysis are marked with the numeric symbols 1,2 and 3.

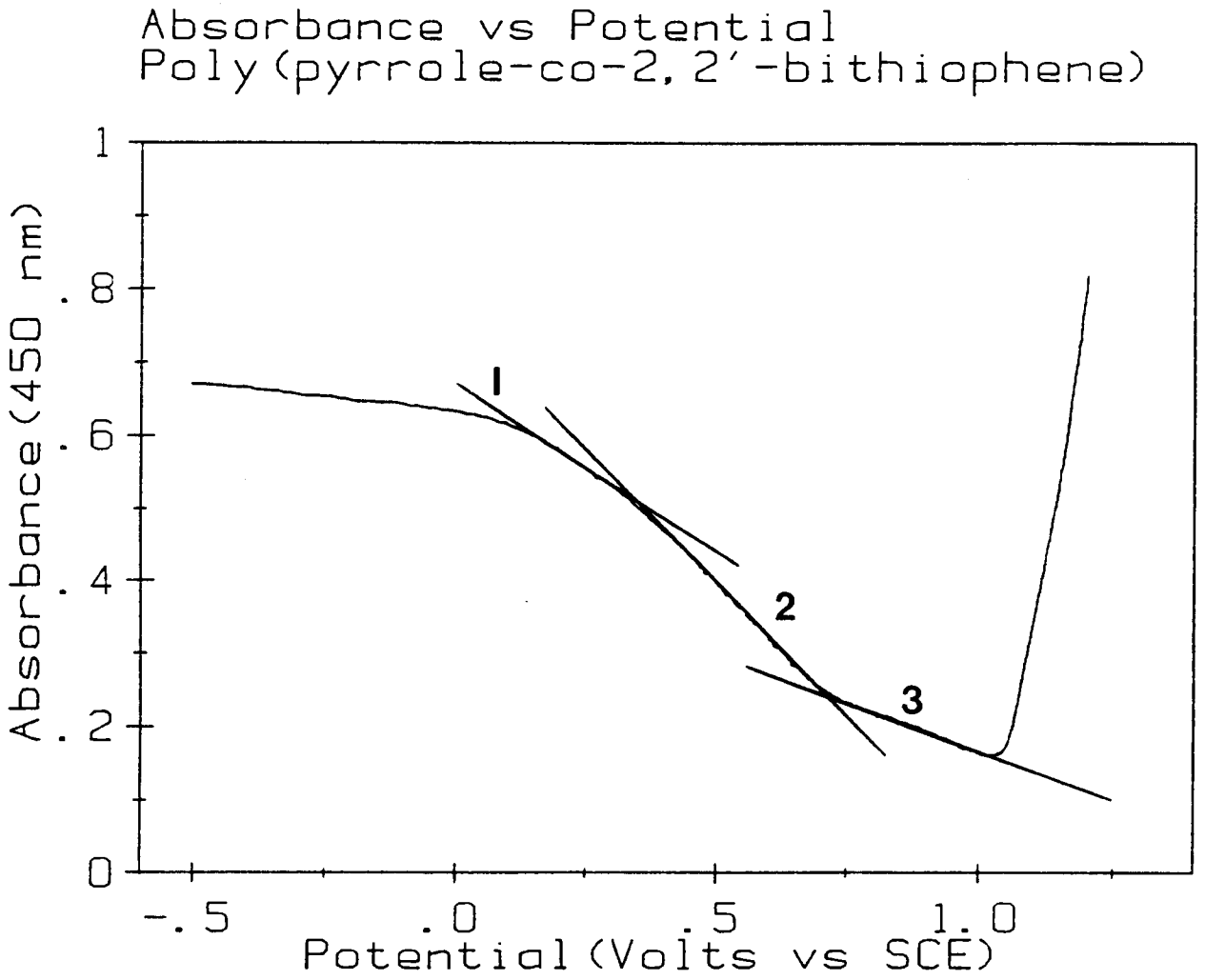
Absorbance vs Potential
Poly(pyrrole-co-2,2'-bithiophene)
Absorbance(450 nm)
1
.8
.6
.4
.2
0
-.5
.0
.5
1.0
Potential(Volts vs SCE)
1
2
3

Figure.VII.8

Nernstian plots were obtained for each of these species and are plotted in Figure VII.9. From these plots slope and intercept values were determined which are also listed in Table VII.1. The intercept values give the standard oxidation potentials (E_o') of +0.215 V, +0.509 V and +0.854 V for PY, PY-BT and BT sequences in the copolymer. The presence of an intermediate oxidation species in the copolymer is significant and provides further evidence that the copolymer has incorporated both PY and BT units in the chain.

The absorbance vs potential plots used in this chapter (Figure VII.5) are an informative method of determining the formal oxidation potentials and irreversible oxidation parameters. This technique could open new areas of research into the physical properties of these polymers. For example, work by Tanaka et al. [122] suggests that the temperature of polymerization significantly effects the polymers ability to be reduced and oxidized. Absorbance vs potential plots for conducting polymers polymerized at various temperatures could show significant changes in the irreversible oxidation boundary.

The Nernstian plots also provide a new method of determining the maximum level of doping for the polymer and the number of units involved in the oxidation of the polymer (n). This method could also be used for temperature dependence or anion substitution studies of the doping level.

Section VII.4 Conclusions

This chapter has demonstrated the application of spectropotentiometric studies for the determination of the formal

Figure VII.9 NERNSTIAN PLOT FOR THE COPOLYMER

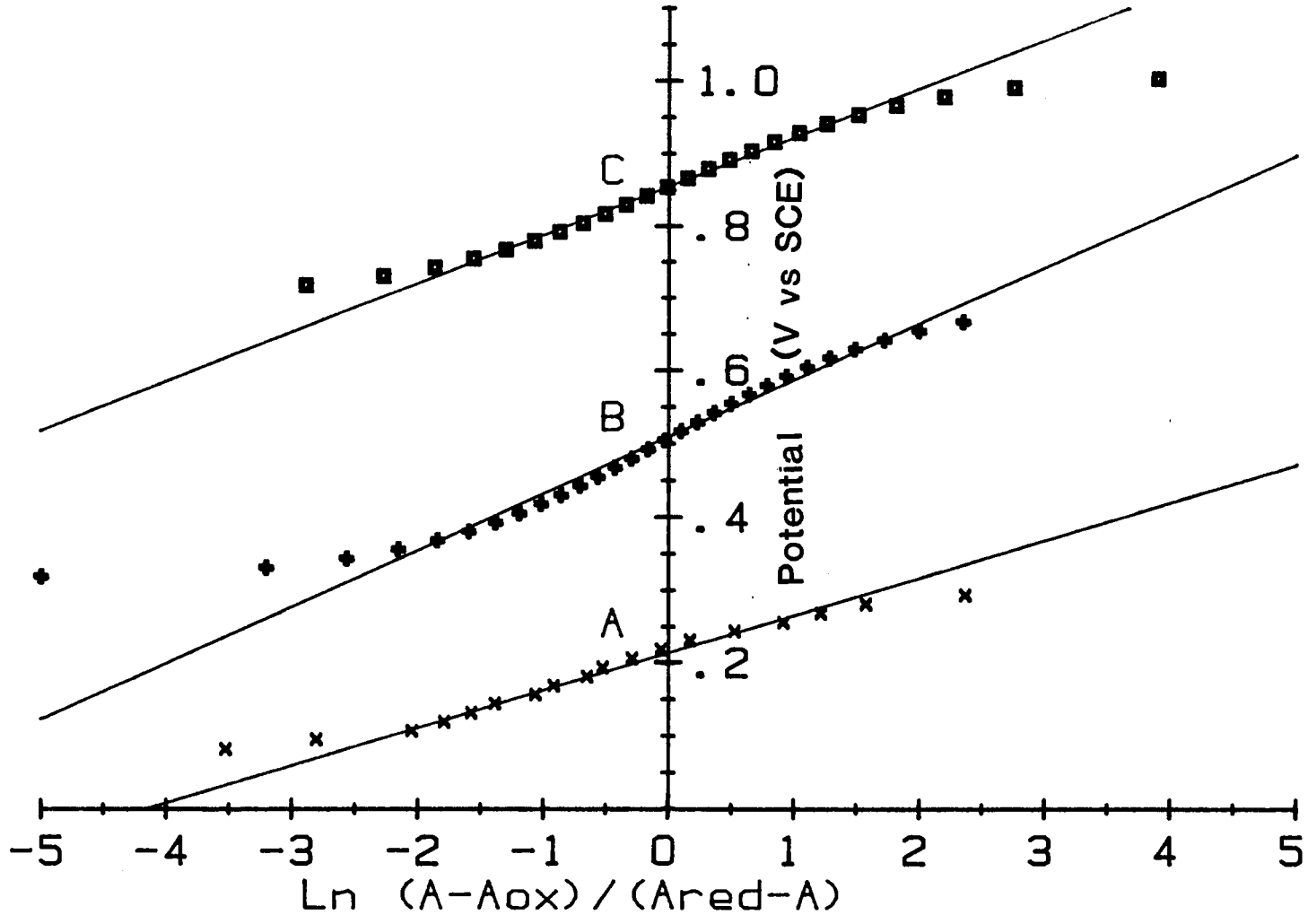

Figure.VII.9

oxidation potential E_o' (or $E_{1/2}$) of conducting polymers. The E_o' for PPY and PBT were determined using this method and the potentials found for their copolymer was compared. The copolymer was found to have two E_o's that compared to those of the homopolymers but one had no counterpart and was characteristic of only the copolymer.

The number of ring units involved in the reaction were also determined using the Nernst equation for the homopolymers and each step in the copolymers oxidation.

CHAPTER VIII CONCLUSIONS

The body of research in this thesis can be broken down into two parts; determination of the copolymers composition (chapter II) and the determination of the physical properties of the copolymer (chapters III-VII). In the first part the Mayo-Lewis equation was used to define the electrocopolymerization reaction of heterocyclic compounds in terms of reactivity ratios (r_1 and r_2). The compositions of the copolymers were shown to be related to the monomer feed ratios. The applied potential on the electrode can be changed to effect the relative rates of monomer incorporation in the copolymers. These results are important as no author had reported even the composition of the copolymers produced. Thus with the results from chapter II [73] the understanding of these systems was expanded from a point where no knowledge of the copolymer's composition was known to a point where the compositions of the copolymers were determined and could be predicted from the monomer feed ratio using the calculated reactivity ratios for the system.

The ability to predict the composition of the copolymer knowing the monomer feed ratio and the electrode potential will be important for commercial applications of conducting polymers. For example; copolymerization of soluble conducting polymers, like those described by Elsenbaumer et. al. [70], improved the conducting and mechanical properties of the polymers. To polymerize commercial quantities of these copolymers with a constant composition, the monomer feed ratio will need to be controlled and the electrode potential monitored. To do this the equations in chapter II will be required.

In the second part of the thesis the physical properties of the PY-BT copolymers were examined. Initially the properties were examined to show that the product formed was a copolymer as predicted. Again this was important as no author had physically characterized their products to prove that it was a copolymer as reported. Thus, the UV-Visible absorption spectra, surface morphology and the oxidation potentials of the copolymers were examined and compared to the parent homopolymers. The UV-visible spectra are the best evidence for the formation of PY-BT copolymers. The positions of the absorbance peaks of the copolymer indicates that the electronic structure of the product is significantly different than either PBT or PPY. If two homopolymers were forming together on the electrode rather than a copolymer the spectra should show the peaks for the homopolymers rather than completely new peaks. The changes in the oxidation potentials and surface morphology although significant are not strong enough evidence to prove that the product formed is a copolymer on their own.

Finally, the conductivities of the copolymers were measured and compared to those of the parent homopolymers. This was done initially to prove that the product formed did conduct electricity and to show that the conductivity of the copolymers is affected by their composition, something that no other author has shown.

There are many intriguing ideals for future research involving conducting copolymers. For example; 4-choromethylstyrene could be copolymerized with butadiene in a 3:1

ratio to form a synthetic rubber. A pyrrole could be attached to the copolymer by reaction with the Cl and pyrrole could be electrochemically polymerized on to the pendent pyrrole to form a conducting graft copolymer using a method similar to the synthesis outlined by A.I. Nazzal and G.B. Street [79]. M. Ogasawara et. al. [103] reported that the conductivity of PPY was enhanced by stretching therefore the conductivity of an elastomeric conducting copolymer like the graft copolymer described would also vary with stretching. Graft copolymers like these would have a large number of applications for devices measuring pressure, stress, strain, and other mechanical parameters. More over elastomeric conducting copolymers may release or absorb charge during elongation. Thus, changing the potential applied on the copolymer may cause the length of the copolymer change. Therefore the copolymer may act as a synthetic muscle.

Conducting copolymer such as those polymerized for the research in this thesis may have applications as chemical sensors due to their multiple oxidation peaks. Devices made using two closely spaced microelectrodes with polymer polymerized between them allow the measurement of the conductivity of small amounts conducting polymers. As the polymer is doped the conductivity of the copolymer changes. If the copolymer is in contact with a chemical oxidant the conductivity would change. Therefore the copolymer could act as a chemical sensor. The multiple oxidation peaks of the copolymer could allow a device made using a copolymer to have a sensitivity to more than one chemical at one time.

REFERENCES

1. H. Shirakawa, S. Ikeda, M. Aizawa, J. Yoshitake, and S. Suzuki; Synthetic Metals; 4 (1981) 43-49.

2. G. Wegner; Angew. Chem. Int. Ed. Engl.; 20 361 (1981) Find other reference

3. G. Froyer, F. Maurice, J.Y. Gobot, J.F. Fauvarque, M.A. Petit, and A. Digua; Mol. Cryst. Liq. Cryst.; 118 (1985) 267-272.

4. G. Zotti and G. Schiavon; J. Electroanal. Chem.; 163 (1984) 385.

5. A.F. Diaz, K.K. Kanazana and G.P. Gardini; J. Chem. Soc. Comm.; (1979) 635.

6. G. Tourillon and F. Garnier; J. Electroanal. Chem.; 135 (1982) 173-178.

7. T. Oshsawa, K. Kaneto, and K. Yoshino; Japanese Journal of Applied Physics; 23 9 (1984) 663-665.

8. S. Tanaka, M. Sato, and K. Kaeriyama; Makromol. Chem.; 185 (1984) 1295-1306.

9. T. Yamamoto and K. Sanechika; Chem. And Ind.; (1982) 301.

10. M. Salmon, A.F. Diaz, A.J. Logan, M. Krounbi, and J. Bargon; Mol. Cryst. Liq. Cryst.; 83 (1982) 265.

11. A.F. Diaz, A. Martinez, K.K. Kanazawa and M. Salmon; J. Electroanal. Chem.; 130 (1981) 181.

12. F. Garnier, G. Tourillon, M. Gazard and J.C. Dubois; J. Electroanal. Chem.; 148 (1983) 299.

13. M. Velazquez Rosenthal, T.A. Skotheim, A. Melo, M.I. Florit and M. Salomon; J. Electroanal. Chem.; 185 (1985) 297-303.

14. K.K. Kanazawa, A.F. Diaz, M.T. Krounbi, and G.B. Street; Synthetic Metals ; 4 (1981) 119.

15. H. Koezuka and S. Etoh ; J. Appl. Phys.; 54 5 (1983) 2511-2516.

16. M. Velazquez Rosenthal, T.A. Skothiem, and C.A. Linkous; Synthetic Metals ; 15 (1986) 219-221.

17. R.A Simon, A.J. Ricco, and M.S. Wrighton; J. Am. Chem. Soc.; 104 (1982) 2031-2034.

18. G. Ahlgren and B. Krische ; J. Chem. Soc., Chem. Commun.; (1984) 946-948.

19. S.E. Lindey and G.B. Street; Synth. Metals ; 10 (1984/85) 67-69.

20. M. De Paoli, R.J. Waltman, A.F. Diaz and J. Bargon; J. Chem. Soc., Chem. Commun.; (1984) 1015.

21. O. Niwa, M. Hikita and T. Tamamura; App. Phy. Lett.; 46 4 (1985) 444-446.

22. A. Dallo'Olio, Y. Dascola, V. Varacca, and V. Bocchi; C. R. Acad. de. Sci. Paris; 267 (1968) 433.

23. K.K. Kanazawa, A.F. Diaz, R.H. Geiss, W.D. Gill, J.F. Kwak, J.A. Logan, J.F. Rabolt, and G.B. Street; J. Chem. Soc. Chem. Commun. ; 1979 (1979) 854.

24. K.K Kanazawa, A.F. Diaz, W.D. Gill, P.M. Grant, G.B. Street, G.P. Gardini and J.F. Kwak; Synthetic Metals; 1 (1980) 329.

25. J. Bargon, S. Mohmand, and R.J. Waltman; IBM J. Res. Dev.; 27 (1983) 330.

26. J. Bargon, S. Mohmand, and R.J. Waltman; Mol. Cryst. Liq. Cryst.; 93 (1983) 279.

27. K. Yoshino, Y. Kohno, T. Shiraishi, and K. Kaneto; Synthetic Metals ; 10 (1985) 319-326.

28. I. Rubinstein; J. Electrochem. Soc. ; 130 (1983) 1506.

29. A. Diaz and J.A. Logan; J. Electroanal. Chem. ; 111 (1980) 111.

30. P. Di Marco, M. Mastragostino, and C. Taliani; Mol. Cryst. Liq. Cryst.; 118 (1985) 241-244.

31. G. Graff; Chem. Week. ; (1985) 20.

32. S. Asavapiriyanont, G.K. Chandler, G.A. Gunawardena and D. Pletcher; J. Electroanal. Chem.; 185 (1985) 297.

33. B.L Funt and S.V. Lowen; Synthetic Metals; 11 (1985) 129.

34. J. Roncali, F. Garnier, M. Lemaire and R. Garreau; Synthetic Metals; 15 (1986) 323-331.

35. G.B. Street, R.H. Geiss, and A. Nazzal; Poly. Mater. Sci.; 49 (1983) 84.

36. J.L. Bredas, B. Themans, J.G. Fripiat, J.M. Andre and R.R. Chance; Physical Review, Part B; 29 12 (1984) 6761.

37. E.M. Genies and J.M. Pernaut; Synthetic Metals; 10 (1984) 117-129.

38. J.C Scott, P. Pfluger, M.T. Krounbi, and G.B. Street; Physical Review, Part B; 28 (1983) 2140.

39. J.L. Bredas, J.C. Scott, K. Yakushi and G.B. Street; Physical Review, Part B; 30 (1984) 1023.

40. J.H. Kaufman, N.C. Colaneri, J.C. Scott and G.B. Street; Physical Review, Letters; 53 (1984) 1005.

41. M. Nechtschien, F. Devreux, F. Genoud, E. Vieil, J.M. Pernaut, and E. Genies; Synthetic Metals; 15 (1986) 59-78.

42. J.L. Bredas and G.B. Street; Acc. Chem. Res.; 18 (1985) 309-315.

43. A.J. Heeger; Polymer Journal; 17 1 (1985) 201-208.

44. J.L. Bredas; Mol. Cryst. Liq. Cryst.; 118 (1985) 49-50.

45. J.L. Bredas, B. Themans, J.M.Andre, R.R. Chance and R. Silbey; Synthetic Metals ; 9 (1984) 265-274.

46. J.C. Scott, J.L. Brecas, K. Yakushi, P. Pfluger and G.B. Street; Synthetic Metals ; 9 (1984) 165-172.

47. F. Genoud, M. Guglielmi, M. Nechtschein, E. Genies and M. Salmon; Physical Review Letters ; 55 1 (1985) 118-121.

48. E.M. Conwell; Synthetic Metals ; 11 (1985) 21-28.

49. K. Kaneto, K. Yoshino and Y. Inuishi; Jpn. J. Appl. Phys.; 21 (1982) 567.

50. M. Ito, H. Shioda and K. Tanaka; J. Polymer Sci., Part C ; 24 (1986) 147-151.

51. S. Tanaka, H.E. Katz, R.S. Hutton, J. Orenstein, G.H. Fredrickson and T.T. Wang; Synthetic Metals ; 16 (1986) 17-30.

52. E.M. Genies, C. Bidan and A.F. Diaz; J. Electroanal. Chem. ; 149 (1983) 101.

53. S. Hotta, W. Shimotsuma and M. Taketani; Synthetic Metals ; 10 (1984/1985) 85.

54. J. E. Frommer, R. L. Elsenbaumer and R. R. Chance, in T. Davidson (ed.);ACS Symposium Series 242, Polymers in Electronics, Am. Chem. Soc.; Washington ,DC, (1984) 447.

55. M. Aldissi and R. Liepins; J. Chem. Soc., Chem Commun.; (1984) 255-256.

56. S. A. Jenekhe, S. T. Wellinghoff and J. F. Reed; Mol. Cryst. Liq. Cryst.; 105 (1984) 175-189.

57. S. J. Jasne and C. K. Chiklis; Synth. Metals ; 15 (1986) 175-182.

58. R. L. Elsenbaumer, K. Y. Jen and R. Oboodi ; Synth. Metals ; 15 (1986) 169-174.

59. T. Iyoda, A. Ohtani, T. Shimidzu, and K. Honda ; Chemistry Letters; (1986) 687-690.

60. T. Ojio and S. Miyata ; Polymer Journal ; 18 1 (1986) 95-98.

61. S.E. Lindsey and G.B. Street; Synth. Metals ; 10 (1984/85) 67-69.

62. M. De Paoli, R. J. Waltman, A.F. Diaz and J. Bargon ; J. Polymer Sci., Polymer Chem Ed. ; 23 (1985) 1687-1698.

63. J. Roncali and F. Garnier ; J. Chem. Soc., Chem Commun.; (1986) 783.

64. H. Shinohara, M. Aizawa, and H. Shirakawa ; Chemistry Letters ; (1985) 179-182.

65. B. Zinger and L.I. Miller ; J. Am. Chem. Soc. ; 106 22 (1984) 6881-6883.

66. A.F Diaz; Chemica Scripta ; 17 (1981) 145-148.

67. D.A. Tirrell; Enclclopedia of Polymer Science and Engineering 2nd. Ed. ; John Wiley and Sons; 4 (1986) 192-233.

68. R.L. Blankespoor and L.L. Miller ; J. Am. Chem. Soc., Chem. Comm. ; (1985) 90.

69. M. Sato, S. Tanaka and K. Kaeriyama ; J. Chem. Soc., Chem. Comm. ; (1986) 873.

70. K.Y. Yen, G.G. Miller and R.L. Elsenbaumer ; J. Chem. Soc., Chem. Comm. ; (1986) 1346.

71. O. Inganas, B. Liedberg and W. Chang-Ru; Synthetic Metals ; 11 (1985) 239-249.

72. S. Naitoh, K. Sanui and N. Ogata; J. Chem. Soc.,Chem. Commun. ; (1986) 1348.

73. B.L. Funt, E.M. Peters and J.D. Van Dyke ; J. Polymer Sci., Part A ; 24 (1986) 1529-1537.

74. N. Kumar, B.D. Malhotra, and S. Chandra; J Polymer Sci., Polymer Lett. Ed ; 23, (1985) 57-61.

75. A.F. Diaz; Chemica Scripta ; 17 (1981) 145-148.

76. Mark A. Druy; J. Electrochem. Soc. ; 23 2 (1986) 353-355.

77. J.A. Moore, and E.M. Partain III; J Polymer Sci, Polymer Chem. Ed. ; 22 (1984) 3581-3583.

78. Matsuahita Electric Co. Ltd.; Jpn. Kokai Tokkyo koho JP 59,207,931 [84,207,931] (Cl. C08G73/06), 26 Nov 1984.

79. A.I. Nazzal and G.B. Street ; J. Chem. Soc., Chem. Commun. ; (1985) 375.

80. G.G. McLoed, M.G.B. Mahboubian-Jones, R.A. Pethrick, S.D. Watson, N.D. Truong, J.C. Galin and J. Francois; Polymer ; 27 (455) 455-458.

81. J. Chen, A.J. Heeger and F. Wudl; Solid State Cumm. ; 58 (1986) 251-257.

82. M. Aizawa, S. Watanabe, H. Shinohara and H. Shirakawa; J. Chem. S (1985) 264.

83. "Principles of Polymerization 2nd Ed." ; pg. 423-507; George Odian; John Wiley and Sons , Toronto (1981).

84. T. Alfrey and G. Goldfinger; J. Chem. Phy. ; 12 (1944) 205.

85. F.R. Mayo and F.M. Lewis; J. Am. Chem. Soc. ; 66 (1944) 1594.

86. F.T. Wall; J. Am. Chem. Soc. ; 66 (1944) 2050.

87. "Encyclopedia of Polymer Science and Engineering 2nd Ed.; pg. 192-233 ; D.A. Tirrell ;John Wiley and Sons, New York New York (1986).

88. G. Goldfinger and T. Kane ; J. Polymer Sci. ; 3 (1948) 462.

89. H.W. Melville, B. Noble, and W.F. Watson; J. Polymer Sci. ; 2 (1947) 229.

90. H. Dostal; Monatsh Chem. ; 69 (1936) 424.

91. "The Elements of Polymer Science and Engineering"; pg. 262-202;Alfred Rudin ; Academic Press New York, New York, (1982).

92. R.C. McFarlane, P.M. Reilly and K.F. O'Driscoll;J. Polymer Sci., Polymer Chem Ed. 18 (1980) 251-257.

93. H. Patino-Leal, P.M. Reilly and K.F. O'Driscoll;J. Polymer Sci.,Polymer Letters ; 18 (1980) 219-227.

94. B. Yamada, M. Itahashi and T. Otsu ;J. Polymer Sci., Polymer chem Ed. ; 16 (1978) 1719-1733.

95. P.W. Tidwell and G.A. Mortimer ; J Polymer Sci., Part A ; 3 (1965) 369-387.

96. M. Fineman and S.D. Ross; J Polymer Sci.; 5 (1950) 259.

97. A.F. Diaz and K.K. Kanazawa; Extended Linear Chain Compounds; 3 (1983) 417.

98. Xiangtong Bi, Youxin Yao, Meixiang Wan, Ping Wang, Ke Xiao, Qiyung Yang and Renyuan Qian; Makromol Chem; 186 (1985) 1101-1108.

99. A.F Diaz, J.I. Castillo, J.A. Logan And W. Lee; J. Electroanal. Chem.; 129 (1981) 115-132.

100. Yong Cao, Ping Wang and Renyuan Qian; Makromol Chem.; 186 (1985) 1093-1100.

101. A. Uhlir; Bell Syst. Tech. J.; (1955) 105.

102. L.J. van der Pauw; Phillips Res. Repts. ; 16 (1961) 187-195.

103. M. Ogasawara, K. Funahashi, T. Demura, T. Hagiwara and K. Iwata ; Synthetic Metals ; 14 (1986) 61-69.

104. M. Ogasawara, K. Funahashi and K. Iwata; Mol. Cryst. Liq. Cryst. ; 118 (1985) 159-162.

105. B. Lundberg, B. Sundqvist, O. Inganas, I. Lundstrom and W.R. Salaneck; Mol. Cryst. Liq. Cryst. ; 118 (1985) 155-158.

106. "Electrical Properties of Polymers"; Page 134 ; A.R. Blythe; Cambridge University Press, Cambridge, (1979).

107. F.M. Smits; Bell Syst. Tech. J. ; 37 (1958) 711.

108. "Laboratory Notes on Electrical and GalvanomagneticB Measurements" ; H.H. Wieder ; Elsevier Scientific Pub. Co., New York, New York, (1979).

109. G.A. Mabbott; J. Chem. Ed. ; 60 9 (1983) 697-702.

110. P.T. Kissinger and W.R. Heineman; J. Chem. Ed. ; 60 9 (1983) 702-706.

111. "Laboratory Techniques in Electrochemistry"; page 86-93 ; P.T. Kissinger and W.R. Heineman; Marcel Dekker Inc., New York, New York; (1984).

112.A. Secvik; Collection Czech. Chem. Commun. ; 13 (1948) 349.

113.J.E.B. Randles; Tran. Faraday Soc. ; 44 (1948) 327.

114."Electrochemical Methods"; page 522 ; A.J. Bard and L.R. Faulkner; John Wiley and Sons; New York, New York; (1980).

115.R.S. Nicholson and I. Shain; Anal. Chem. ; 36 (1964) 706.

116.G. Tourillon and F. Garnier; J. Electroanal. Chem. ; 161 (1984) 51-58.

117.P.G. Pickup, C.R. Liedner, P. Denisevich, and R.W. Murray; J. Electroanal. Chem. ; 164 (1984) 39-61.

118.O. Inganas and I. Lundstrom; J. Electrochem. Soc., Solid - State Science and Technology ; 131 5 (1984) 1129-1132.

119.M. Okano and A. Fujishima; J. Electroanal. Chem. ; 185 (1985) 393-396.

120."Organic Chemistry 3th ed."; page 413 ; R.T. Morrison and R.N. Boyd ; Allyn and Bacon ; Boston, Mass. (1973).

121.J.K. Kaufman, N. Colaneri, J.C. Scott, K.K. Kanazawa and G.B. Street; Mol. Cryst. Liq. Cryst. ; 118 (1985) 171-177.

122.K. Tanaka, T. Shichiri and T. Yamabe; Synthetic Metals ; 16 (1986) 207-214.

123.W.R. Heineman, F.M. Hawkridge and H.N. Blount in "Electroanalytical Chemistry"; Vol 13 ; A.J. Bard (Ed.); Marcel Dekker, New York, New York (1984) page 17-20.

124.P.M. Hoang, S. Holdcroft, B.L. Funt; J. Electrochem. Soc. ; 132 (1985) 2129.

125."Electrochemical Methods"; page 525-527 ; A.J. Bard and L.R. Faulkner; John Wiley and Sons; Toronto, Ont. (1980).

126."Electrochemical Methods"; page 86-118 ; A.J. Bard and L.R. Faulkner; John Wiley and Sons; Toronto, Ont. (1980).

APPENDIX I

In section II.1 the statement is made that if equations 2.10 and 2.11 are rate controlling, then the results will still fit the Mayo-Lewis Equation. This relationship has never been demonstrated before therefore some proof is required.

$$M_1 \xrightarrow{k_a} M_1^{+\cdot} \qquad [2.10]$$

$$M_2 \xrightarrow{k_b} M_2^{+\cdot} \qquad [2.11]$$

In equation 2.10 and 2.11 the monomers react at the electrode to form radical cations. The rate of formation of these radical cations depends on the electrode potential and concentrations of M_1 and M_2 in the monomer mixture. This relationship is described by the Butler-Volmer formulation of electrode kinetics [126].

If the potential on the electrode is constant throughout polymerization then:

$$[M_1^{+\cdot}] \quad \alpha \quad [M_1] \qquad [I.1]$$

$$[M_2^{+\cdot}] \quad \alpha \quad [M_2] \qquad [I.2]$$

therefore:

$$[M_1^{+\cdot}] = k_a[M_1] \qquad [I.3]$$

$$[M_2^{+\cdot}] = k_b[M_2] \qquad [I.4]$$

where k_a and k_b are the reaction rate constants.

If we create data using these relationships (I.3 and I.4) then we can easily show that copolymers polymerized with 2.10 and 2.11 the rate controlling step can fit the Mayo-Lewis equation. In Table 1.1 the concentrations of two monomers M_1 and M_2 are varied between 0 and 1. Concentration values for $M_1^{+\cdot}$ and $M_2^{+\cdot}$ are calculated from the M_1 and M_2 values using equation I.3 and I.4. k_a and k_b were arbitrarily given the values 0.1 and 0.05

respectively. If all $M_1^{+\cdot}$ and $M_2^{+\cdot}$ cation radials formed polymerize to form polymer, then the concentrations of the cation radicals formed are equal to the concentrations of monomer units in the polymer. The percent M_1 units in the polymers are plotted against the percent M_1 in the comonomer feed to give the compositional curve Figure 1.1.

F and f are calculated for the Fineman and Ross linearization (equation II.37) of the Mayo-Lewis equation (see section II.3.2). These values are used to calculate F_2f and F(1-f). F(1-f) is plotted against F^2f to give a straight line with a slope of 2.0 (r_1) and an intercept of -0.5 ($-r_2$). This plot (Figure 1.2) gives a straight line fit indicating that the data calculated fits the Mayo-Lewis equation. Thus the Mayo-Lewis equation can be used to descibe polymerizations which have equations 2.10 and 2.11 as their rate controlling steps.

Table 1.1

$[M_1]$	$[M_2]$	F	$[M_1^{+\cdot}]$	$[M_2^{+\cdot}]$	f	F^2f	F(1-f)
0.00	1.00	0.00	0.00	0.05			
0.05	0.95	0.05	0.01	0.05	9.50	0.0263	-0.45
0.10	0.90	0.11	0.01	0.05	4.50	0.0556	-0.39
0.20	0.80	0.25	0.02	0.04	2.00	0.1250	-0.25
0.30	0.70	0.43	0.03	0.04	1.17	0.2143	-0.07
0.40	0.60	0.67	0.04	0.03	0.75	0.3333	0.17
0.50	0.50	1.00	0.05	0.03	0.50	0.5000	0.50
0.60	0.40	1.50	0.06	0.02	0.33	0.7500	1.00
0.70	0.30	2.33	0.07	0.02	0.21	1.1667	1.83
0.80	0.20	4.00	0.08	0.01	0.12	2.0000	3.50
0.90	0.10	9.00	0.09	0.01	0.06	4.5000	8.50
1.00	0.00						

If reaction steps 2.10 and 2.11 are rate controlling, then the reactions can be described in terms of the monomer mixture composition, the rates k_a and k_b, and the reactivity ratios r_1

Figure 1.1 Calculated Compositional Curve for Stage 1 controlled polymerization

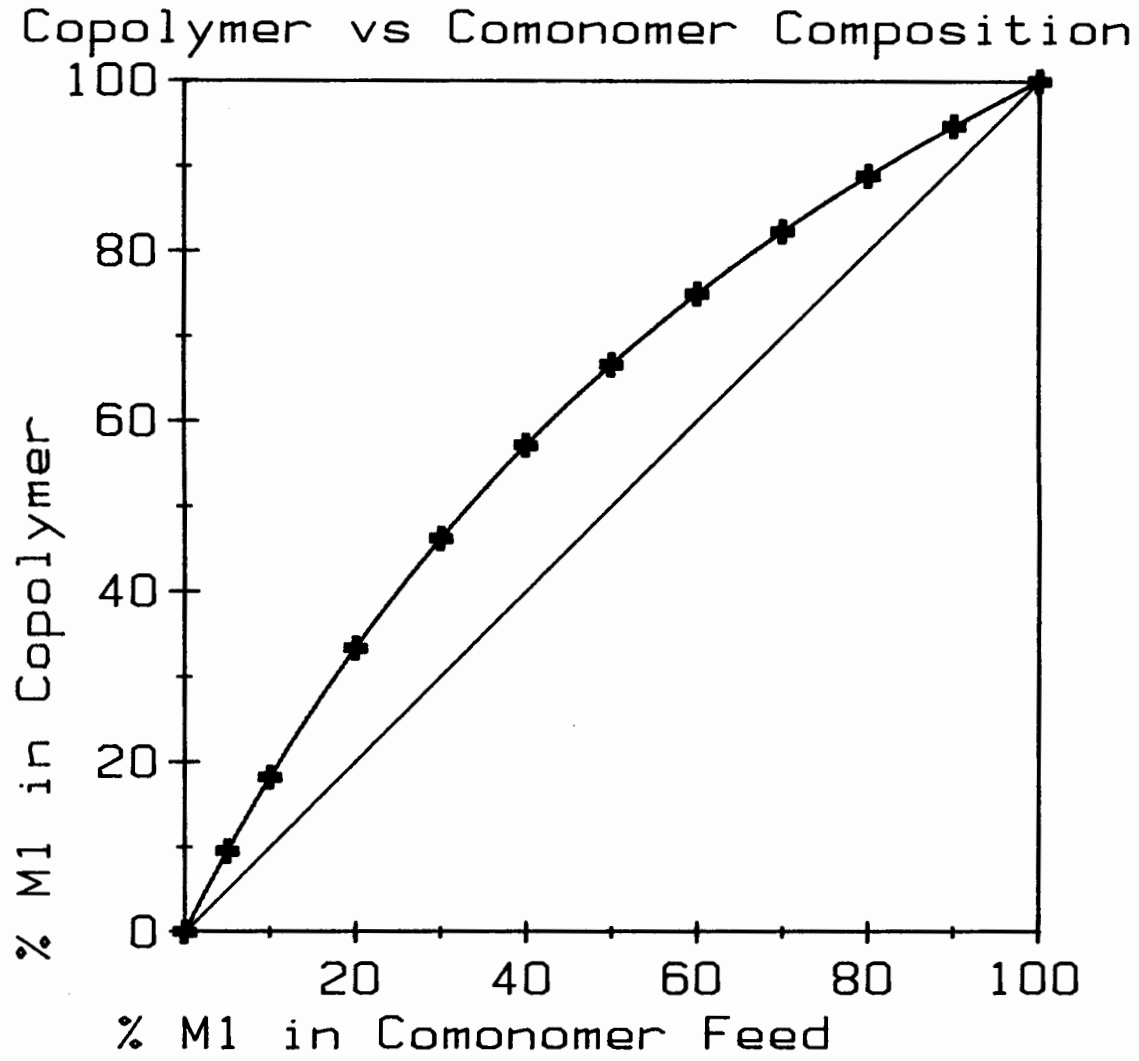
Copolymer vs Comonomer Composition
100
80
60
40
20
0
% M1 in Copolymer
20
40
60
80
100
% M1 in Comonomer Feed

Figure 1.1

Figure 1.2 Fineman and Ross plot for calculated data

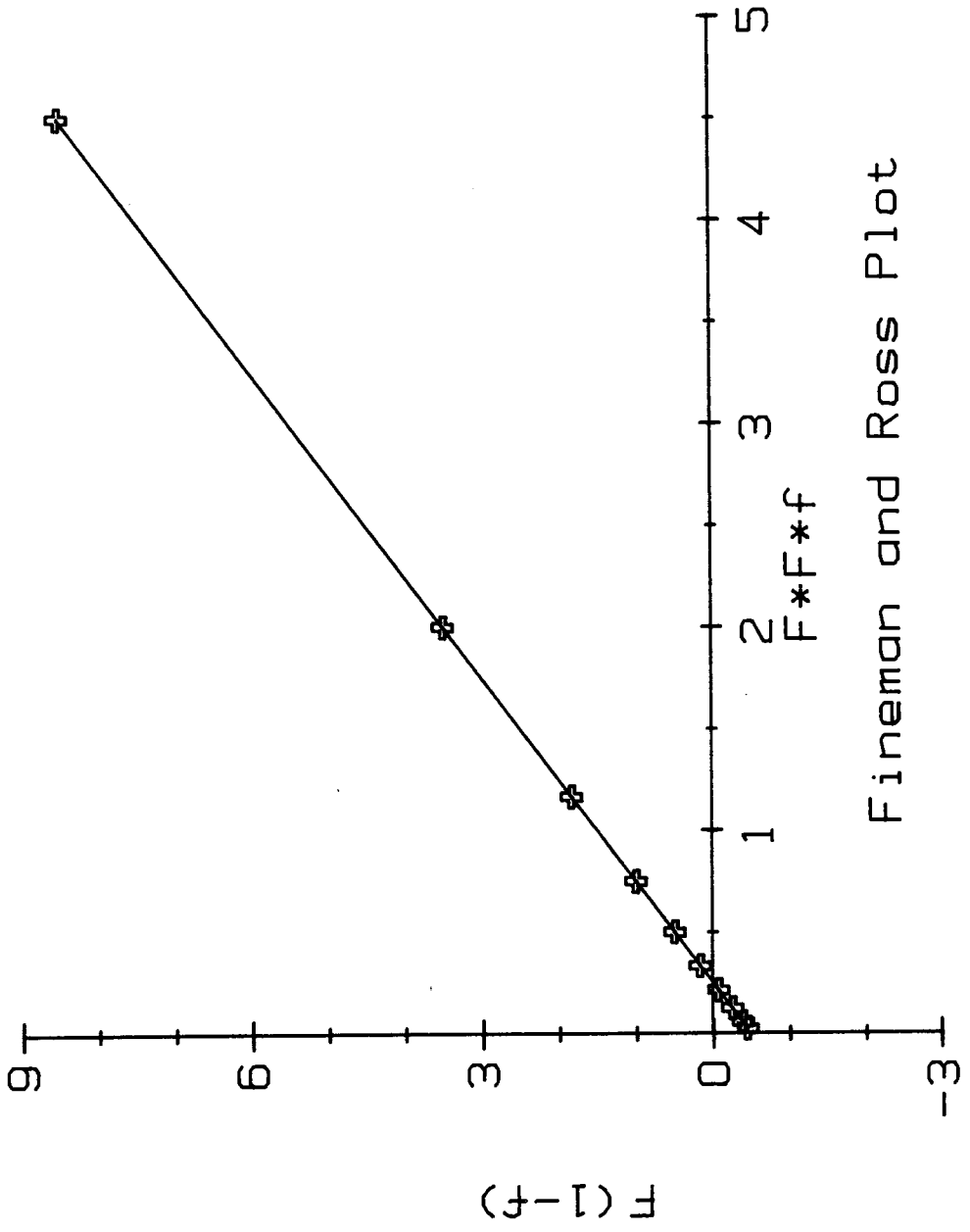

Figure 1.2

and r_2.

If one defines k_b/k_a as equal to Ø, then the polymer composition ratio (f) can be related to the ratio of monomers in the polymerization mixture (F):

$$F = [M_1]/[M_2]$$

$$f = d[M_2]/d[M_1] = [M_2^{+\cdot}]/[M_1^{+\cdot}] = k_b[M_2]/k_a[M_1] = k_b/k_aF = Ø/F$$

Substituting this relationship into the Fineman and Ross equation (2.37) one obtains the form:

$$F(1-f) = -r_2 + r_1F^2f \qquad [2.37]$$

$$F - Ø = -r_2 + r_1ØF$$

Therefore if the reaction rate constants of the monomers are known (k_a and k_b), then for homopolymerizations at a constant potential the reactivity ratios for the copolymers can be determined. Also, the copolymer compositions for the various feed ratios can be predicted. Furthermore the rate constants of the monomers can be calculated using the Butler-Volmer equation [126] for a wide range of potentials if the rate constants are experimentially determined for two or more potentials with in that range. Thus if the these reaction steps are rate controlling, then the experimental determination of the reaction rate constants at two potentials for the various monomers of interest could theoretically allow the prediction of the compositions of all the possible conducting copolymers, polymerized using radical cation coupling.